Topological materials and flat band superconductivity

Aalto University *G. Volovik* Landau Institute

Russian Academy of Sciences
L.D Landau Institute for Theoretical Physics

Cryocourse 2016, September 29

1. From topological defects to topological matter

* monopoles, half quantum vortices (Alice strings), skyrmions, etc.
* topological confinement, hybridization of topological defects
* Topological materials as defects & skyrmions in momentum space

2. From Fermi surface to flat bands

* Fermi surface as vortex in p-space
* from Fermi surface to flat band: route to room T_c superconductivity

3. Weyl point - Berry phase monopole

* chiral superfluids, Weyl semimetals, vacuum of Standard Model in massless phase
* topological origin of physical laws: chiral fermions, gauge fields & gravity as emergent phenomena
* type-I & and type-II Weyl fermions
* chiral anomaly, chiral magnetic & chiral vortical effects

4. Nodal line semimetals, graphene & graphite

* flat band in nodal line semimetals
* topological route to room-temperature superconductivity

5. fully gapped topological materials: *p*-space skyrmion

* topological insulators & vacuum of Standard Model in massive phase
* fermion zero modes on surface and on vortices & strings

hedgehog in magnets
’t Hooft-Polyakov magnetic monopole in hep

ground state in magnets
quantum vacuum in hep

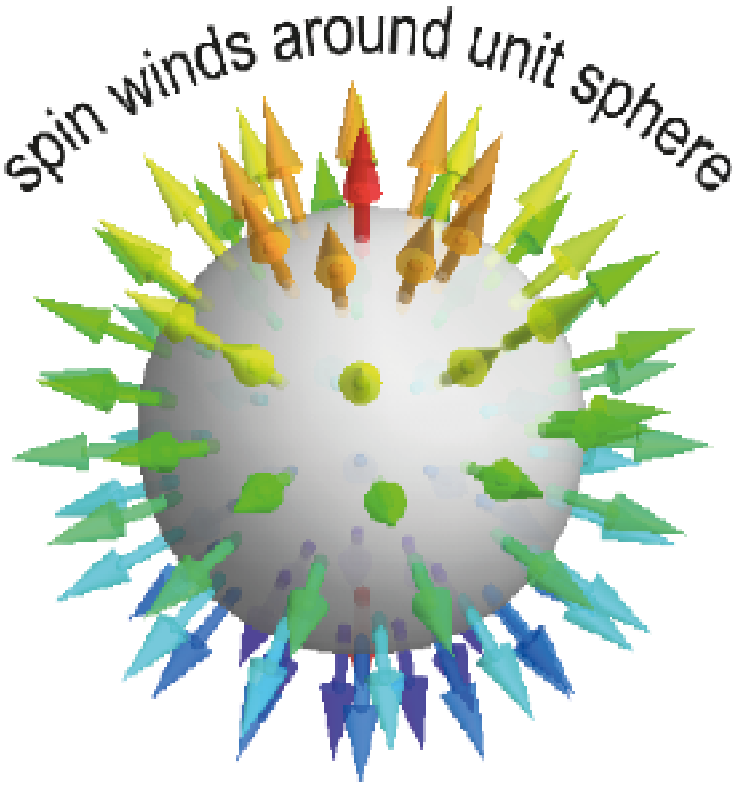

$\neq$

no winding

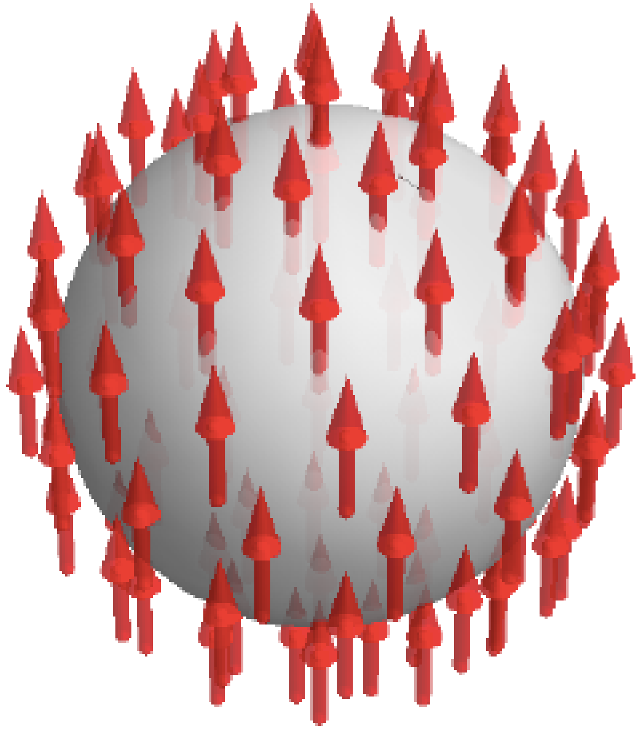

cannot smoothly be transformed into each other
$\Leftrightarrow$ hedgehog is topologically stable

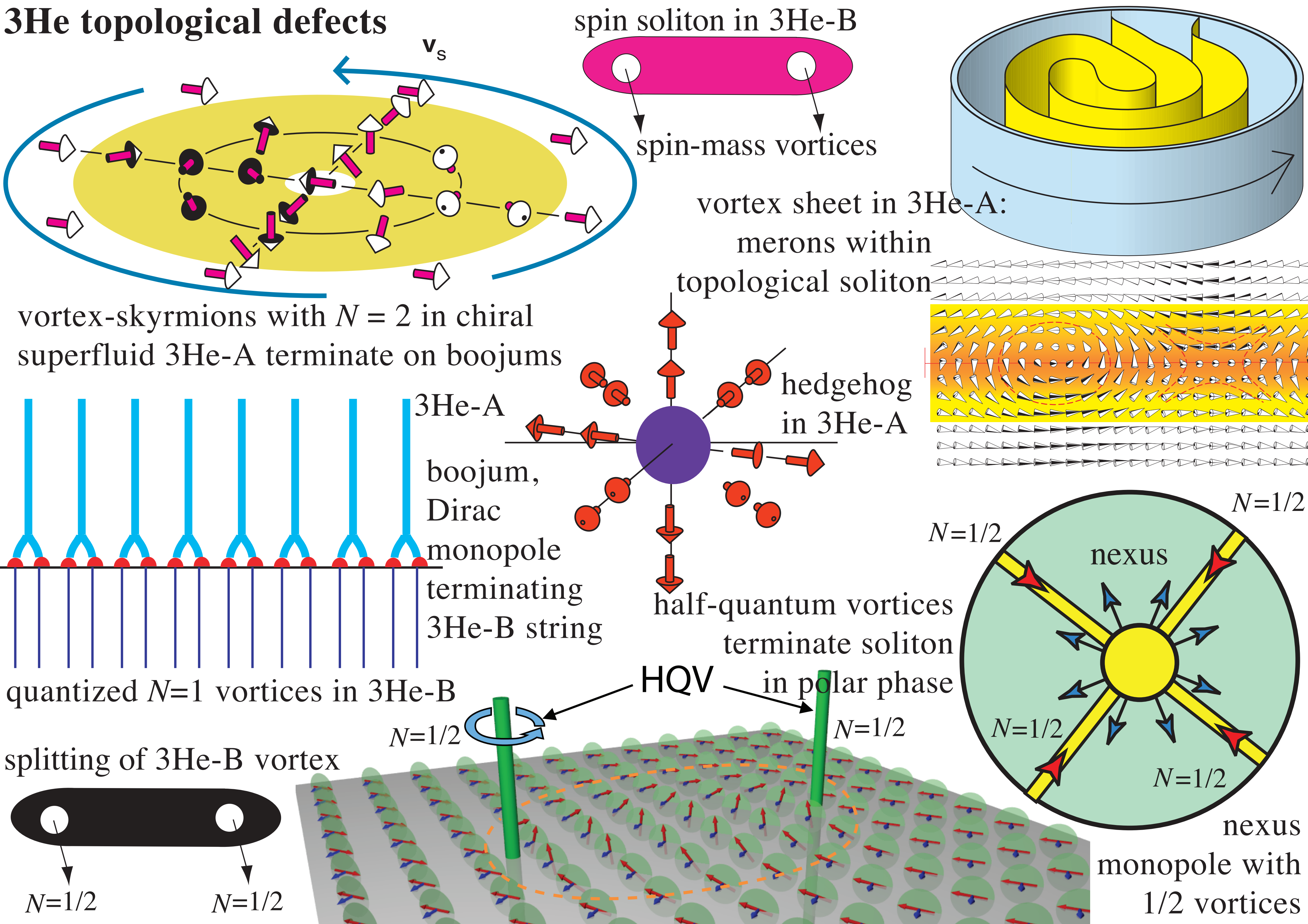
3He topological defects
v_s
vortex-skyrmions with $N = 2$ in chiral superfluid 3He-A terminate on boojums
spin soliton in 3He-B
spin-mass vortices
vortex sheet in 3He-A: merons within topological soliton
hedgehog in 3He-A
3He-A
boojum, Dirac monopole terminating 3He-B string
quantized N=1 vortices in 3He-B
splitting of 3He-B vortex
N=1/2
N=1/2
half-quantum vortices terminate soliton in polar phase
HQV
N=1/2
N=1/2
nexus
N=1/2
N=1/2
N=1/2
N=1/2
nexus monopole with 1/2 vortices

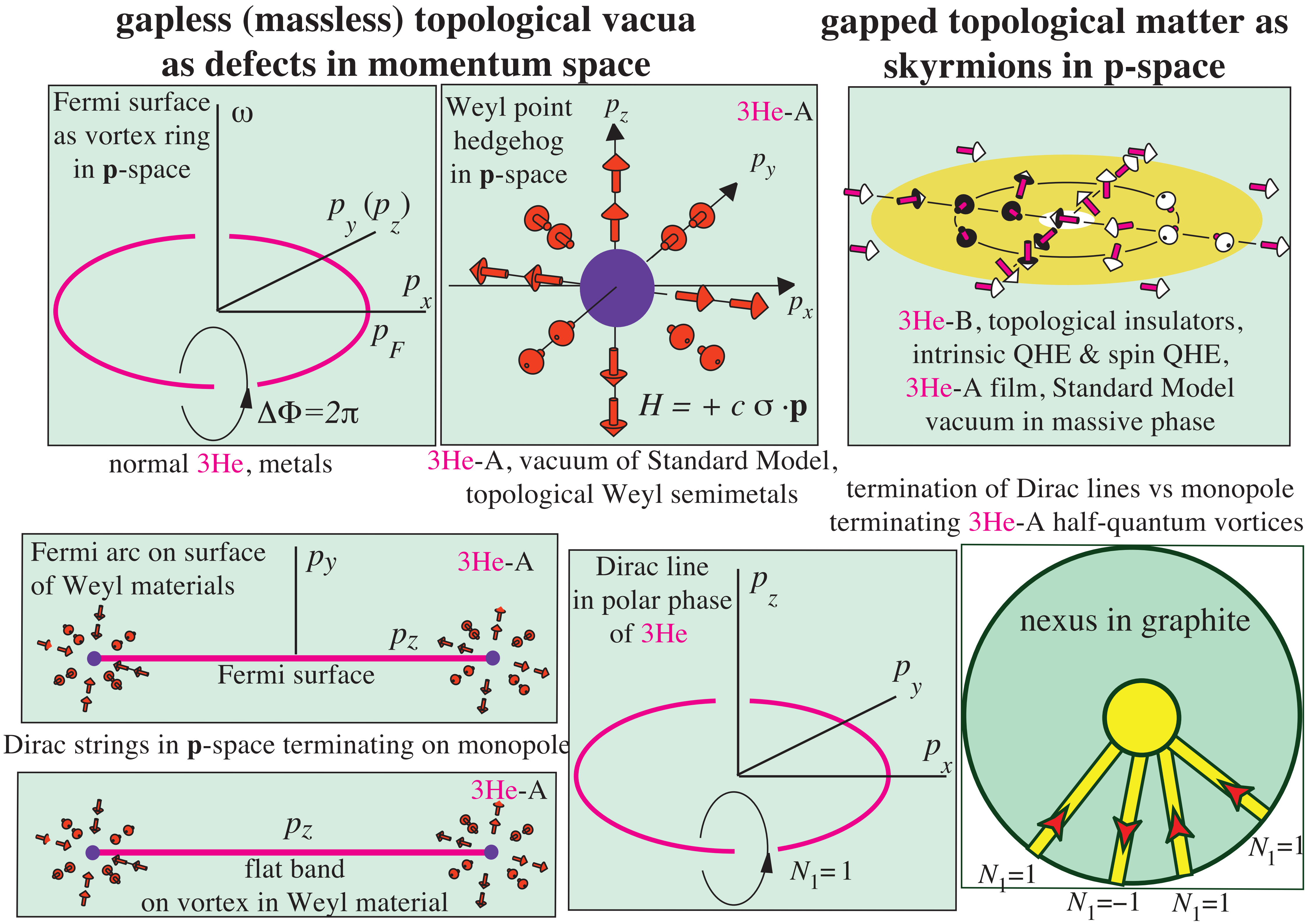

gapless (massless) topological vacua as defects in momentum space
gapped topological matter as skyrmions in p-space
Fermi surface as vortex ring in p-space
ω
p_y (p_z)
p_x
p_F
ΔΦ=2π
normal 3He, metals
Weyl point hedgehog in p-space
p_z
3He-A
p_y
p_x
$H = + c\, \sigma \cdot \mathbf{p}$
3He-A, vacuum of Standard Model, topological Weyl semimetals
3He-B, topological insulators, intrinsic QHE & spin QHE, 3He-A film, Standard Model vacuum in massive phase
termination of Dirac lines vs monopole terminating 3He-A half-quantum vortices
Fermi arc on surface of Weyl materials
p_y
3He-A
p_z
Fermi surface
Dirac strings in p-space terminating on monopole
3He-A
p_z
flat band on vortex in Weyl material
Dirac line in polar phase of 3He
p_z
p_y
p_x
N_1= 1
nexus in graphite
N_1=1
N_1=−1
N_1=1
N_1=1

Fermi surface as topological object (vortex) in p-space

Energy spectrum of
non-interacting gas of fermionic atoms

$$\varepsilon(p) = \frac{p^2}{2m} - E_F = \frac{p^2}{2m} - \frac{p_F^{\,2}}{2m}$$

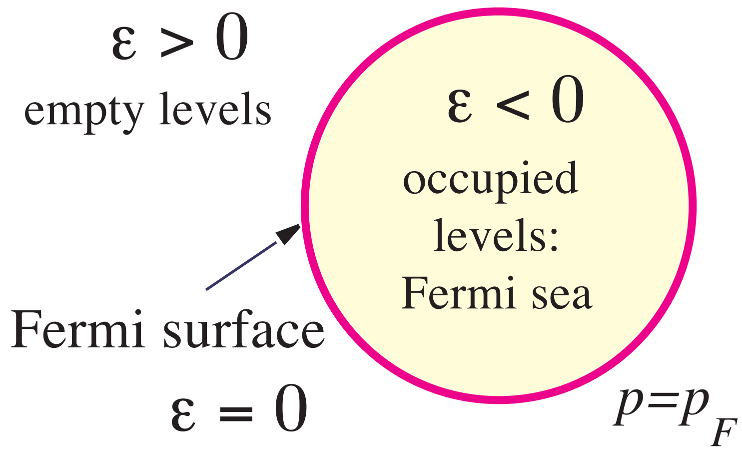

Green's function

$$G^{-1} = i\omega - \varepsilon(p)$$

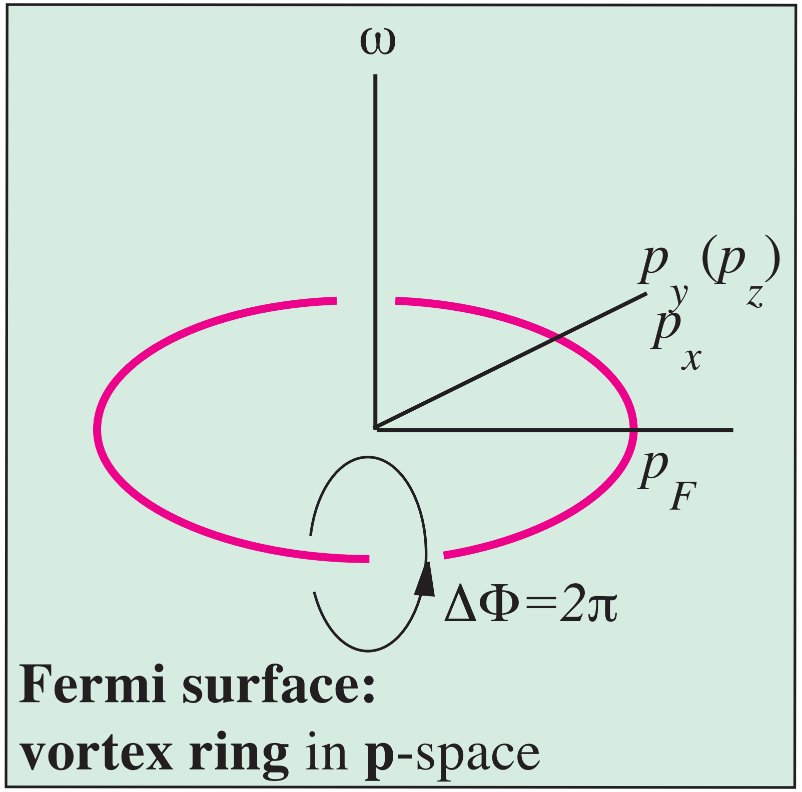

phase of Green's function

$$G(\omega,\mathbf{p}) = |G| e^{\,i\Phi}$$

has winding number $N = 1$

$$N = \frac{1}{4\pi i}\,\mathbf{tr}\left[\oint dl\, \mathbf{G}\,\nabla_l\, \mathbf{G}^{-1}\right]$$

Fermi surface survives in metals due to integer topological invariant

$$N = \frac{1}{4\pi i}\mathbf{tr}\left[\oint dl\, \mathbf{G}\,\nabla_l\, \mathbf{G}^{-1}\right]$$

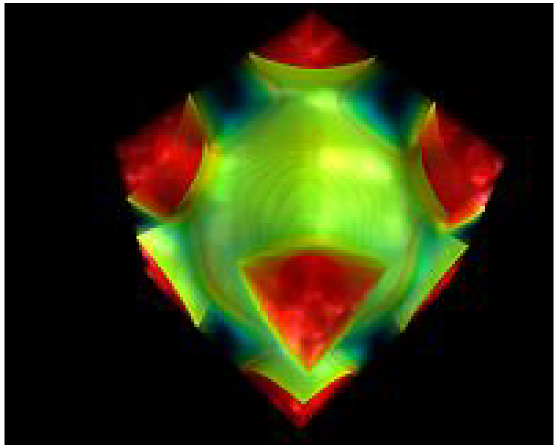

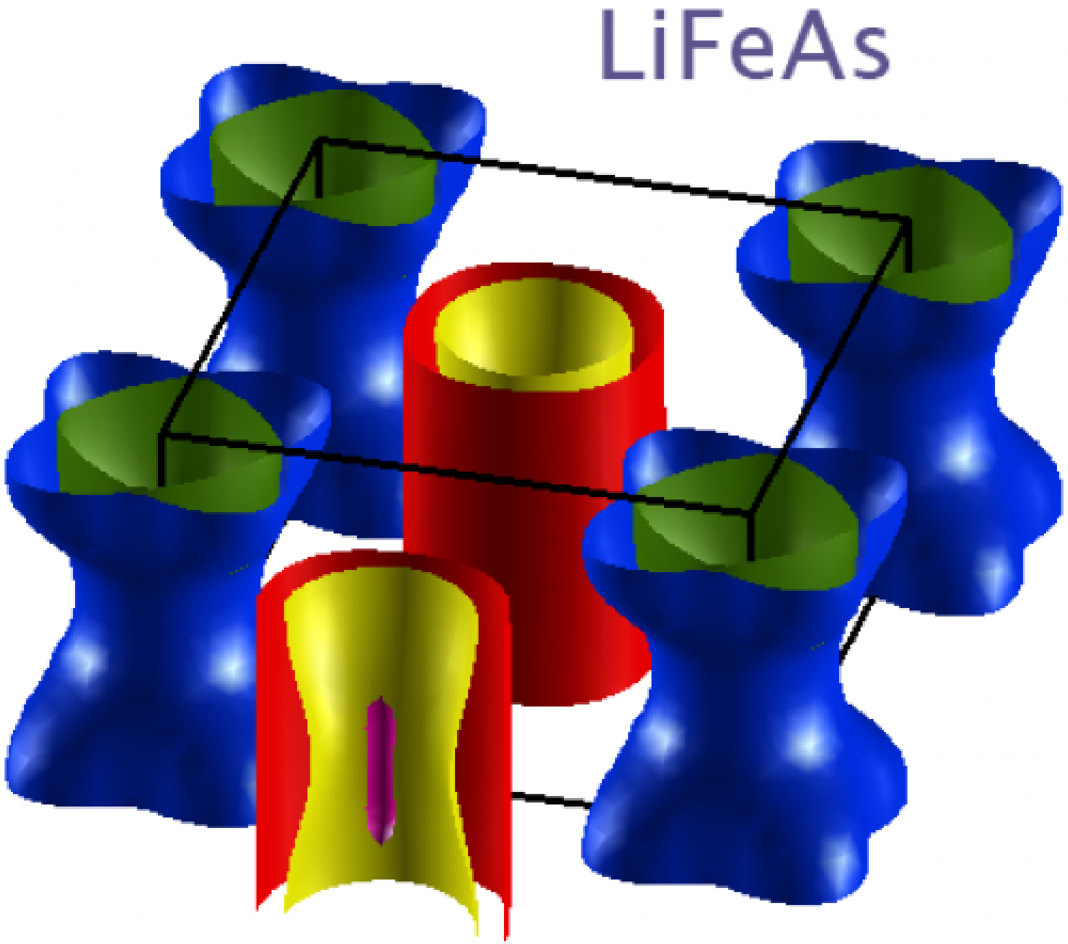

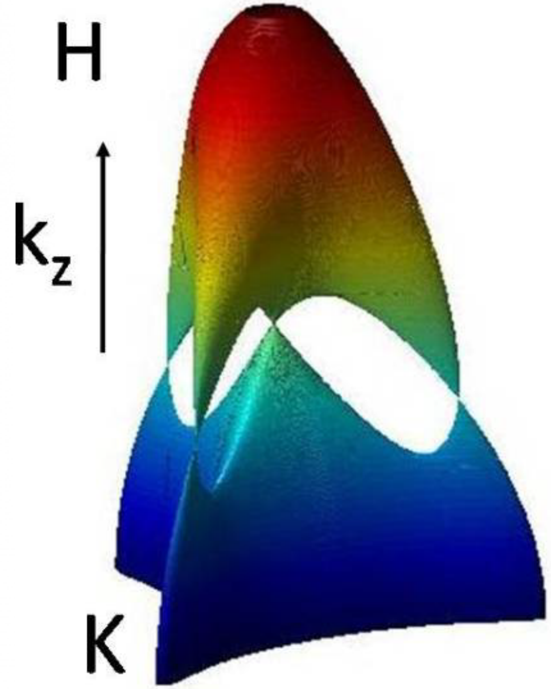

why metals are ubiquitous ?

because Fermi surface is topologically protected origin of topological stability of **vortex** in **r**-space & **Fermi surface** in **p**-space

homotopy group π_1

Topology in **r**-space

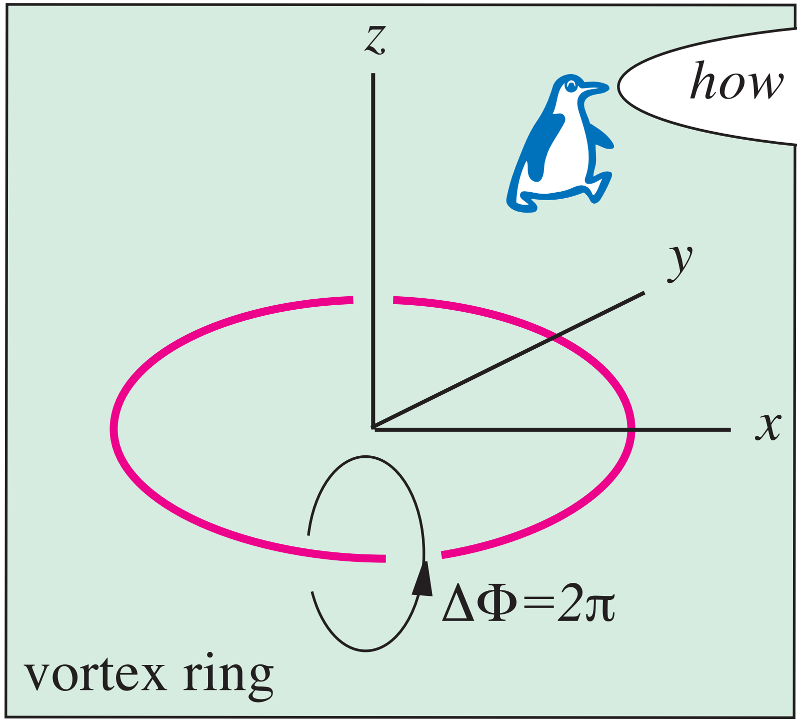

winding number $N_1 = 1$

Topology in **p**-space

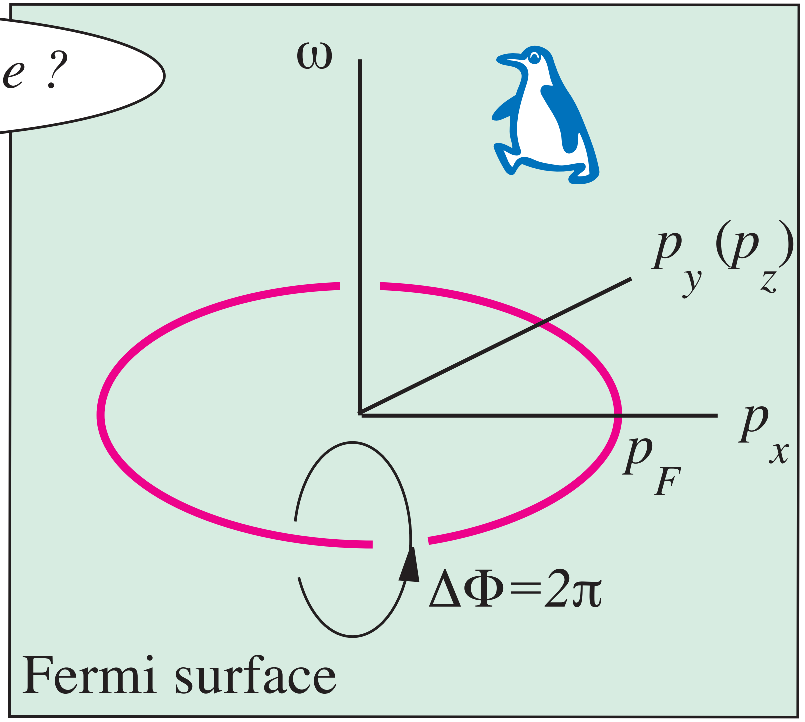

$\Psi(\mathbf{r})=|\Psi|\, e^{\,i\Phi}$

scalar order parameter of superfluid & superconductor

$G(\omega,\mathbf{p})=|G|e^{\,i\Phi}$

Green's function (propagator)

classes of mapping S^1 to $U(1)$

manifold of broken symmetry vacuum states

classes of mapping S^1 to $GL(\mathrm{n,C})$

space of non-degenerate complex matrices

Fermi liquids & non-Fermi liquids

Singularity at Fermi surface is robust to perturbations:

winding number N=1 cannot change continuously,
interaction (perturbative) cannot destroy singularity
but behavior near FS can be different

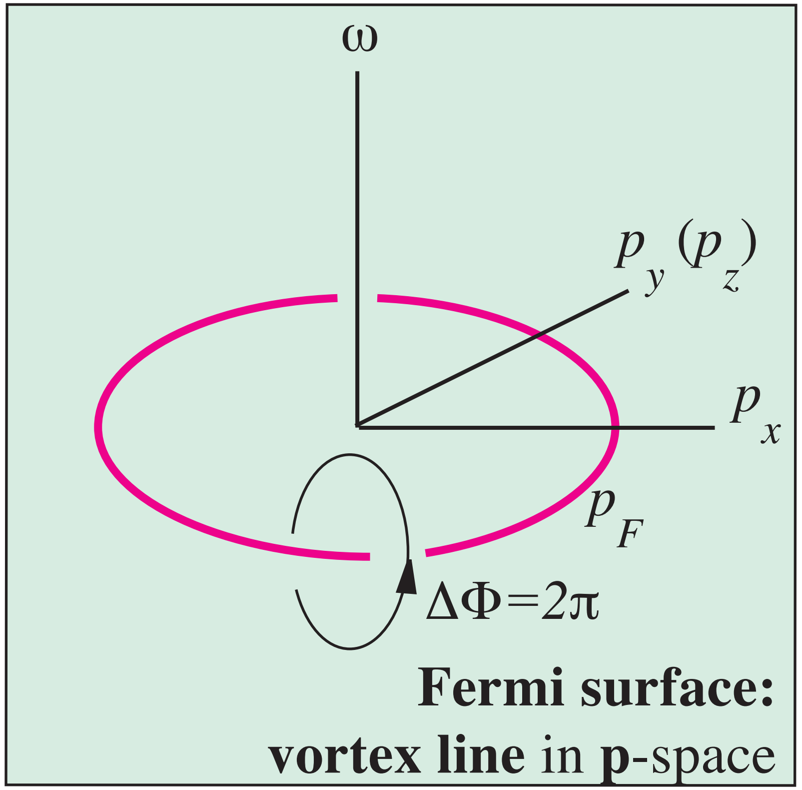

$G(\omega,\mathbf{p})=|G|e^{i\Phi}$

Landau Fermi-liquid

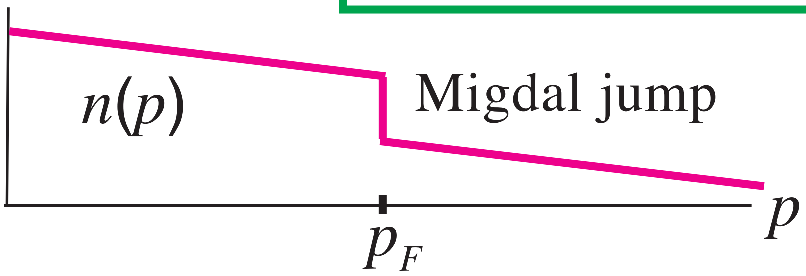

Fermi surface exists in superfluids/superconductors
examples: 3He-A in flow & Gubankova-Schmitt-Wilczek,
PRB74 (2006) 064505, but no Luttinger theorem

Luttinger Fermi liquid, marginal Fermi liquid

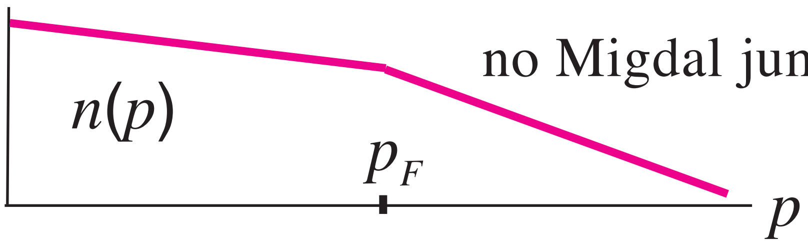

unparticles in particle physics

zeroes in $G(\omega,\mathbf{p})$ have the same N=1 as poles

$$G(\omega,\mathbf{p}) = \frac{Z(p,\omega)}{i\omega - \varepsilon(p)}$$

$$Z(p,\omega) = (\omega^2 + \varepsilon^2(p))^\gamma$$

zeroes in $G(\omega,\mathbf{p})$

for $\gamma > 1/2$

from Fermi-surface to flat band

Khodel-Shaginyan flat band from Landau theory

Khodel-Shaginyan, JETP Lett. **51**, 553 (1990)
GV, JETP Lett. **53**, 222 (1991)
Nozieres, J. Phys. (Fr.) **2**, 443 (1992)

$$E\{n(p)\}$$

$$\delta E\{n(p)\} = \int \varepsilon(p)\, \delta n(p)\, d^{d}p = 0$$

two solutions: $\delta n(p)=0$ & $\varepsilon(p) = 0$

weak interaction:
Fermi surface (Landau Fermi-liquid)

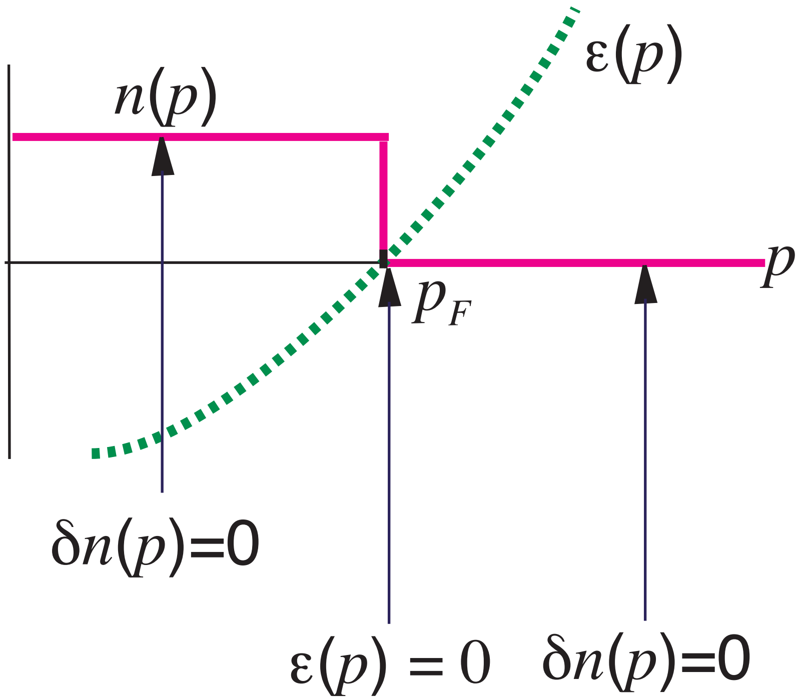

strong interaction:
Fermi ball (flat band)

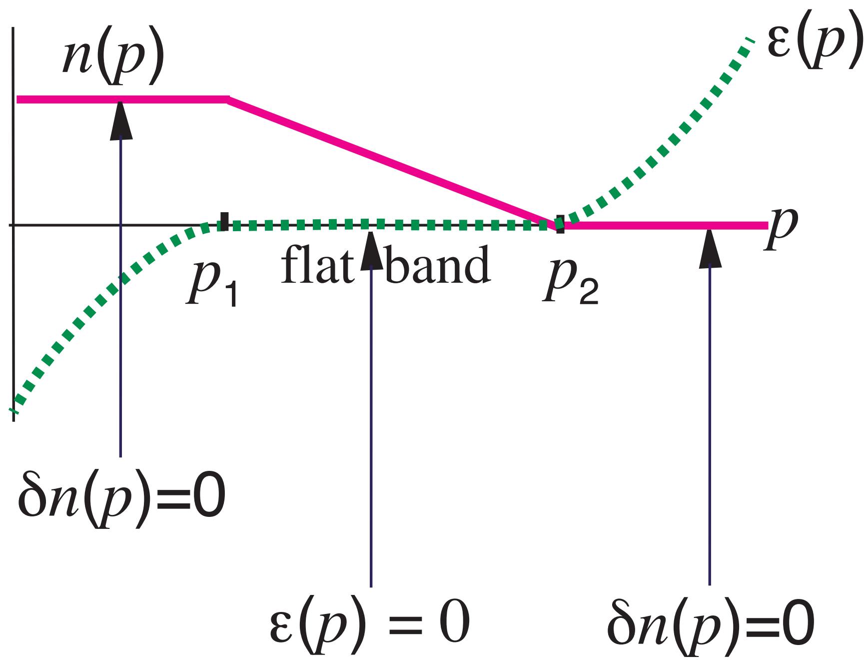

S.-S. Lee
Non-Fermi liquid from a charged black hole: A critical Fermi ball
PRD 79, 086006 (2009)

anti-de Sitter/conformal field theory correspondence

From Fermi surface topology to flat band topology

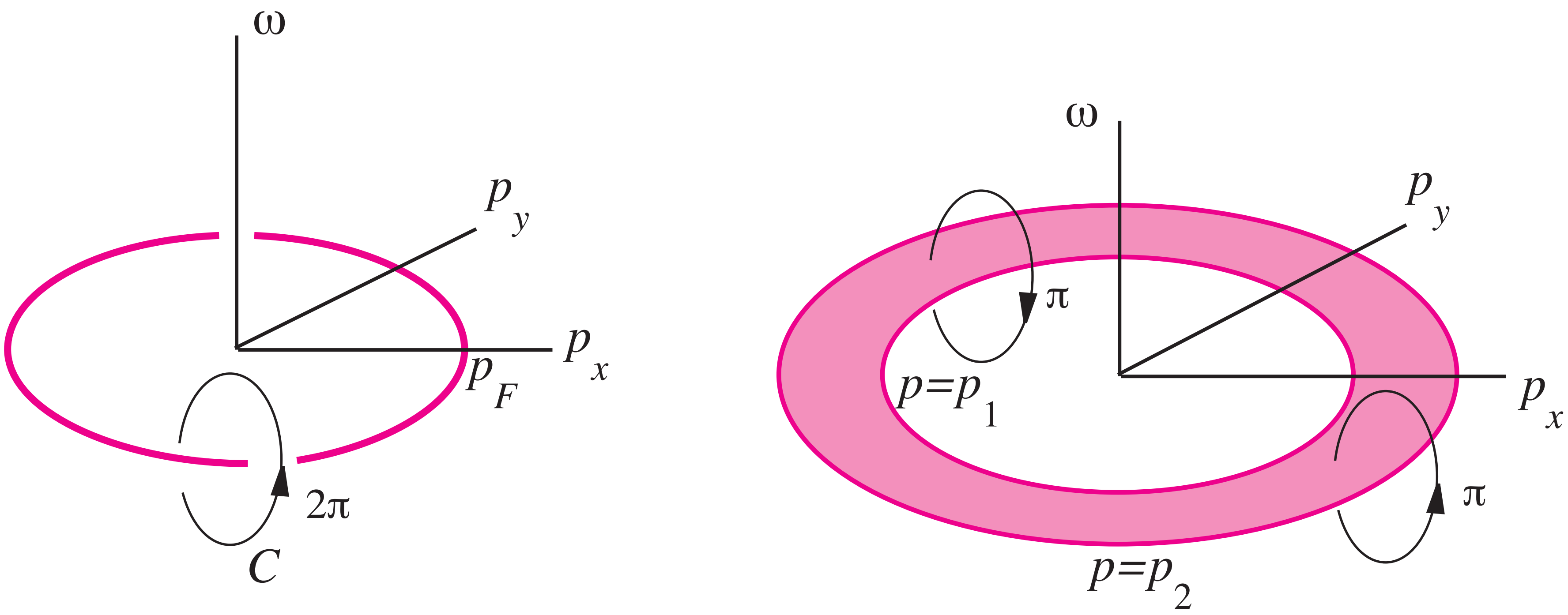

p-space vortex splits into two half-quantum vortices (p-space Alice strings), separated by p-space domain wall (p-space soliton)

GV 1991

Extremely high DoS in flat band - route to room-T superconductivity

gap equation

$$\boxed{1 = W \int \frac{d^3p}{2h^3} \frac{1}{E(p)}}$$

W - coupling in Cooper channel

$$E^2(p) = \Delta^2 + \varepsilon^2(p)$$

conventional metal with Fermi surface

$$\varepsilon(p) = v_F\,(p - p_F)$$

$$E^2(p) = \Delta^2 + v_F^{\,2}(p - p_F)^2$$

$$1 = WN(0) \int \frac{d\varepsilon}{E(\varepsilon)} = WN(0) \ln \frac{E_c}{\Delta}$$

normal superconductors:
exponentially suppressed
transition temperature

$$\boxed{T_c \sim \Delta = E_c \exp\,[-1/\underbrace{W}_{\text{coupling}}\underbrace{N(0)}_{\text{DOS}}]}$$

coupling ***DOS***

system with flat band

$$\varepsilon(p) = 0 \quad \text{in flat band}$$

$$E(p) = \Delta \quad \text{in flat band}$$

$$1 = \frac{W}{\Delta} \int \frac{d^3p}{2h^3} = \frac{W\,V_{FB}}{\Delta}$$

flat band superconductivity:
linear dependence
of T_c on coupling W

$$\boxed{T_c \sim \Delta = W\,V_{FB}}$$

coupling ***flat band volume***

PRL 112, 070403 (2014) PHYSICAL REVIEW LETTERS week ending 21 FEBRUARY 2014

Fermi Condensation Near van Hove Singularities Within the Hubbard Model on the Triangular Lattice

Dmitry Yudin,[1] Daniel Hirschmeier,[2] Hartmut Hafermann,[3] Olle Eriksson,[1]
Alexander I. Lichtenstein,[2] and Mikhail I. Katsnelson[4,5]

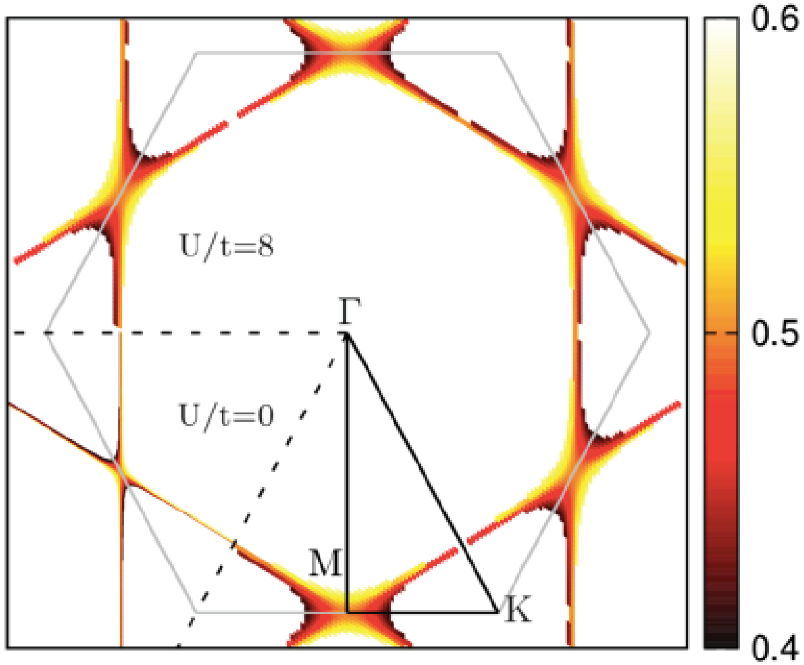

FIG. 4 (color online). Broadened Fermi surface within ±0.1 electrons for $U/t = 8$ and $T/t = 0.1$. The lower left sextant shows the noninteracting result.

flat band near Lifshitz transition

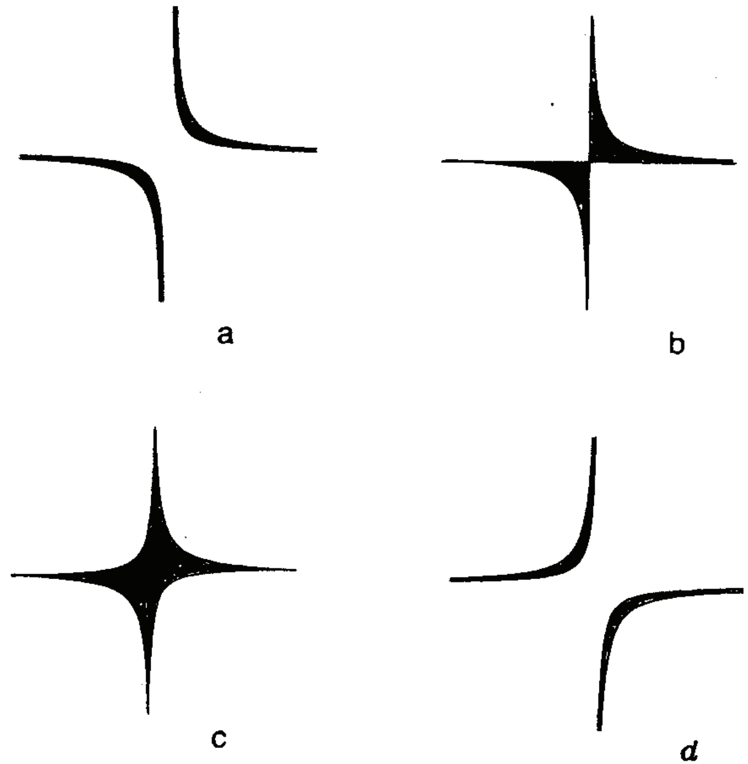

Письма в ЖЭТФ, том 59, вып.11, стр.798 - 802, ©1994 г. 10 июня

ON FERMI CONDENSATE: NEAR THE SADDLE POINT AND WITHIN THE VORTEX CORE

G.E. Volovik

van Hove singularity & room-T superconductivity

Conventional superconductivity at 203 K at high pressures

A.P. Drozdov[1]*, M. I. Eremets[1]*, I. A. Troyan[1], V. Ksenofontov[2], S. I. Shylin[2]

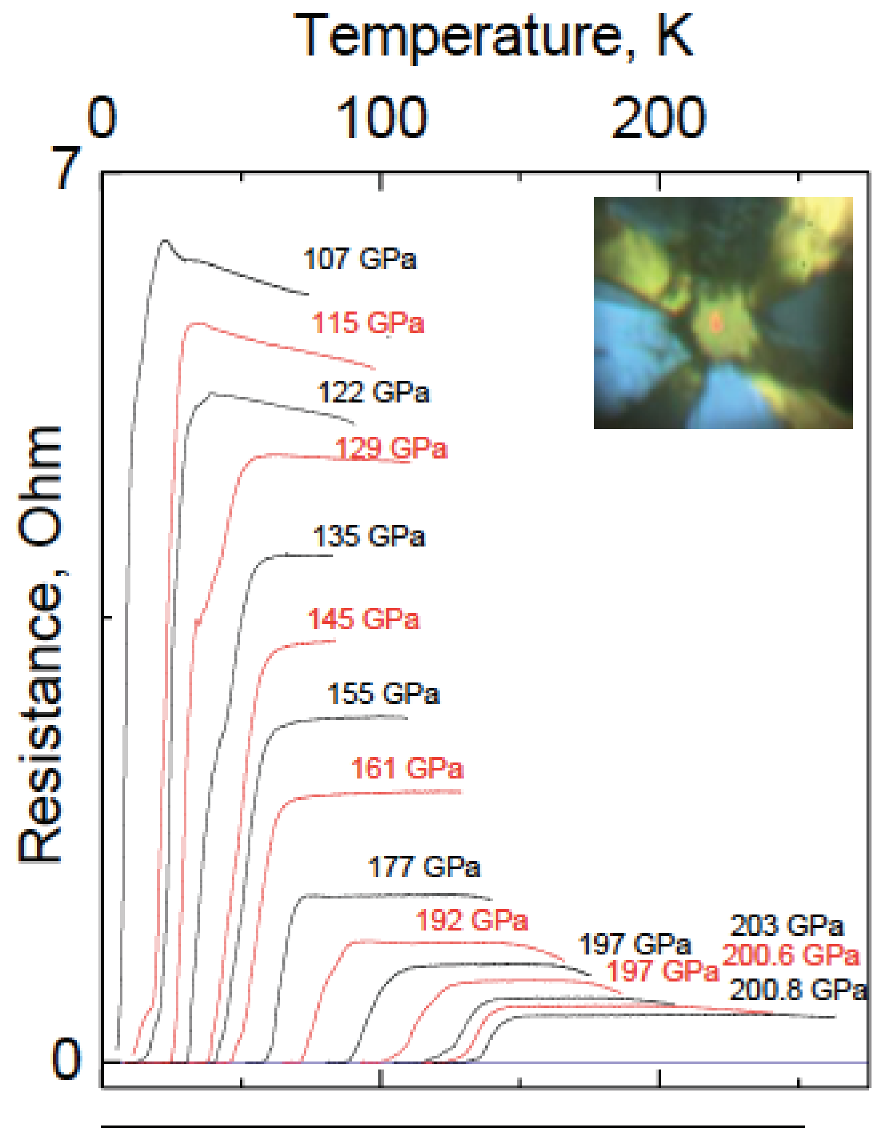

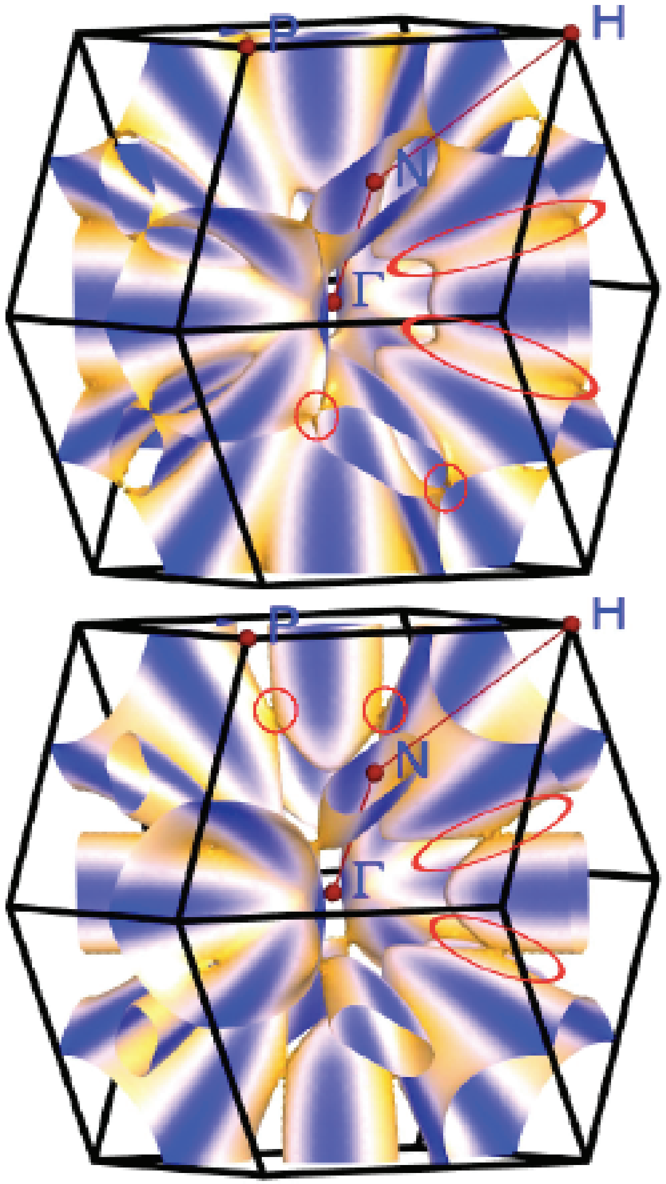

Impact of van Hove singularities in the strongly coupled high temperature superconductor H_3S

Yundi Quan and Warren E. Pickett*

3. Classes of Fermi points & nodal lines:

superfluid ^{3}He-A, Standard Model, semimetals, graphene, cuprate SC, ...
surface of ^{3}He-B & topological insulators

magnetic hedgehog

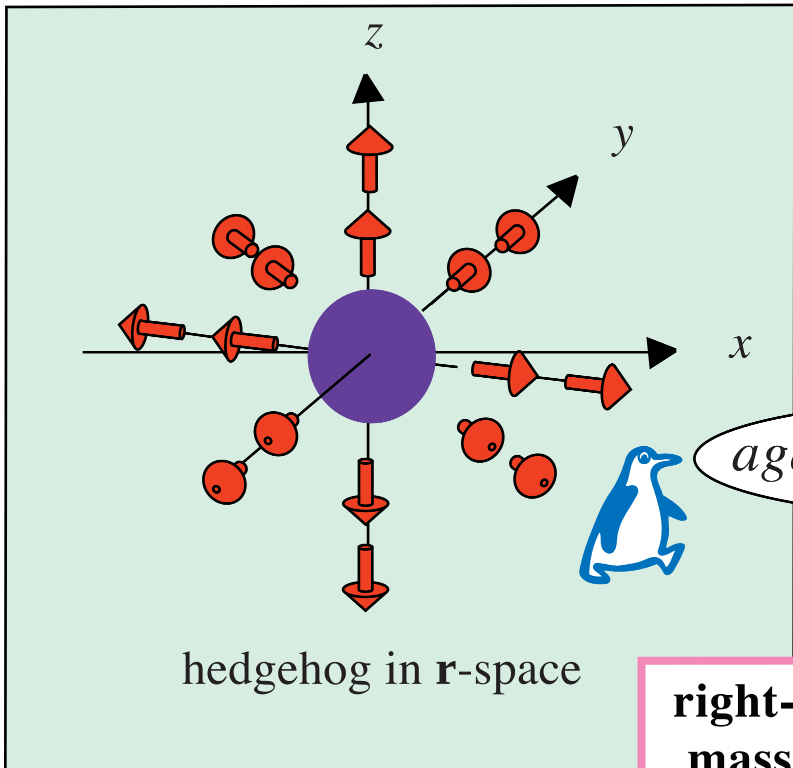

$\sigma(\mathbf{r})=\hat{\mathbf{r}}$

again no difference ?

Weyl point
or *Berry phase Dirac monopole*

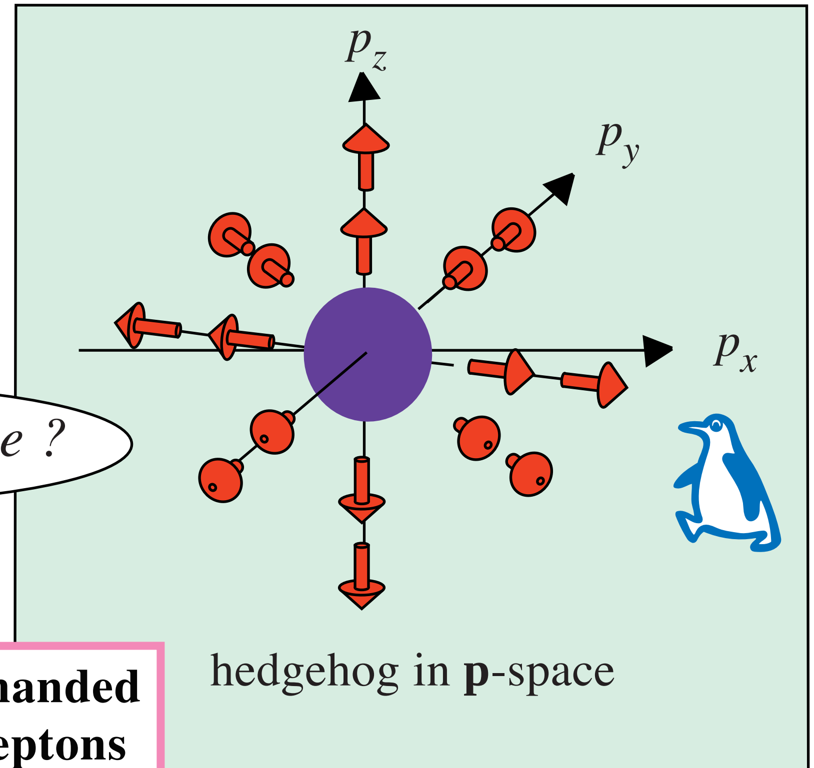

$\sigma(\mathbf{p}) = \hat{\mathbf{p}}$

right-handed and left-handed massless quarks and leptons are elementary particles in Standard Model

Landau CP symmetry is emergent

close to Fermi point

$$H = + c\, \sigma \cdot \mathbf{p}$$

right-handed Weyl electron =
hedgehog in **p**-space with spines = spins

Weyl point is the exceptional point of level crossing in the space of 3 parameters
now these parameters are p_x , p_y , p_z

von Neumann and Wigner, 1929

- In QMs, 3 parameters must be tuned to make 2 levels cross

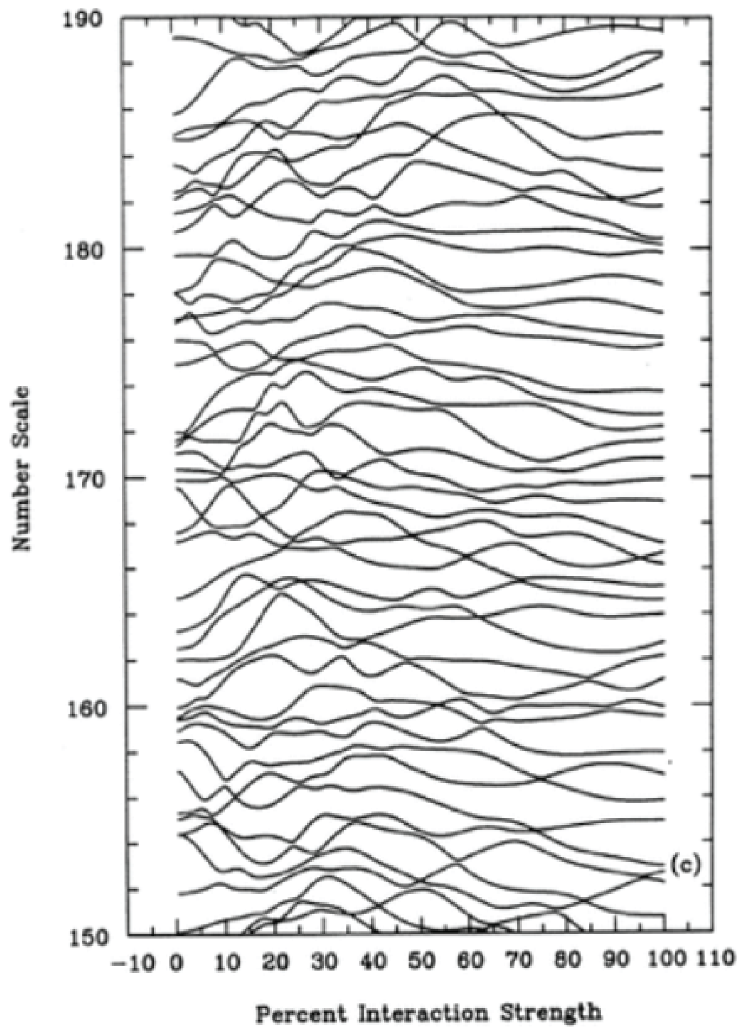

avoided crossing of energy levels & Weyl point

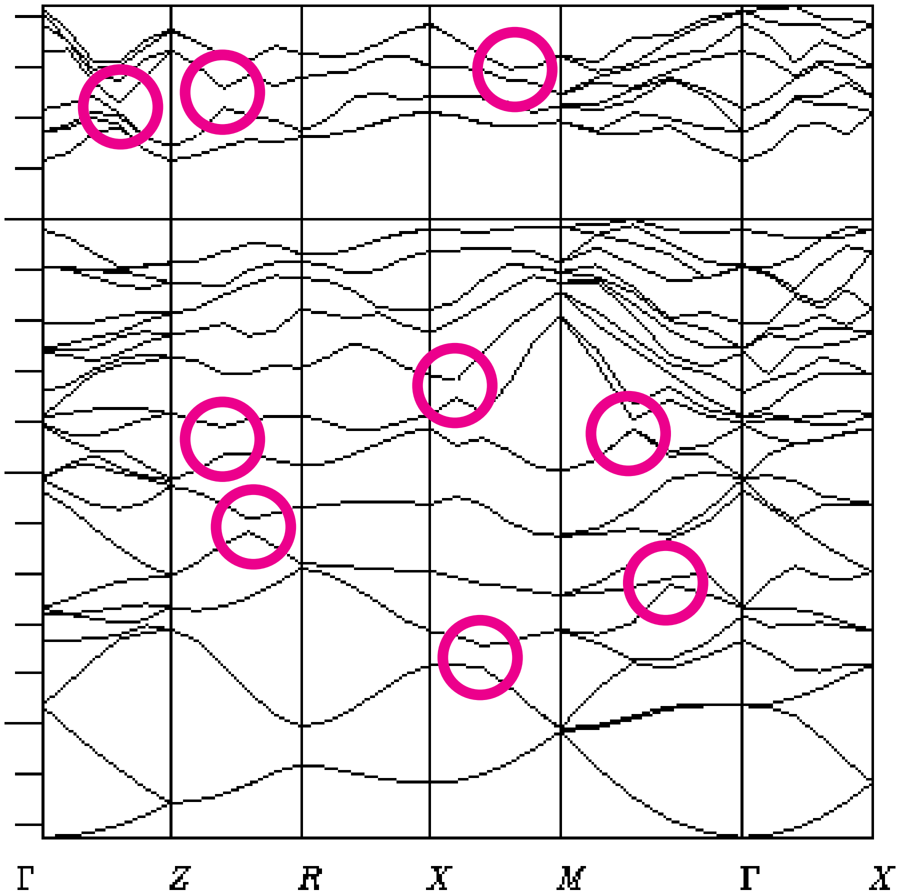

two-level effective Hamiltonian
is enough to describe the crossing of energy levels

$$H = E_0 + \begin{pmatrix} g_3(\mathbf{p}) & g_1(\mathbf{p}) + i\, g_2(\mathbf{p}) \\ g_1(\mathbf{p}) - i\, g_2(\mathbf{p}) & -g_3(\mathbf{p}) \end{pmatrix} = E_0 + \sigma \cdot \mathbf{g}(\mathbf{p})$$

σ are 3 Pauli matrices (emergent spin)

$$E_{\pm} = E_0 \pm \left(g_1{}^2 + g_2{}^2 + g_3{}^2\right)^{1/2}$$

for contact of two levels in general
3 parameters should be fitted

Weyl point: exceptional point of level contact in 3D momentum space p_x , p_y , p_x

Right-handed & left-handed particles

$$E^2 = c^2 p^2$$

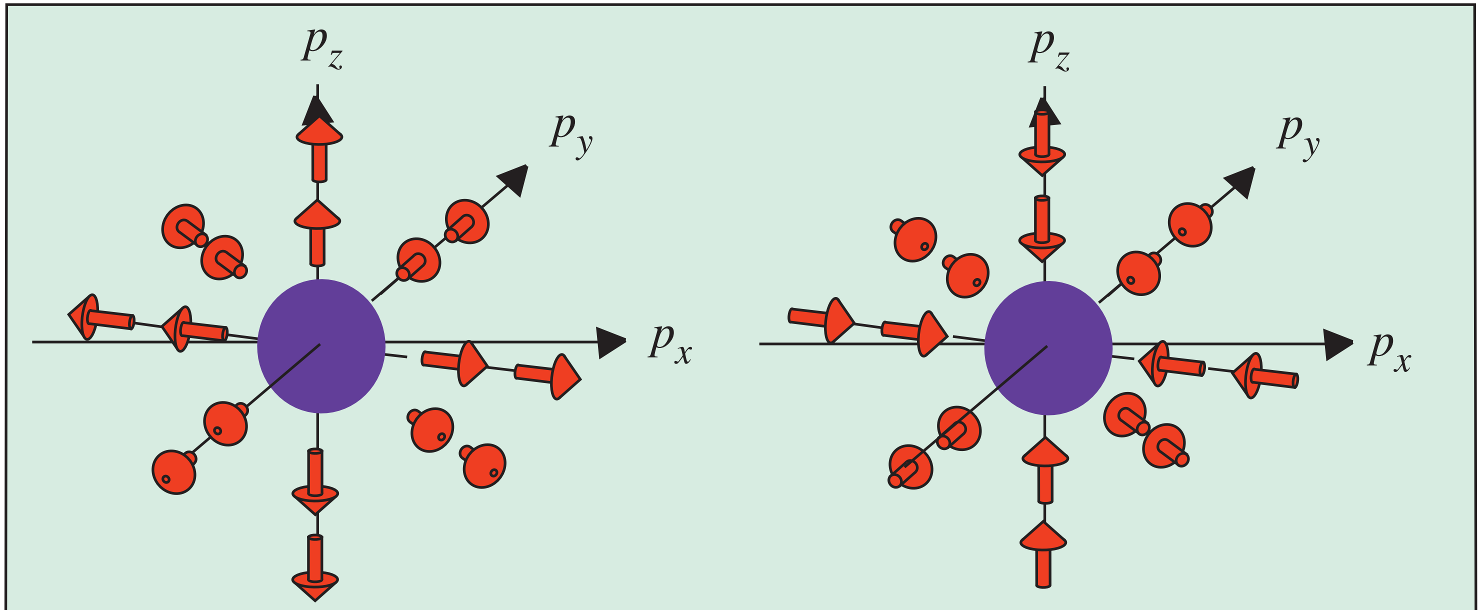

hedgehog with spines (spins) outward ($N_3 = +1$)

hedgehog with spines (spins) inward ($N_3 = -1$)

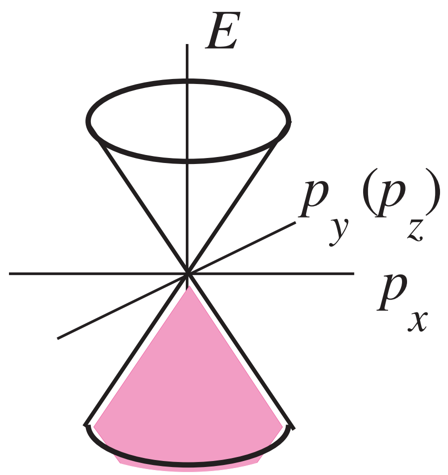

Weyl point: conical (diabolical) crossing point in fermionic spectrum in momentum space

right $H = +c\,\sigma \cdot \mathbf{p}$

$\mathbf{g}(\mathbf{p}) = +c\mathbf{p}$

$$\boxed{H = \sigma \cdot \mathbf{g}(\mathbf{p})}$$

$H = -c\,\sigma \cdot \mathbf{p}$ **left**

$\mathbf{g}(\mathbf{p}) = -c\mathbf{p}$

$$N = \frac{1}{8\pi}\, e^{ijk} \int dS_i\, \mathbf{g}\cdot(\nabla_{p_j}\mathbf{g} \times \nabla_{p_k}\mathbf{g})$$

over 2D surface S in 3D p-space

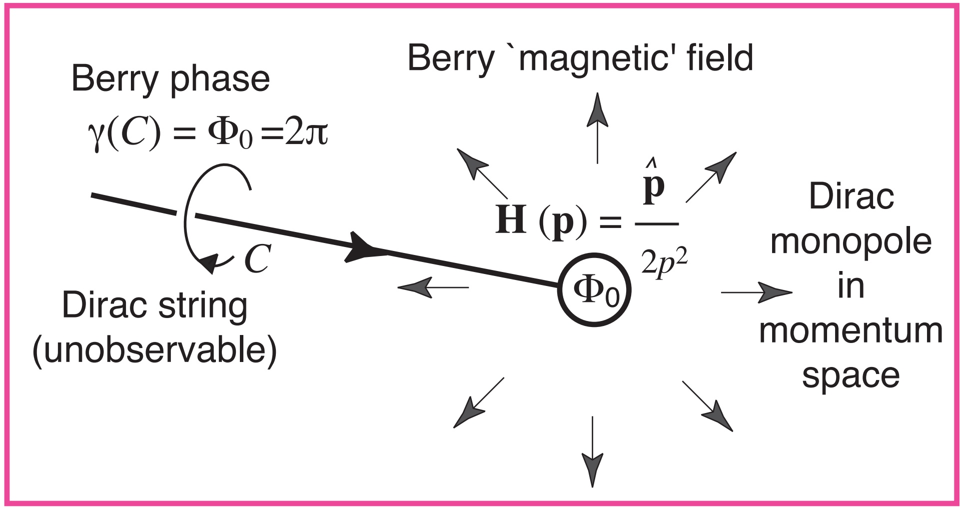

Chiral Weyl fermions in Standard Model

Family #1 of quarks and leptons

left particles

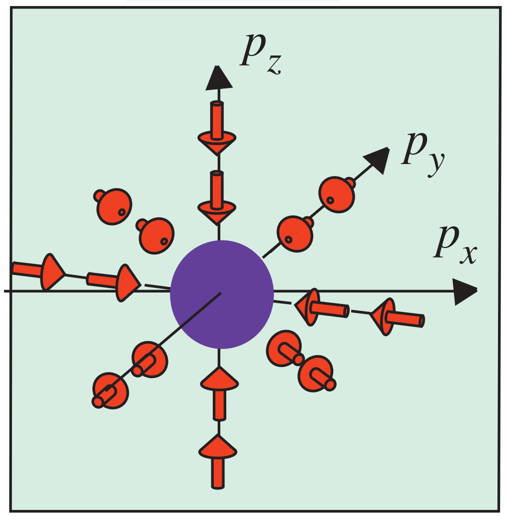

hedgehog with spines (spins) inward ($N_3 = -1$)

quarks

$SU(3)_C$

+2/3 u_L +1/6	-1/3 d_L +1/6
+2/3 u_L +1/6	-1/3 d_L +1/6
+2/3 u_L +1/6	-1/3 d_L +1/6

$SU(2)_L$

+2/3 u_R +2/3		-1/3 d_R -1/3	
+2/3 u_R +2/3		-1/3 d_R -1/3	
+2/3 u_R +2/3		-1/3 d_R -1/3	

leptons

0 ν_L -1/2	-1 e_L -1/2

0 ν_R 0	-1 e_R -1

$$H = -\, c\, \sigma \cdot \mathbf{p}$$
$$N_3 = -1$$

$$H = +\, c\, \sigma \cdot \mathbf{p}$$
$$N_3 = +1$$

right particles

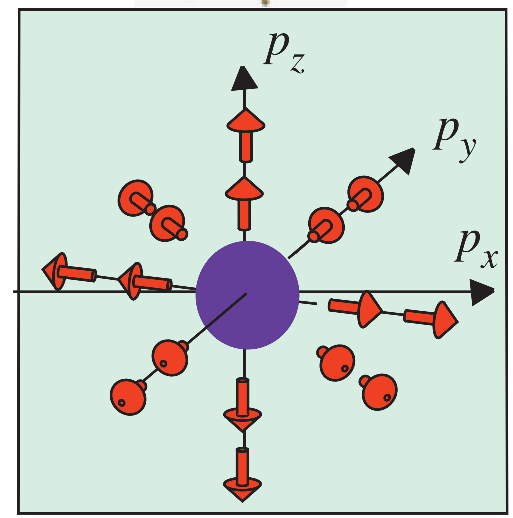

hedgehog with spines (spins) outward ($N_3 = +1$)

$$N_3 = \frac{1}{24\pi^2}\, e_{\mu\nu\lambda\gamma}\, \mathbf{tr} \int dS^\gamma\, \mathbf{G}^\mu\, \mathbf{G}^{-1}\, \mathbf{G}^\nu\, \mathbf{G}^{-1} \mathbf{G}^\lambda\, \mathbf{G}^{-1}$$

over 3D surface S in 4D momentum space

general topological invariant
in terms of Green's function
for interacting systems

From massless Weyl particles to massive Dirac particles

where are massive Dirac particles?

Dirac particle - composite object: mixture of left and right Weyl particles

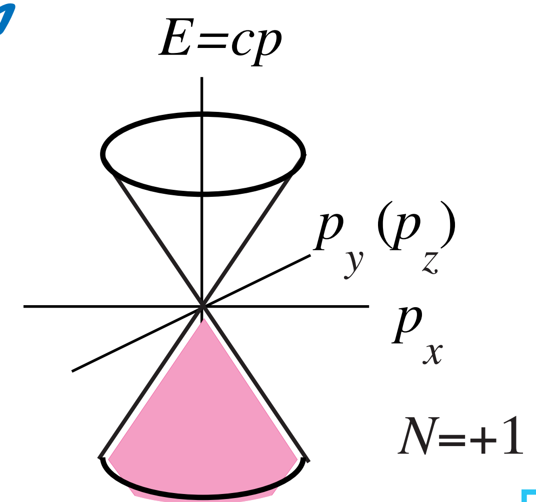

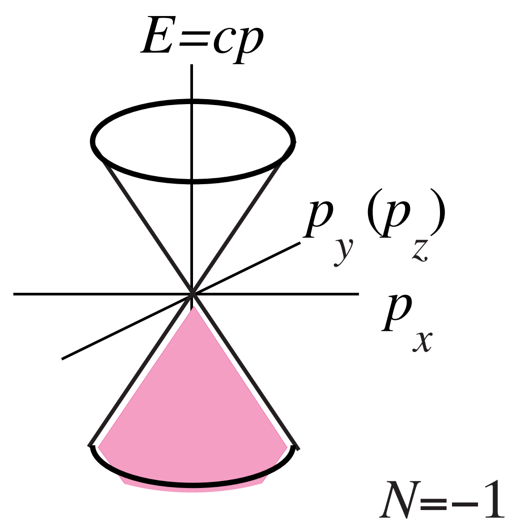

$T_{\mathrm{ew}} \sim 1$ TeV$\sim 10^{16}$K

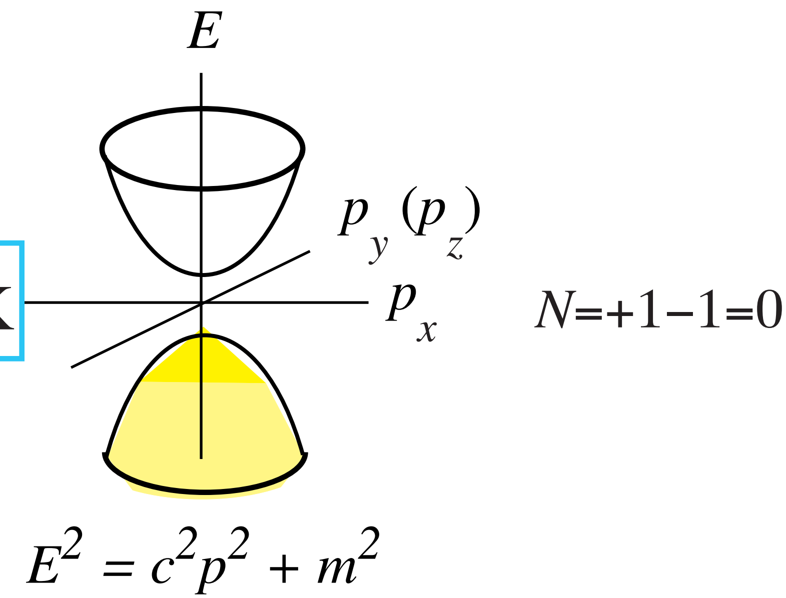

is Dirac vacuum topologically trivial ?

fully gapped vacua can be also topologically nontrivial (3He-B, topological insulators, ...)

Weyl fermions in 3+1 gapless topological cond-mat

topologically protected Weyl points in:

topological semi-metal or Weyl metals (Abrikosov-Beneslavskii 1971), ^{3}He-A (1982), triplet Fermi gases, $CoSb_3$ (arXiv:1204.5905)

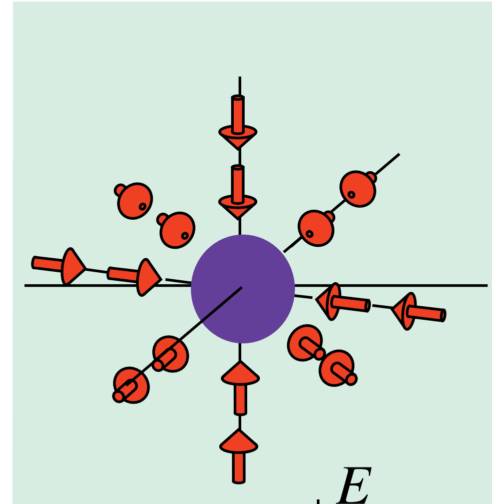

$$N_3 = \frac{1}{8\pi} e_{ijk} \int dS^k \; \hat{\mathbf{g}} \cdot \left(\nabla_{p_i} \hat{\mathbf{g}} \times \nabla_{p_j} \hat{\mathbf{g}}\right)$$

over 2D surface S in 3D p-space

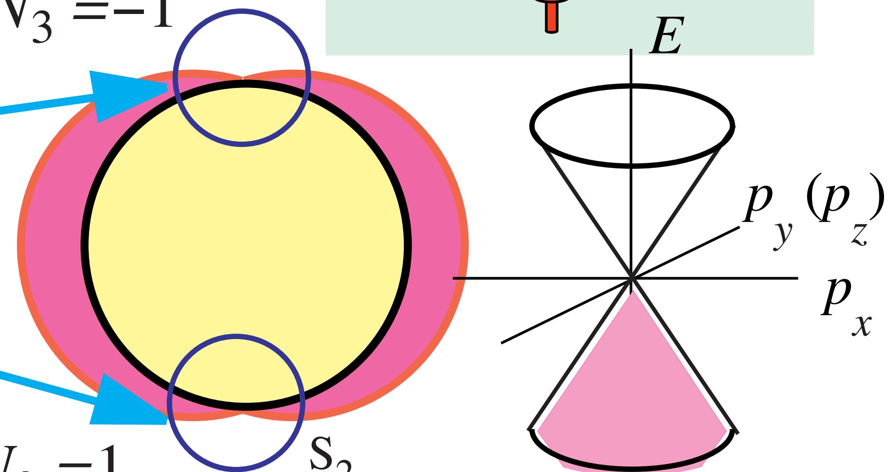

$$p^2 = p_x^{\,2} + p_y^{\,2} + p_z^{\,2}$$

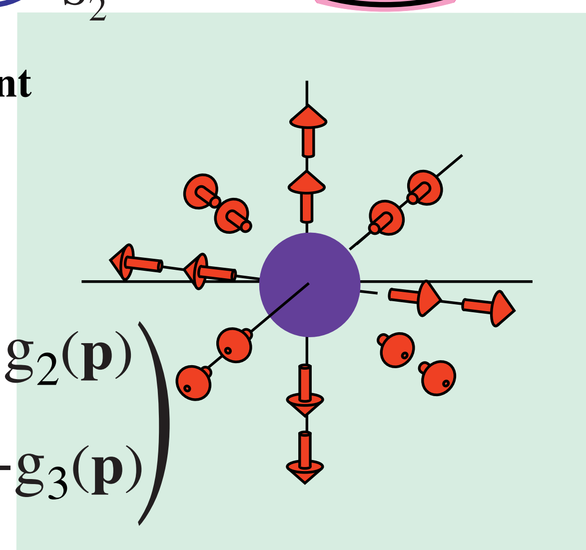

$$H = \begin{pmatrix} \frac{p^2}{2m} - \mu & c(p_x + ip_y) \\ c(p_x - ip_y) & -\frac{p^2}{2m} + \mu \end{pmatrix} = \begin{pmatrix} g_3(\mathbf{p}) & g_1(\mathbf{p}) + i\, g_2(\mathbf{p}) \\ g_1(\mathbf{p}) - i\, g_2(\mathbf{p}) & -g_3(\mathbf{p}) \end{pmatrix}$$

emergence of relativistic chiral Weyl fermions near Fermi points

original non-relativistic Hamiltonian

$$H = \begin{pmatrix} \frac{p^2}{2m} - \mu & c(p_x + ip_y) \\ c(p_x - ip_y) & -\frac{p^2}{2m} + \mu \end{pmatrix} = \begin{pmatrix} g_3(\mathbf{p}) & g_1(\mathbf{p}) + i\, g_2(\mathbf{p}) \\ g_1(\mathbf{p}) - i\, g_2(\mathbf{p}) & -g_3(\mathbf{p}) \end{pmatrix} = \boldsymbol{\tau} \cdot \mathbf{g}(\mathbf{p})$$

close to nodes, i.e. in low-energy corner
relativistic chiral fermions emerge

$$H = N_3\, c\, \boldsymbol{\tau} \cdot (\mathbf{p} - \mathbf{p}_0)$$

$$E = -c\tilde{p}$$

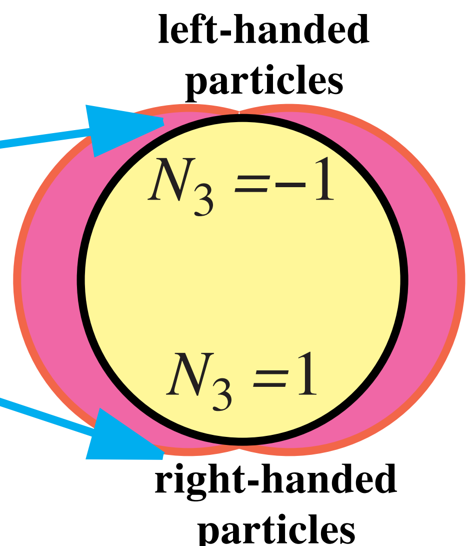

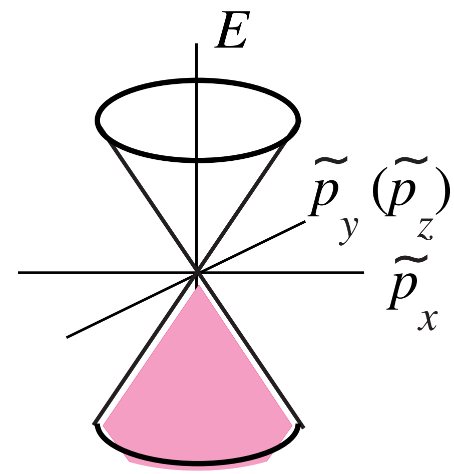

chirality is emergent ??

what else is emergent ?

top. invariant determines chirality in low-energy corner

relativistic invariance as well

bosonic collective modes in two generic fermionic vacua

Landau theory of Fermi liquid

collective Bose modes of fermionic vacuum:
propagating
oscillation of **shape**
of Fermi surface

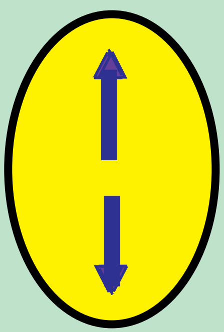

Landau, ZhETF **32**, 59 (1957)

Standard Model + gravity

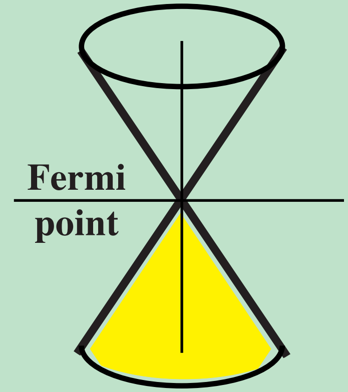

collective Bose modes:

propagating
oscillation of **position**
of Fermi point

$$\mathbf{p} \rightarrow \mathbf{p} - e\mathbf{A}$$

form effective dynamic
electromagnetic field

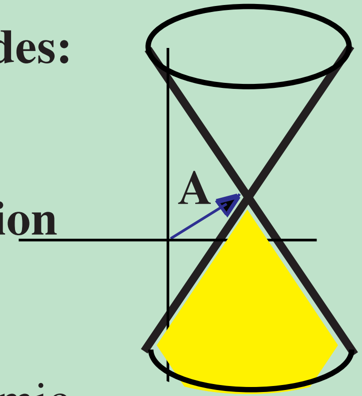

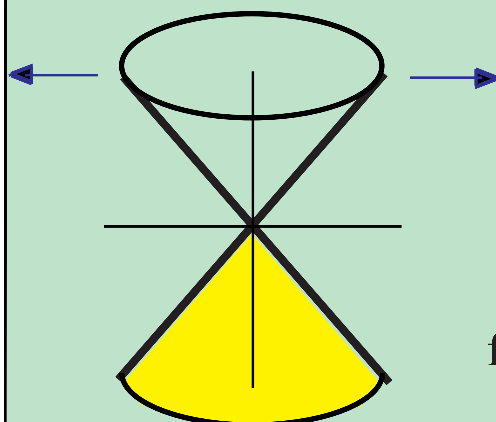

propagating
oscillation of **slopes**

$$E^2 = c^2p^2 \rightarrow g^{ik}p_i p_k$$

form effective dynamic
gravity field

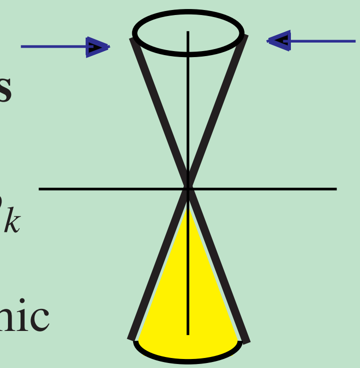

two generic quantum field theories of interacting bosonic & fermionic fields

relativistic quantum fields & gravity emerging near Weyl point

Atiyah-Bott-Shapiro construction:
linear expansion of Hamiltonian near the nodes in terms of Dirac Γ-matrices

primary object:
tetrad
$e_a^{\ \mu}$

$$\boxed{E = v_F\,(p - p_F)}$$

emergent relativity

$$\boxed{H = e_a^{\ k}\,\Gamma^a \cdot (p_k - p_k^0)}$$

linear expansion near Fermi surface

linear expansion near Weyl point

secondary object:
metric

$$g^{\mu\nu} = \eta^{ab}\, e_a^{\ \mu}\, e_b^{\ \nu}$$

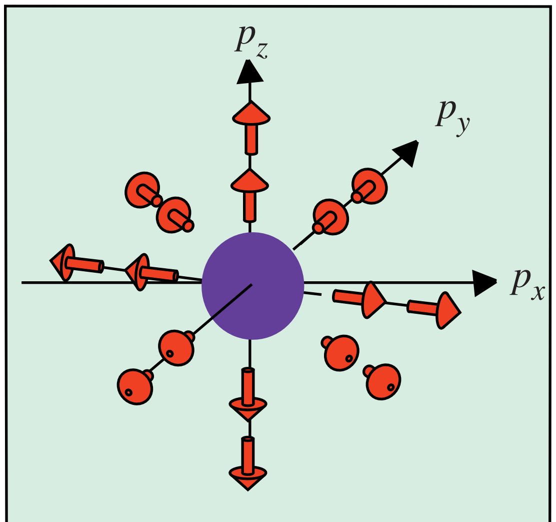

hedgehog in **p**-space

$$\boxed{g^{\mu\nu}(p_\mu - eA_\mu - e\tau\cdot\mathbf{W}_\mu)(p_\nu - eA_\nu - e\tau\cdot\mathbf{W}_\nu) = 0}$$

effective metric:
emergent gravity

effective
electromagnetic
field

effective
$SU(2)$ gauge
field

effective
electric charge
$e = +1$ or -1

effective
isotopic spin

all ingredients of Standard Model :
chiral fermions & gauge fields
emerge in low-energy corner
together with spin, Dirac Γ−matrices,
gravity & physical laws:
Lorentz & gauge invariance,
equivalence principle, etc

gravity & gauge fields
are collective modes
of vacua with Weyl point

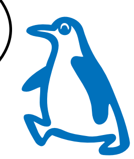

Einstein-Cartan-Sciama-Kibble theory
with tetrads, spin connection & torsion

crossover from Landau 2-fluid hydrodynamics to Einstein general relativity

they represent two different limits of hydrodynamic type equations

equations for $g^{\mu\nu}$ depend on hierarchy of ultraviolet cut-off's:
Planck energy scale E_{Planck} vs Lorentz violating scale E_{Lorentz}

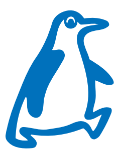

$E_{\text{Planck}} >> E_{\text{Lorentz}}$

emergent Landau two-fluid hydrodynamics

$E_{\text{Planck}} << E_{\text{Lorentz}}$

emergent general covariance & general relativity

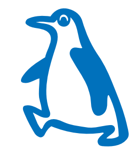

^{3}He-A with Fermi point

$E_{\text{Lorentz}} << E_{\text{Planck}}$

$E_{\text{Lorentz}} \sim 10^{-3}\, E_{\text{Planck}}$

Universe

$E_{\text{Lorentz}} >> E_{\text{Planck}}$

$E_{\text{Lorentz}} > 10^{9}\, E_{\text{Planck}}$

type II Weyl fermions in semimetals

GV & Zubkov
Emergent Weyl spinors in multi-fermion systems
NPB **881**, 514 (2014)

$$H = c\,\sigma\cdot\mathbf{p} - v p_z$$

$v > c$ $v = c$ $v < c$

Soluyanov et al.
Type-II Weyl semimetals
Nature **527**, 495 (2015)

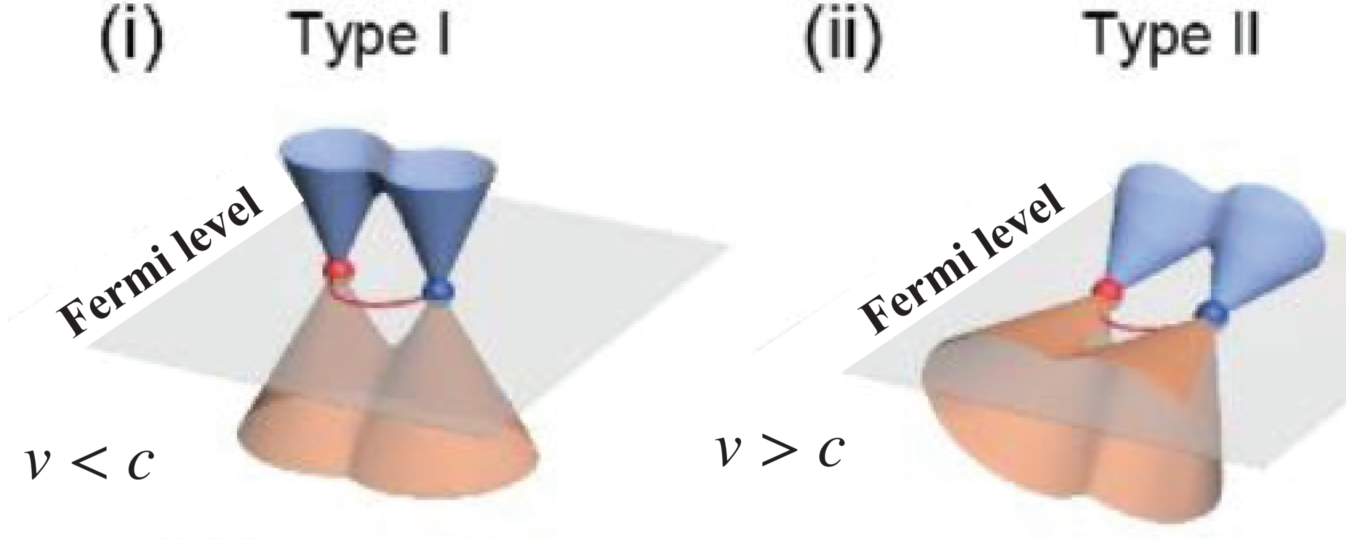

Fermi surface

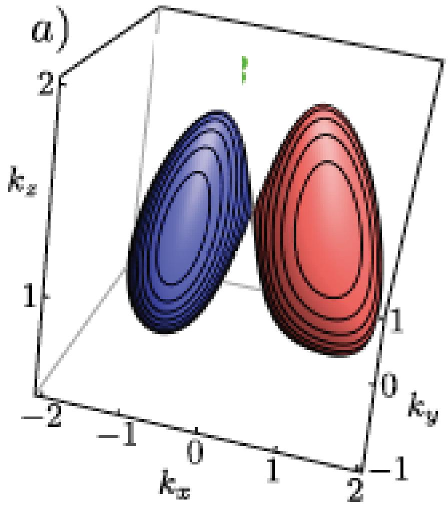

type II Weyl fermions behind event horizon

$$H = c\,\sigma\cdot\mathbf{p} - v(r)p_r$$

$v(r)$ velocity of free-falling observer

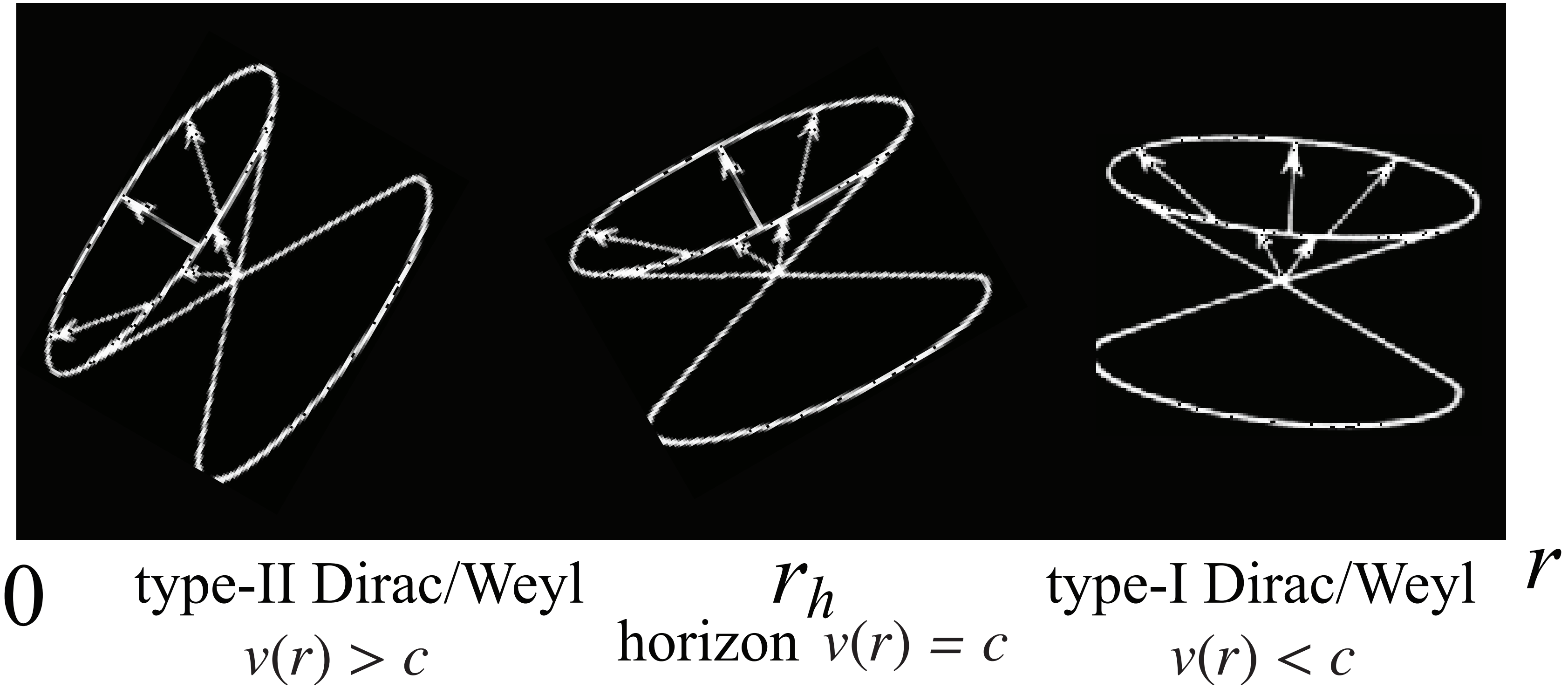

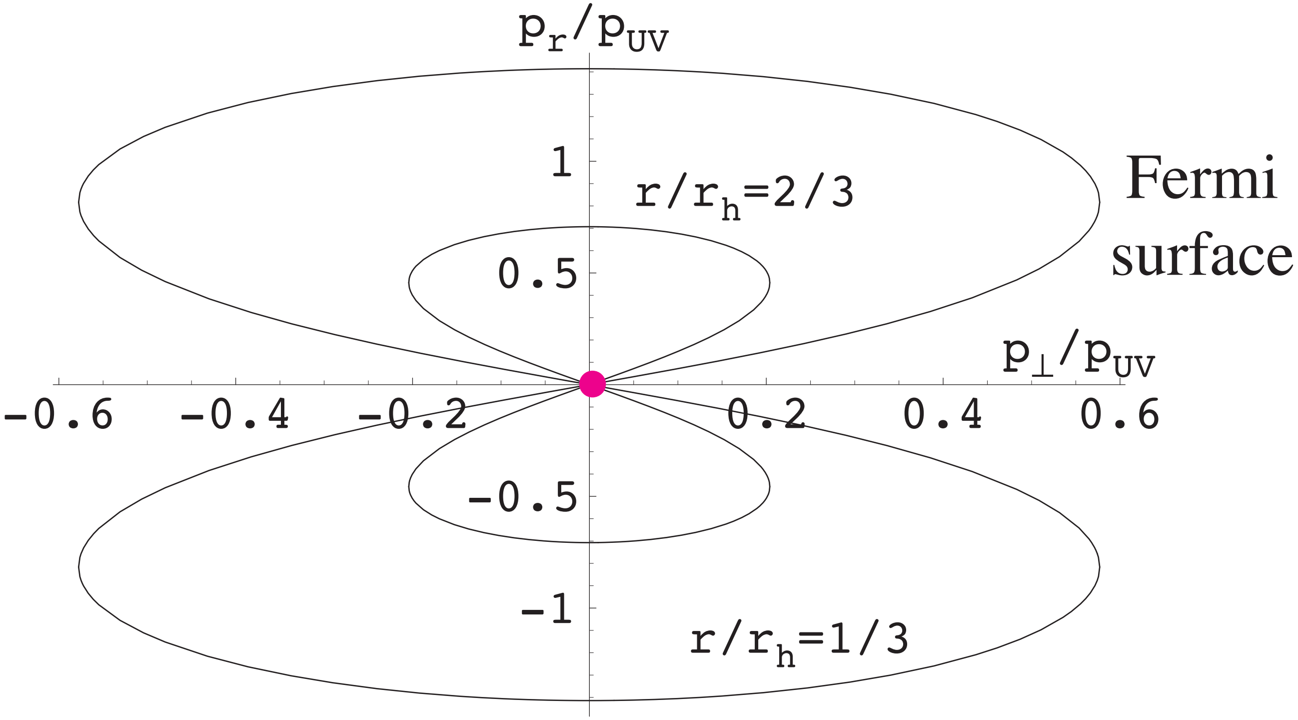

Huhtala & GV
Fermionic microstates within Painleve-Gullstrand black hole
JETP **94**, 853 (2002)

Weyl particles in magnetic field

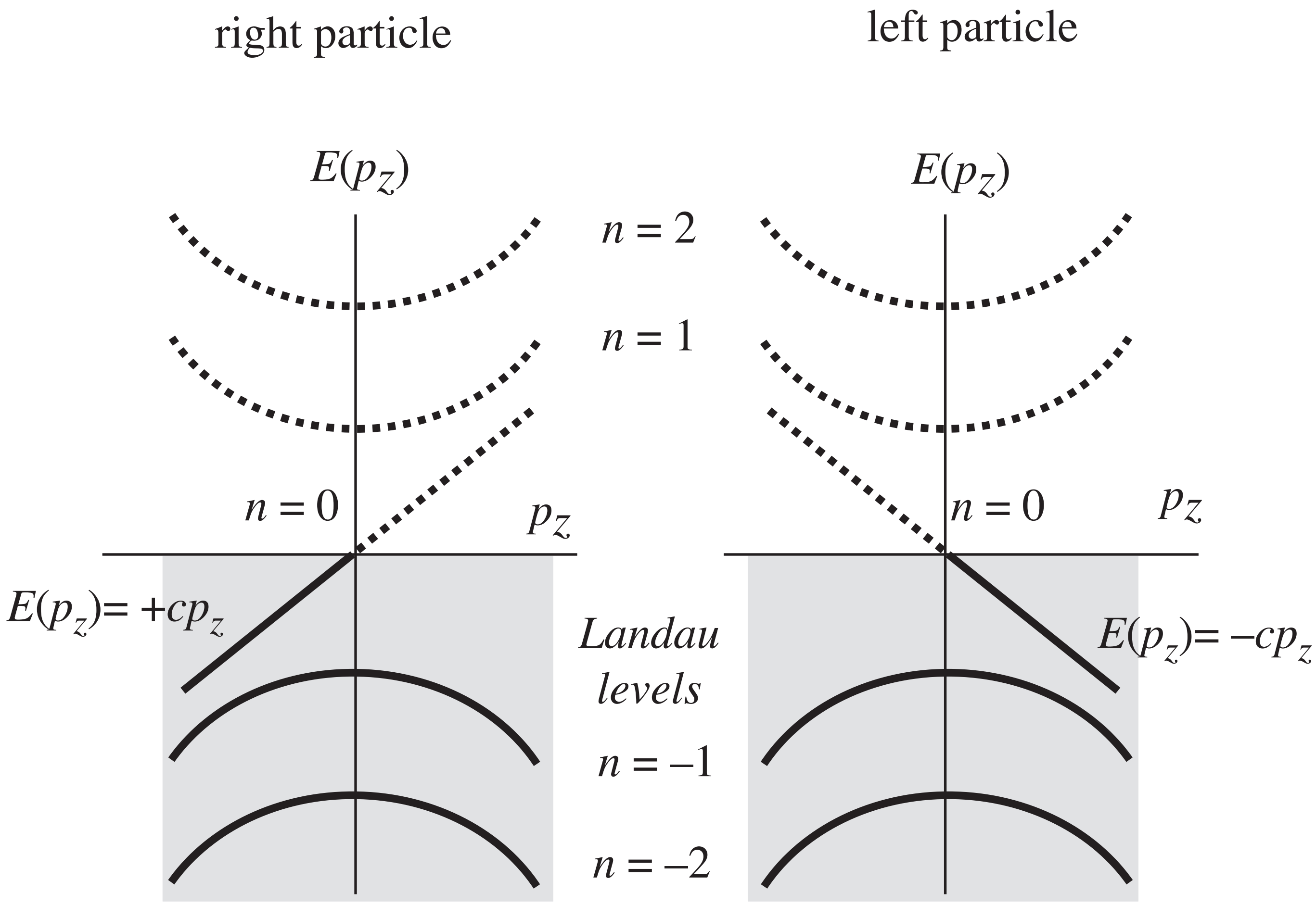

Asymmetric branches
on n=0 Landau level
cross zero energy

Chiral anomaly: spectral flow of left and right particles from vacuum in electric field

Newton law $\dot{p}_z = qE_z$

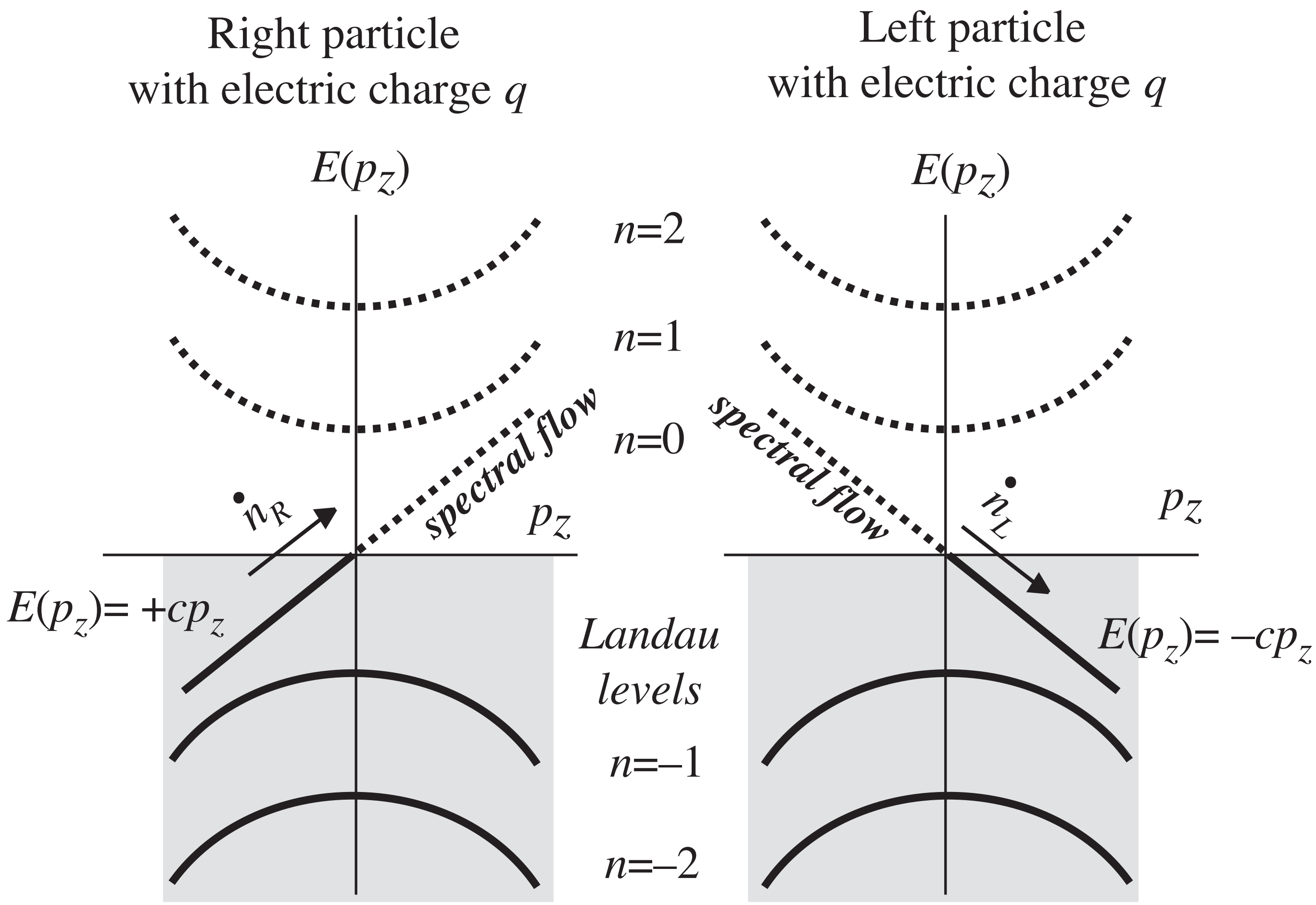

$$\dot{n}_R = -\dot{n}_L = \frac{1}{4\pi^2} q^2 \mathbf{B}_{\text{eff}}(\mathbf{r}, t) \cdot \mathbf{E}_{\text{eff}}(\mathbf{r}, t)$$

chiral anomaly in topological Weyl vacua: Standard Model & 3He-A

electroweak baryogenesis in Standard Model of particle physics
baryon production from vacuum by hypermagnetic field in early Universe

chiral anomaly equation
(Adler, Bell, Jackiw)

$$\dot{B} = \frac{1}{4\pi^2} N_B\, \mathbf{B}_Y \cdot \mathbf{E}_Y$$

topological origin
of quantization of physical parameters

symmetry protected integer valued topological invariant

$$N_B = \frac{1}{24\pi^2} e_{\mu\nu\lambda}\, \mathbf{tr} \int_{\text{over } S^3} dV\, \mathbf{B}\mathbf{Y}^2\, \mathbf{G}\, \nabla^{\mu}\, \mathbf{G}^{-1}\, \mathbf{G} \nabla^{\nu}\, \mathbf{G}^{-1} \mathbf{G} \nabla^{\lambda}\, \mathbf{G}^{-1}$$

matrix of baryonic charge **matrix of hypecharge**

$$\dot{B} = \frac{1}{4\pi^2} \mathbf{B}_Y \cdot \mathbf{E}_Y \sum_a B_a N_a Y_a^2$$

B_a -- **baryonic charge**
Y_a -- **hypercharge**
N_a -- **chirality** $= +1$ **for right**
-1 **for left**

triangle
Feynman diagram

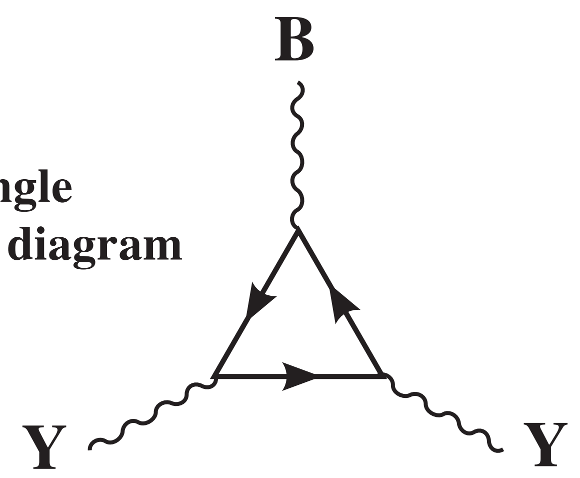

experimental verification of chiral anomaly equation

measurement of *Kopnin force*

$$\mathbf{A} = p_F \mathbf{l} \qquad \mathbf{B} = p_F \nabla \times \boldsymbol{l}$$

$$\mathbf{E} = p_F \dot{\boldsymbol{l}} \qquad \mathrm{B}_a = \mathbf{P}_a$$

translation from SM to language of 3He-A

momentum from vacuum of fermion zero modes

baryogenesis in early Universe

$$\dot{\mathbf{P}} = \sum \mathbf{P}_a \dot{n}_a$$

$$\dot{\mathrm{B}} = \sum \mathrm{B}_a \dot{n}_a$$

$\mathbf{P}_a$ -- momentum of Weyl point (fermionic charge)

e_a -- effective electric charge

B_a -- baryonic charge

Y_a -- hypercharge

$$\dot{\mathbf{P}} = (1/4\pi^2)\, \mathbf{B} \bullet \mathbf{E} \sum_a \mathbf{P}_a N_a q_a^2$$

applied to ³He-A

N_a = +1 for right
-1 for left

chiral anomaly equation (Adler, Bell, Jackiw)

$$\dot{\mathrm{B}} = (1/4\pi^2)\, \mathbf{B}_Y \bullet \mathbf{E}_Y \sum_a \mathrm{B}_a N_a \mathrm{Y}_a^2$$

applied to Standard Model

N_a = +1 for right
-1 for left

quasiparticles move from vacuum to the positive energy world, where they are scattered by quasiparticles in bulk and transfer momentum from vortex to normal component

this is the source of Kopnin spectral flow force

Bevan, Manninen, Cook, Hook, Hall, Vachaspati & GV
Momentum creation by vortices in superfluid 3He as a model of primordial baryogenesis, Nature **386**, 689 (1997)

observation of chiral anomaly in Manchester experiments

$$\mathbf{B}_{\rm eff} = p_F \nabla \times \hat{\mathbf{l}} \qquad \mathbf{E}_{\rm eff} = -p_F \partial_t \hat{\mathbf{l}} = p_F (\mathbf{v}_{\rm L} \cdot \nabla)\hat{\mathbf{l}}$$

$$\mathbf{F}_{\text{spectral flow}} = \frac{p_F^3}{2\pi^2} \int d^2x\, \hat{\mathbf{l}} \left((\nabla \times \hat{\mathbf{l}}) \cdot (\mathbf{v}_{\rm L} \cdot \nabla)\hat{\mathbf{l}} \right) = -\pi \mathcal{N} C_0 \hat{\mathbf{z}} \times \mathbf{v}_{\rm L}$$

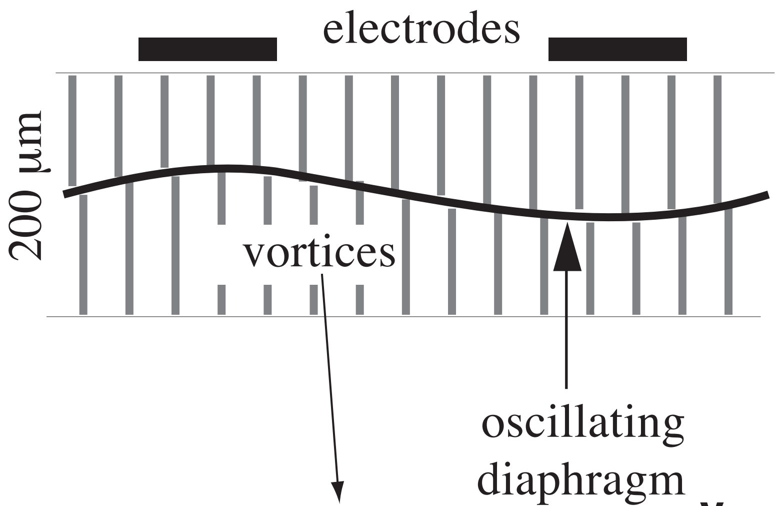

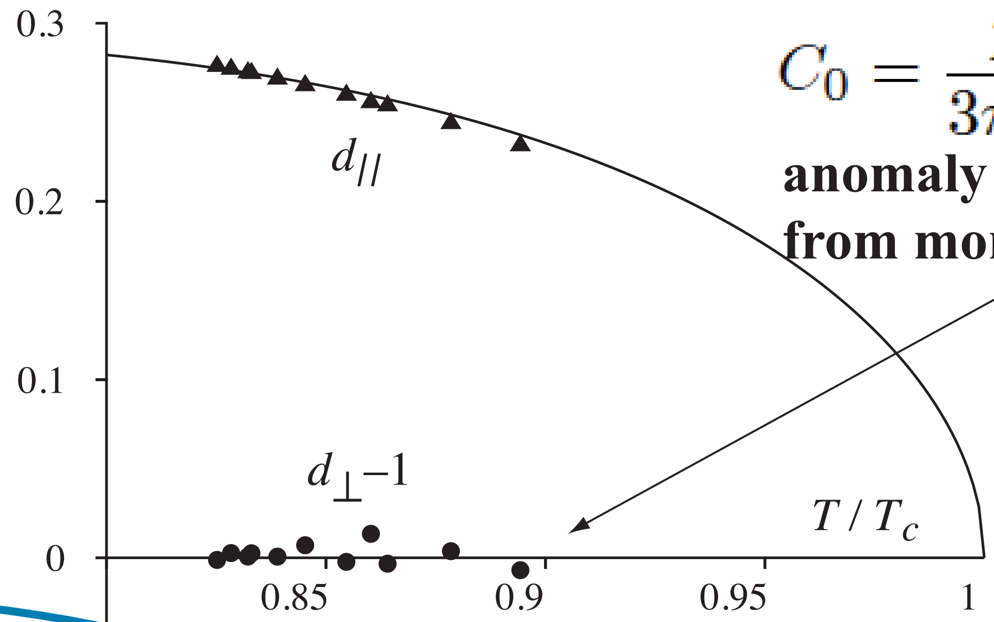

$$C_0 = \frac{p_F^3}{3\pi^2\hbar^2} \approx n$$

anomaly parameter from momentogenesis

l - field:

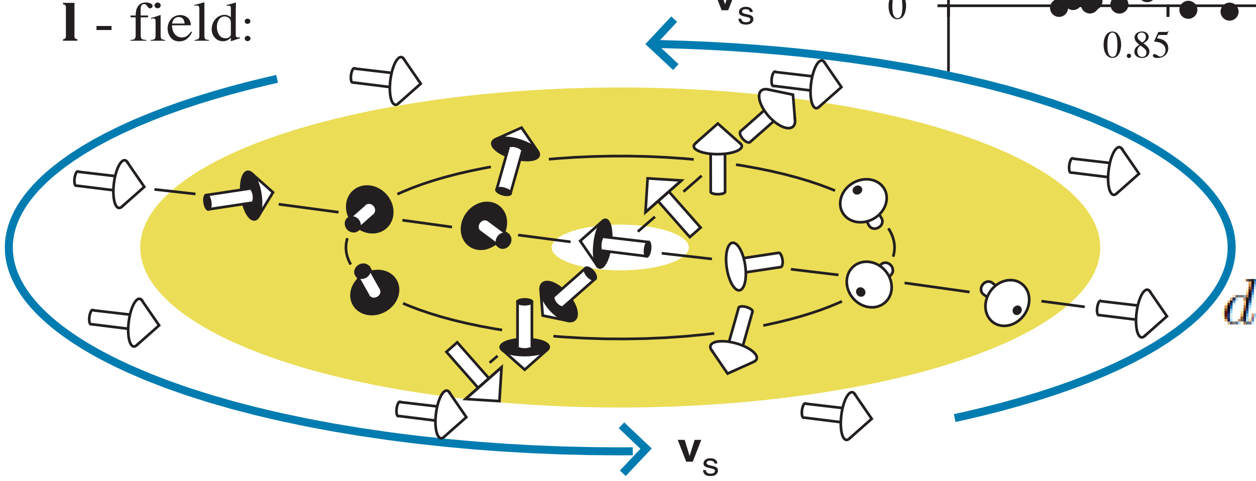

skyrmion

anomaly parameter

$$d_\perp = 1 - \frac{n - C_0}{n_{\rm s}(T)} \; , \quad d_\parallel = \frac{\gamma}{\pi n_1 n_{\rm s}(T)}$$

Symmetry protected invariants and chiral anomaly

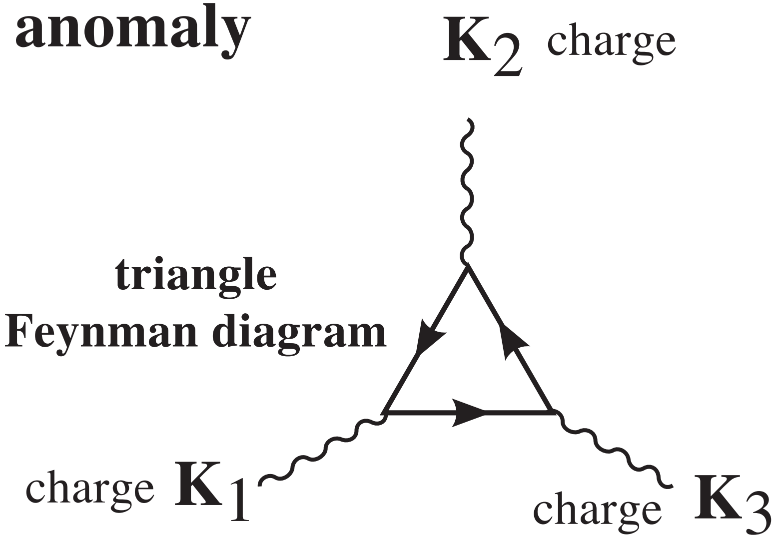

prefactors of $\boldsymbol{r}$-space topological terms
are $\boldsymbol{p}$-space topological invariant

chiral anomaly from 3+1 Weyl points

$$K_{123} = \frac{1}{24\pi^2}\, e_{\mu\nu\lambda}\, \mathbf{tr} \int_{\text{over } S^3} dV\; \mathbf{K}_1\mathbf{K}_2\mathbf{K}_3\; \mathbf{G}\,\nabla^{\mu}\,\mathbf{G}^{-1}\,\mathbf{G}\nabla^{\nu}\,\mathbf{G}^{-1}\mathbf{G}\,\nabla^{\lambda}\,\mathbf{G}^{-1}$$

chiral magnetic effect $\mathbf{K}_1 = \mu_a \qquad \mathbf{K}_2 = \mathbf{K}_3 = q_a$

chiral vortical effect $\mathbf{K}_1 = \mathbf{K}_2 = \mu_a \qquad \mathbf{K}_3 = q_a$

momentogenesis (Kopnin force) $\mathbf{K}_1 = \mathbf{K}_2 = q_a \qquad \mathbf{K}_3 = \boldsymbol{p}_a$

Chiral magnetic effect (CME): equilibrium current along magnetic field

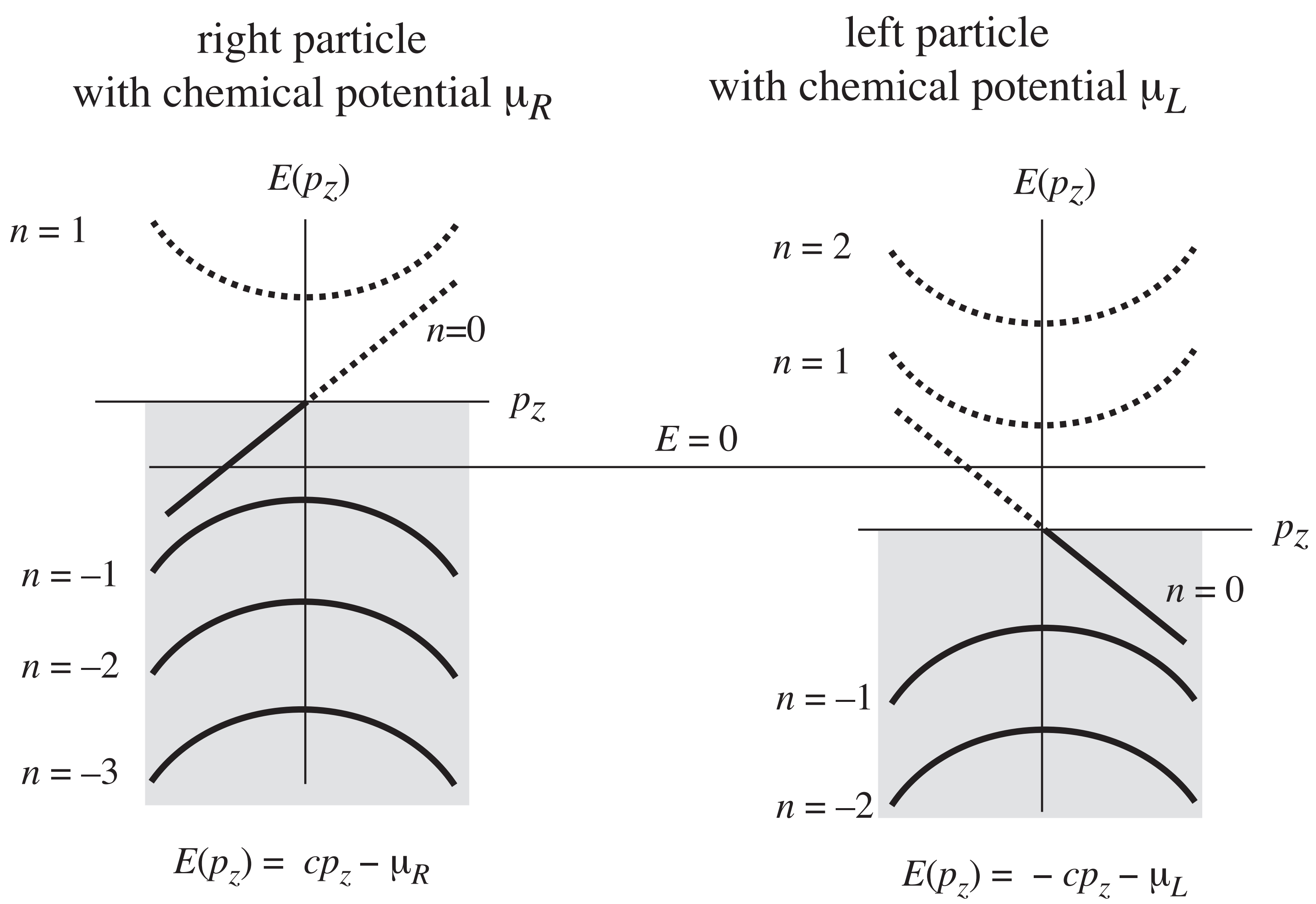

disbalance between chemical potentials of right μ_R and left μ_L particles leads to electric current along **B**

$$\boxed{\mathbf{J}_{\mathrm{CME}} = \frac{e\mu_5}{2\pi^2}\mathbf{B}}$$

$$\mu_5 = \mu_R - \mu_L$$

CVE (chiral vortical effect - current along rotation axis)

$$F_{\mathrm{CME}} = \frac{1}{8\pi^2}\int d^3x\,\mathbf{A}_{\mathrm{eff}}(\mathbf{r},t)\cdot\mathbf{B}_{\mathrm{eff}}(\mathbf{r},t)\sum_a \mu^{(a)} N_a q_a^2$$

$$F_{\mathrm{CVE}} = \frac{1}{8\pi^2}\int d^3x\,\mathbf{A}_{\mathrm{eff}}(\mathbf{r},t)\cdot\mathbf{B}_{g}(\mathbf{r},t)\sum_a (\mu^{(a)})^2 N_a q_a \qquad \mathbf{B}_g = 2\mathbf{\Omega}/c^2$$

N_a - chirality

q_a - (effective) electric charge

$\mathbf{B}_g$ - gravimagnetic field

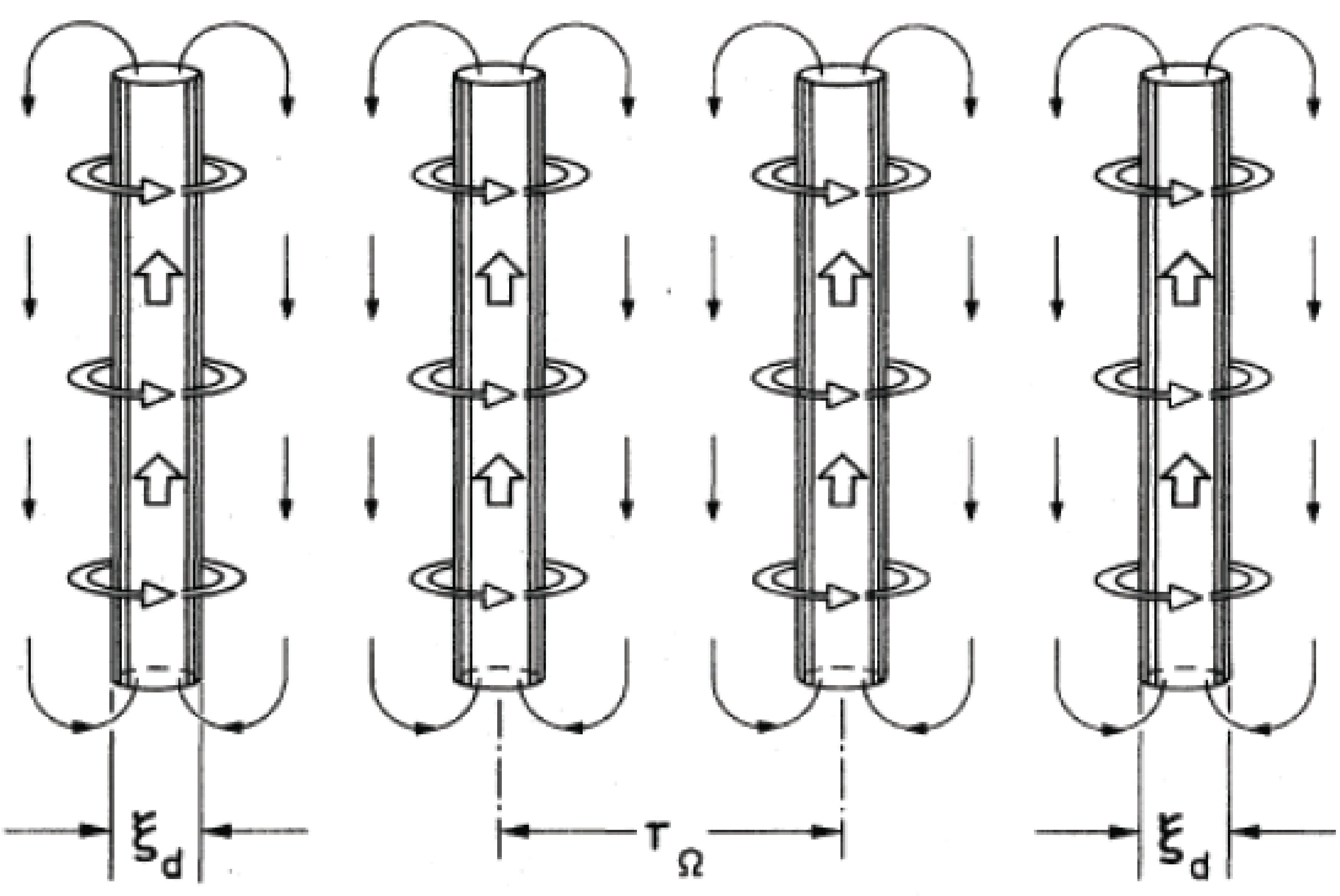

CVE in chiral superfluid 3He-A

p-space analogs of graphene

emergence of 2+1 gapless relativistic fermions in 2D graphene

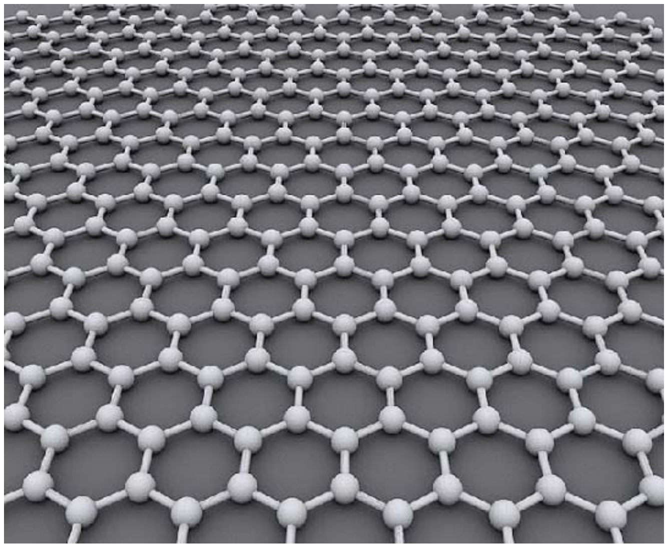

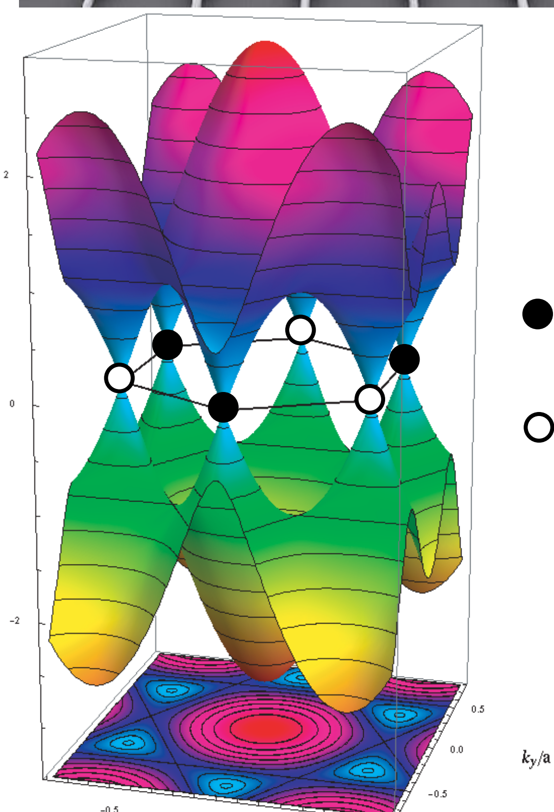

● Weyl/Dirac point $N = +1$

○ Weyl/Dirac point $N = -1$

p-space analog of
4D graphene in lattice QCD

Kaplan 1993, 2011, Creutz JHEP 04 (2008) 017

quantum vacuum as crystal

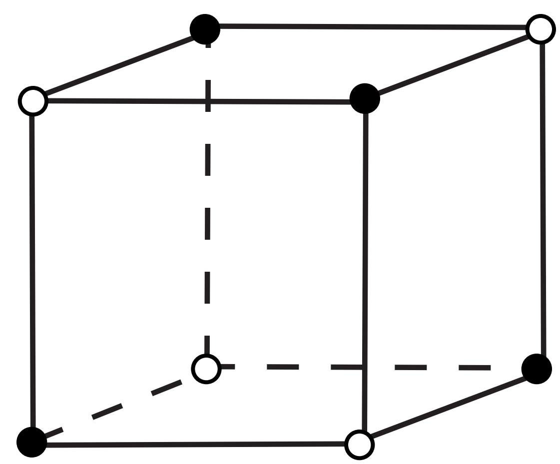

p-space analog of 3D graphene: superconductor α - phase

emergence of 2+1 relativistic fermions due to topology of graphene nodes

$$\boxed{N = \frac{1}{4\pi i}\,\mathbf{tr}\left[\mathbf{K}\oint dl\,\mathbf{H}^{-1}\nabla_l\,\mathbf{H}\right]}$$

$\mathbf{K}$ - symmetry operator,
commuting or anti-commuting with $\mathbf{H}$

close to nodes:

$$\mathbf{H}_{N=+1} = \tau_x p_x + \tau_y p_y$$

$$\mathbf{H}_{N=-1} = \tau_x p_x - \tau_y p_y$$

$$\mathbf{K} = \tau_z$$

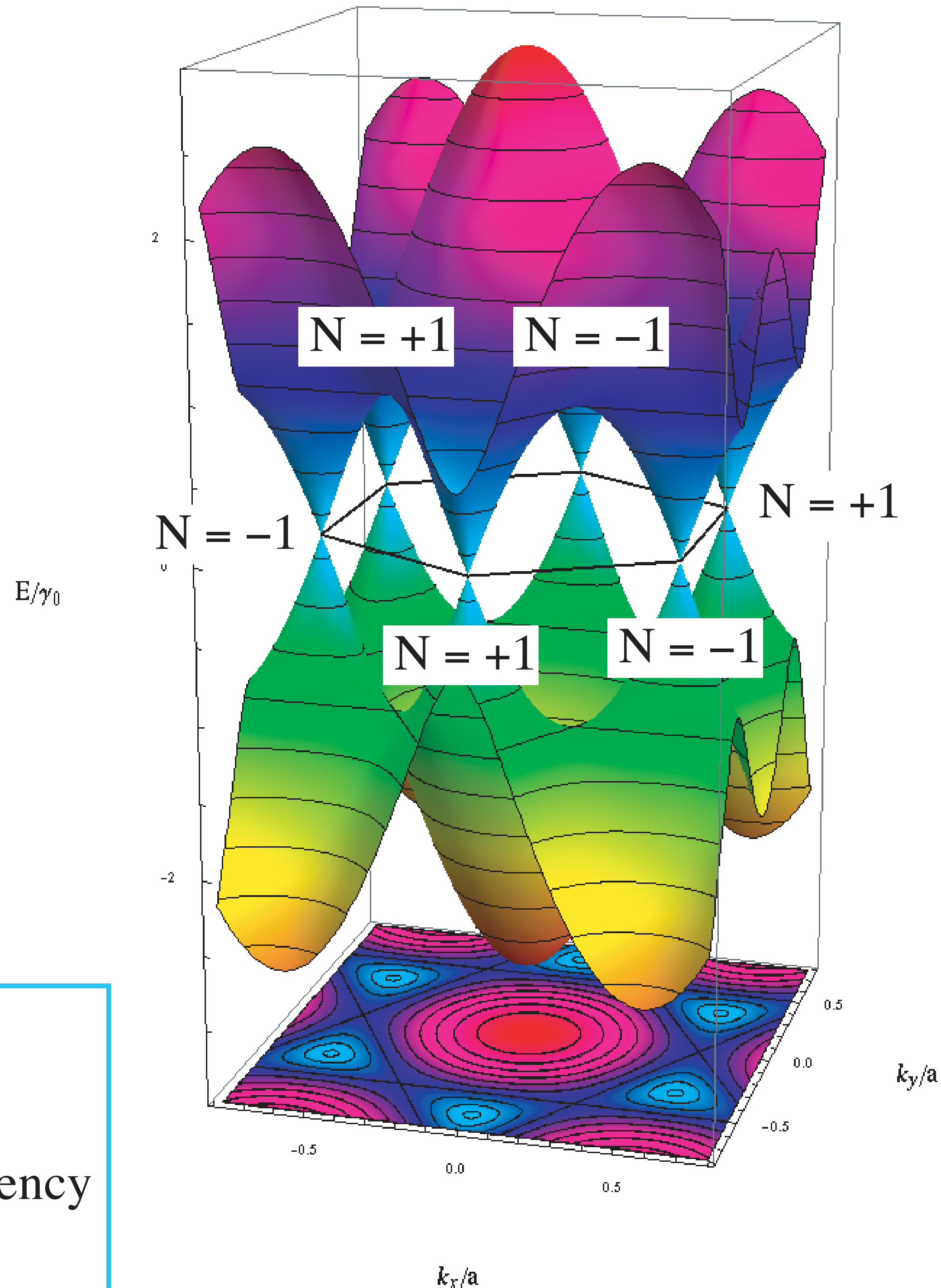

for real interacting systems
the Hamiltonian $\mathbf{H}(\mathbf{p})$ is substituted
by inverse Green's function at zero frequency
$\mathbf{G}^{-1}(\omega=0,\mathbf{p})$

SU(2) gauge fields emerging near Weyl & Dirac points

Atiyah-Bott-Shapiro construction:
linear expansion of Hamiltonian near the nodes in terms of Dirac Γ-matrices

$$\boxed{H = e_a^{\ k}\, \Gamma^a \cdot (p_k - eA_k - e\tau \cdot \mathbf{W}_k)}$$

effective tetrad: emergent gravity

effective electromagnetic field

effective isotopic spin

effective $SU(2)$ gauge field

$SU(2)$ gauge field is collective mode of vacuum with Weyl point

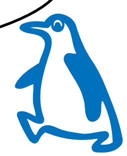

isotopic spin comes from spin or from band indices

SU(2) field near Dirac points in graphene

$$\mathbf{H}_{N=+1} = \tau_x(p_x - A_x - \sigma \cdot \mathbf{W}_x) + \tau_y(p_y - A_y - \sigma \cdot \mathbf{W}_y)$$

Summation of topological charges in action

exotic fermions:
massless fermions with quardatic,
cubic & quartic dispersion
semi-Dirac fermions

$$\boxed{N = \frac{1}{4\pi i}\,\mathbf{tr}\,\left[\mathbf{K}\oint dl\,\mathbf{H}^{-1}\nabla_l\,\mathbf{H}\right]}$$

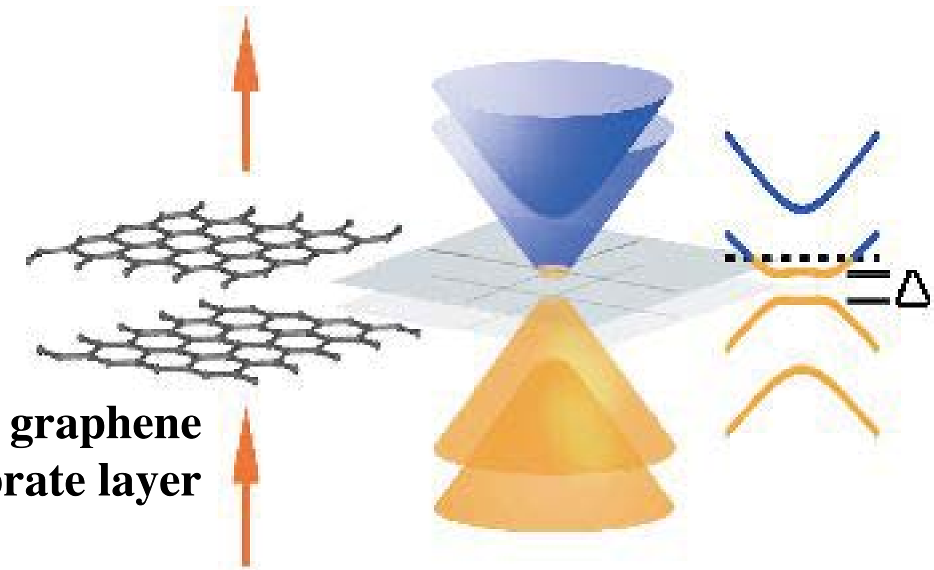

bilayer graphene
double cuprate layer

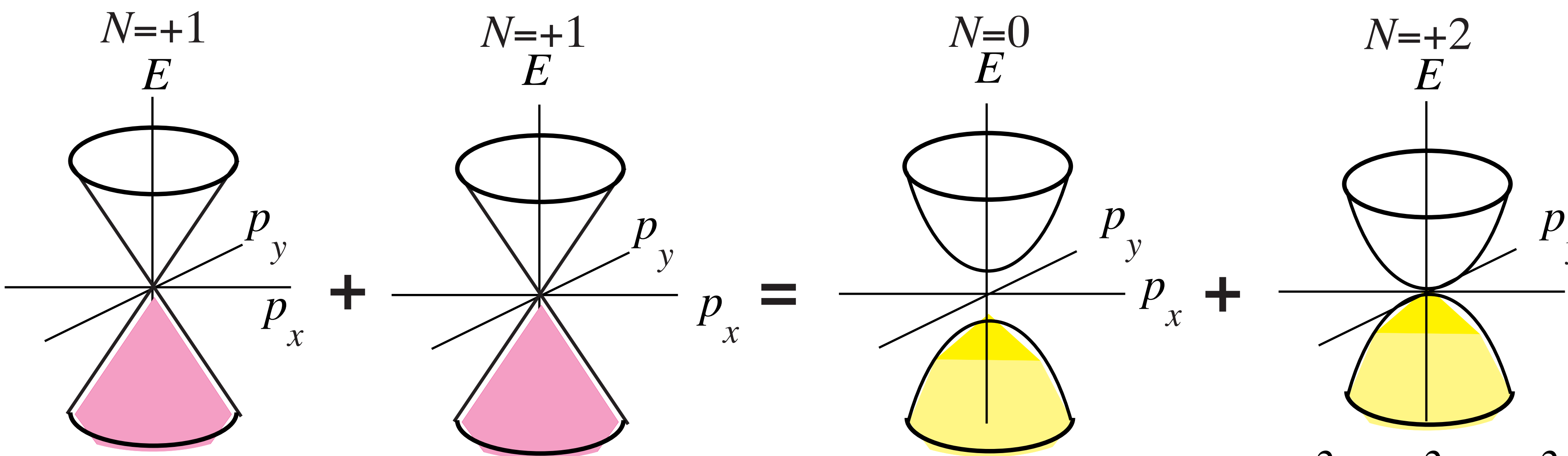

$E=cp$ $E=cp$

relativistic massless fermions

$E^2 = 2c^2p^2 + 4m^2$

Dirac fermion

$E^2 = (p^2/\,2m)^2$

nonrelativistic Dirac fermion
with quadratic dispersion

re-entrant violation of Lorentz invariance & neutrino physics Klinkhamer & GV arXiv:1109.6624

multiple Fermi point

T. Heikkila & GV arXiv:1010.0393

cubic spectrum in trilayer graphene

$$N = 1 + 1 + 1 = 3$$

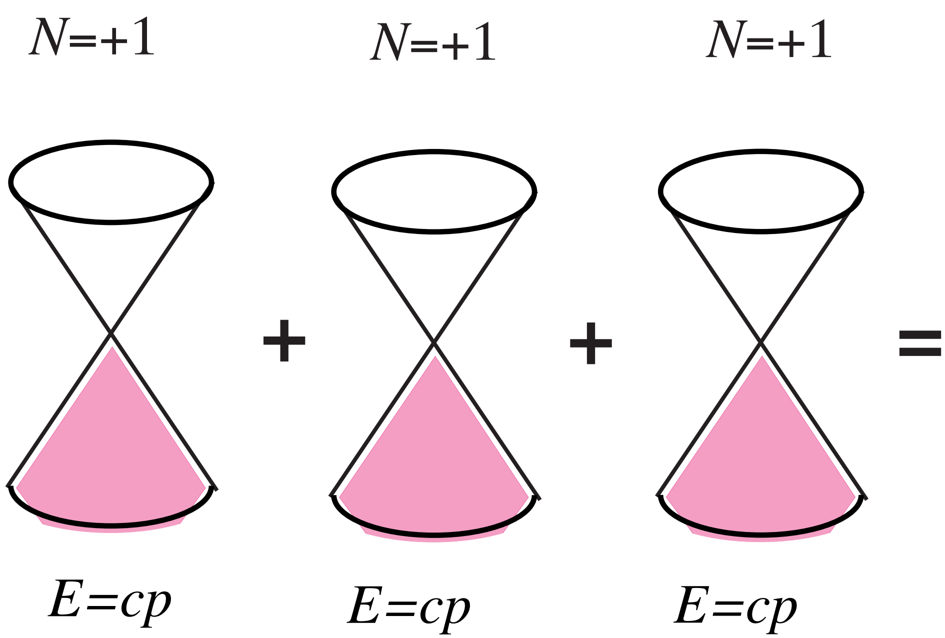

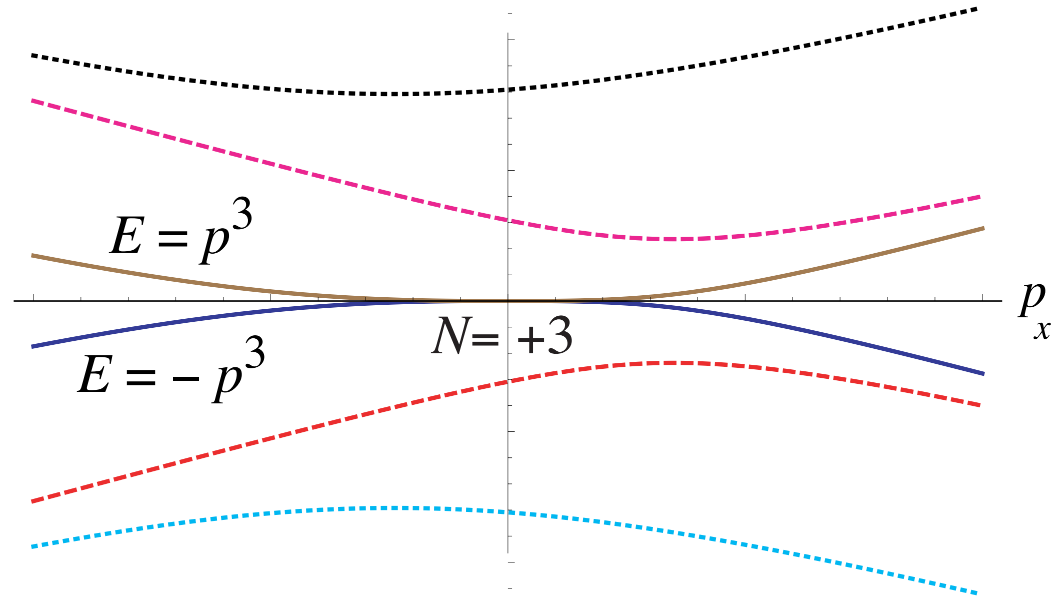

multilayered graphene

$$N = 1 + 1 + 1 + \ldots$$

spectrum in the outer layers

$$E = p^N$$

$$E = -\,p^N$$

what kind of induced gravity emerges near degenerate Fermi point?

route to topological flat band on the surface of 3D material

Fermions in 2+1 bylayer graphene

single layer

$$\mathrm{H} = \begin{pmatrix} 0 & p_x + ip_y \\ p_x - ip_y & 0 \end{pmatrix} = \sigma_x p_x + \sigma_y p_y = \begin{array}{c} \text{zweibein} \\ \begin{pmatrix} 0 & (\mathbf{e}_1 + i\,\mathbf{e}_2)\cdot(\mathbf{p} - \mathbf{A}) \\ (\mathbf{e}_1 - i\,\mathbf{e}_2)\cdot(\mathbf{p} - \mathbf{A}) & 0 \end{pmatrix} \end{array}$$

double layer

$$\mathrm{H} = \begin{pmatrix} 0 & (p_x + ip_y)^2 \\ (p_x - ip_y)^2 & 0 \end{pmatrix} = \begin{array}{c} \text{zweibein} \\ \begin{pmatrix} 0 & [(\mathbf{e}_1 + i\,\mathbf{e}_2)\cdot(\mathbf{p} - \mathbf{A})]^2 \\ [(\mathbf{e}_1 - i\,\mathbf{e}_2)\cdot(\mathbf{p} - \mathbf{A})]^2 & 0 \end{pmatrix} \end{array}$$

anisotropic scaling: $x = b\, x'$, $t = b^2\, t'$

Horava-Lifshitz gravity:
Horava, Quantum gravity at a Lifshitz point
PRD **79**, 084008 (2009)

2+1 anisotropic QED emerging in bylayer graphene

$$\mathrm{H} = \begin{pmatrix} 0 & (p_x + ip_y)^2/2\mathrm{m} \\ (p_x - ip_y)^2/2\mathrm{m} & 0 \end{pmatrix} = \begin{pmatrix} 0 & [(\mathbf{e}_1 + i\,\mathbf{e}_2)(\mathbf{p} - \mathbf{A})]^2/2\mathrm{m} \\ [(\mathbf{e}_1 - i\,\mathbf{e}_2)(\mathbf{p} - \mathbf{A})]^2/2\mathrm{m} & 0 \end{pmatrix}$$

Heisenberg-Euler action

anisotropic scaling: $\mathrm{x} = \mathrm{b\,x}'$, $\mathrm{t} = \mathrm{b}^2\ \mathrm{t}'$, $\mathrm{B} = \mathrm{b}^{-2}\,\mathrm{B}'$, $\mathrm{E} = \mathrm{b}^{-3}\,\mathrm{E}'$, $\mathrm{S} = \mathrm{S}'$

$$S = 1/m \int \underset{\mathrm{b}^2}{d^2x}\ \underset{\mathrm{b}^2}{dt}\ \underset{\mathrm{b}^{-4}}{B^2}\ g(\mu)$$

$g(\mu)$ – dimensionless fuction of dimensionless parameter $\mu = m^2 \underset{\mathrm{b}^{-6}}{E^2} / \underset{\mathrm{b}^{6}}{B^3}$

magnetic field asymptote

$$S_{\mathrm{B}} = 1/m \int d^2x\ dt\ B^2\ ln\ 1/B^2$$

electric field asymptote

$$S_{\mathrm{E}} = 1/m \int \underset{\mathrm{b}^2}{d^2x}\ \underset{\mathrm{b}^2}{dt}\ (-\,m^2 \underset{\mathrm{b}^{-4}}{E^2}\,)^{2/3}$$

Schwinger pair production $\sim E^{4/3}$

pair production mainly occurs at $\mu > 1$ **i.e at** $E^2 > B^3/m^2$

Flat bands in topological matter

flat band: half-quantum vortex in **p**-space

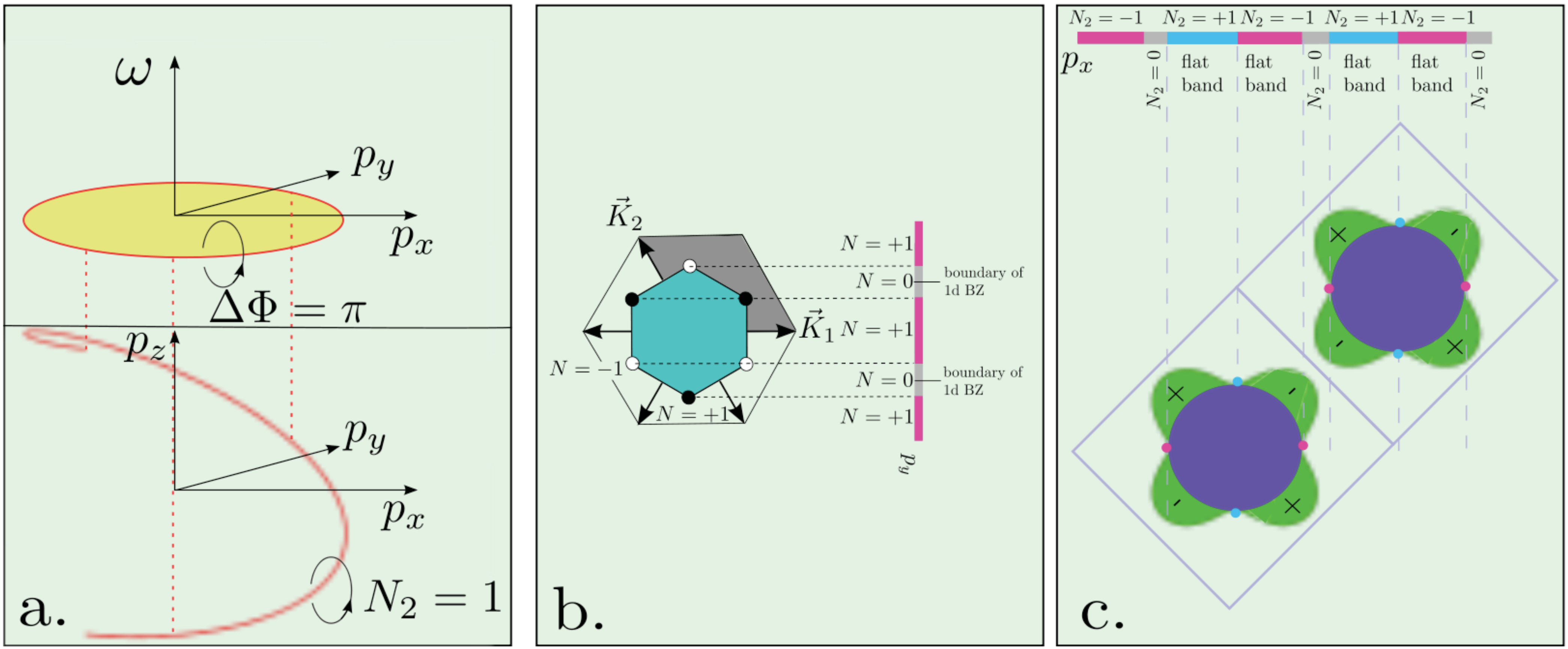

nodal spiral in multilayered graphene
generates flat band with zero energy
in the top and bottom layers

Hekilla, Kopnin, GV

nodes in graphene
generate flat band on zigzag edge

nodal lines
in cuprate superconductors
generate flat band on side surface

Shinsei Ryu

approximate flat band on side surface
of graphite

formation of nodal spiral in bulk (together with flat band on the surface) by stacking of graphene layers

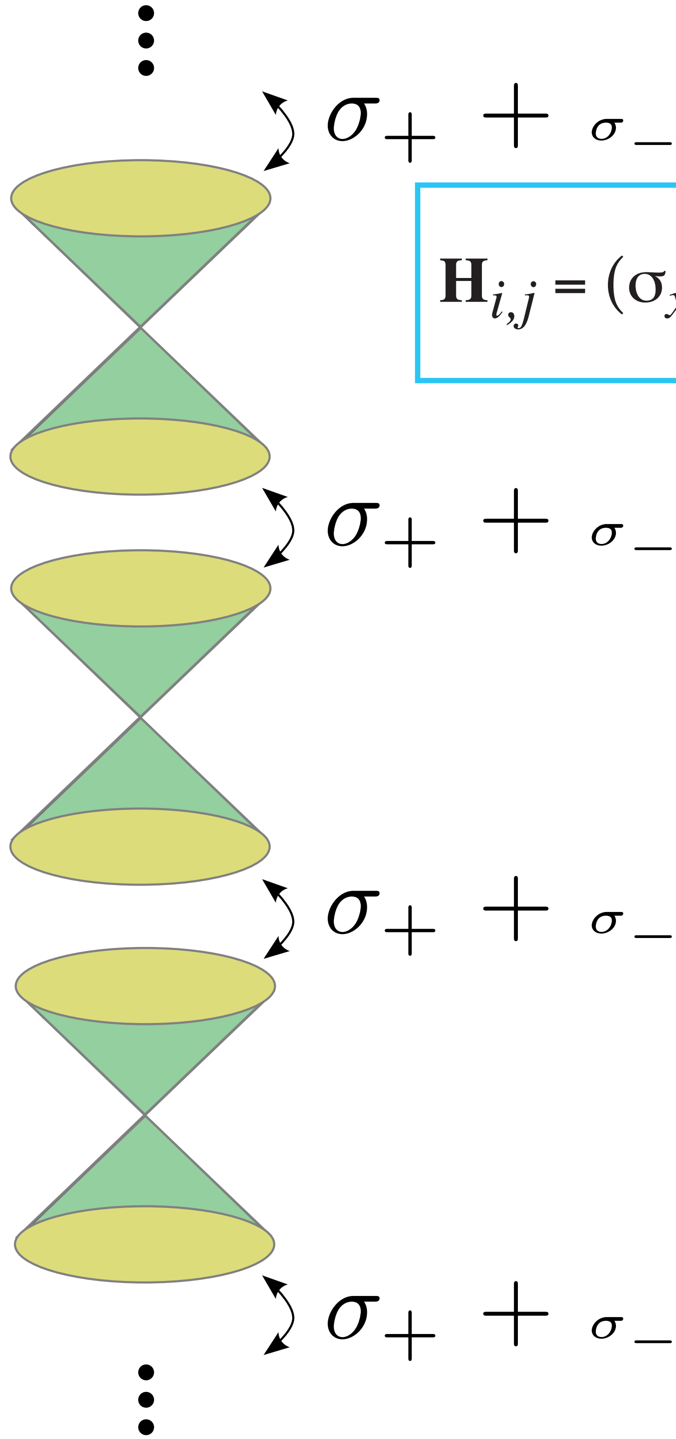

$$\mathbf{H}_{i,j} = (\sigma_x p_x + \sigma_y p_y)\delta_{i,j} + (\sigma_+ t_+ + \sigma_- t_-)\delta_{i,j+1}$$

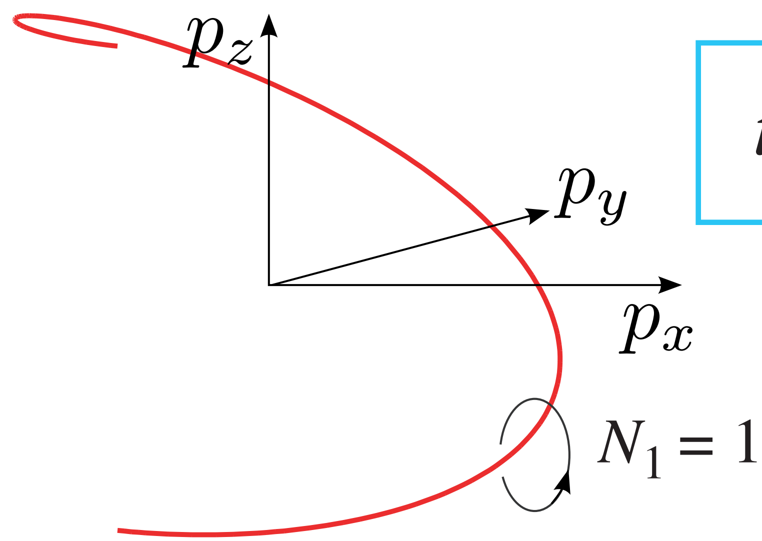

$$t_+ > t_-$$

$$N_1 = \frac{1}{4\pi i}\,\mathbf{tr}\left[\mathbf{K}\oint dl\,\mathbf{H}^{-1}\nabla_l\,\mathbf{H}\right]$$

Emergence of nodal line from gapped branches by stacking graphene layers

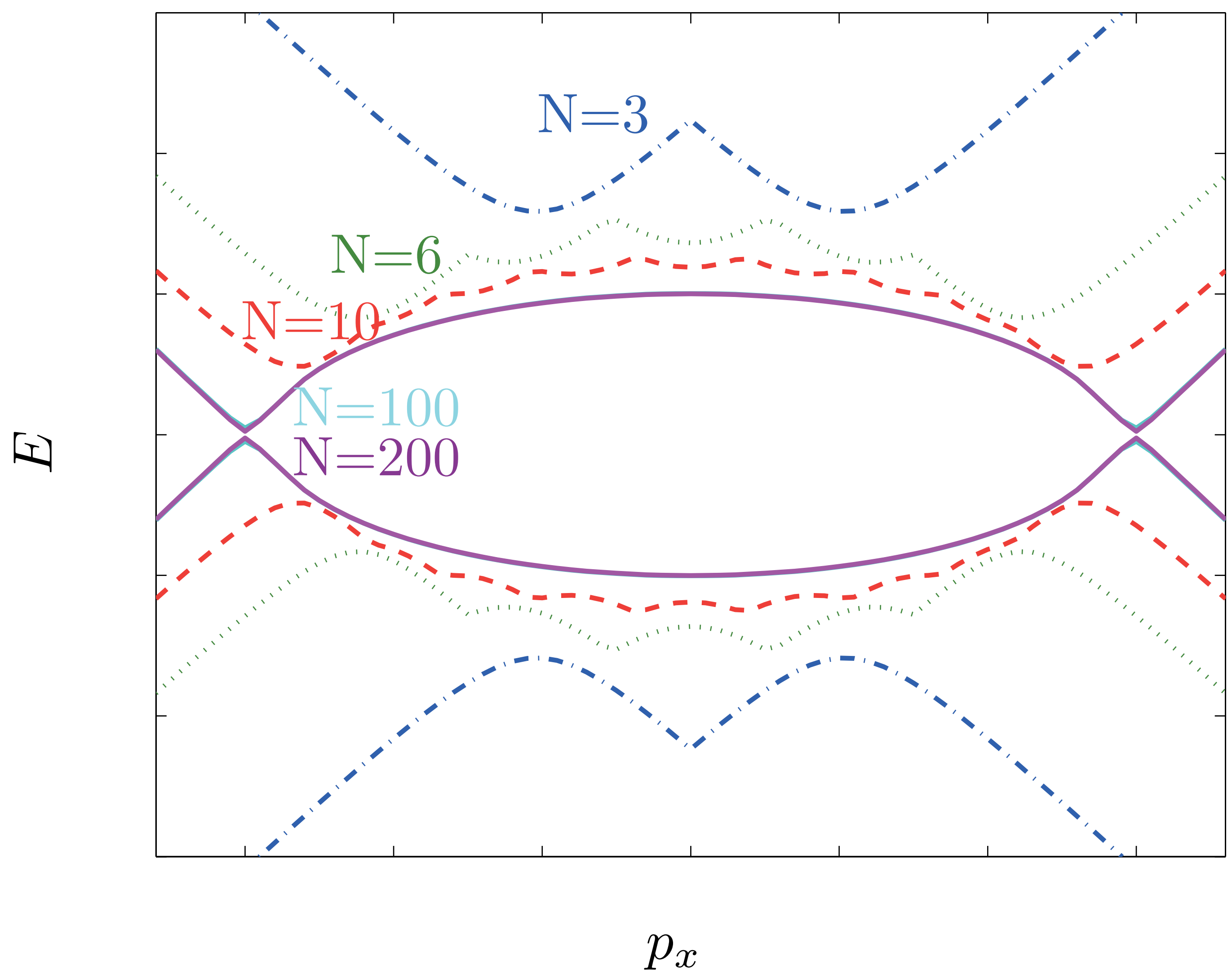

example of topological bulk-surface correspondense:
Nodal spiral generates flat band on the surface

projection of spiral on the surface determines boundary of flat band

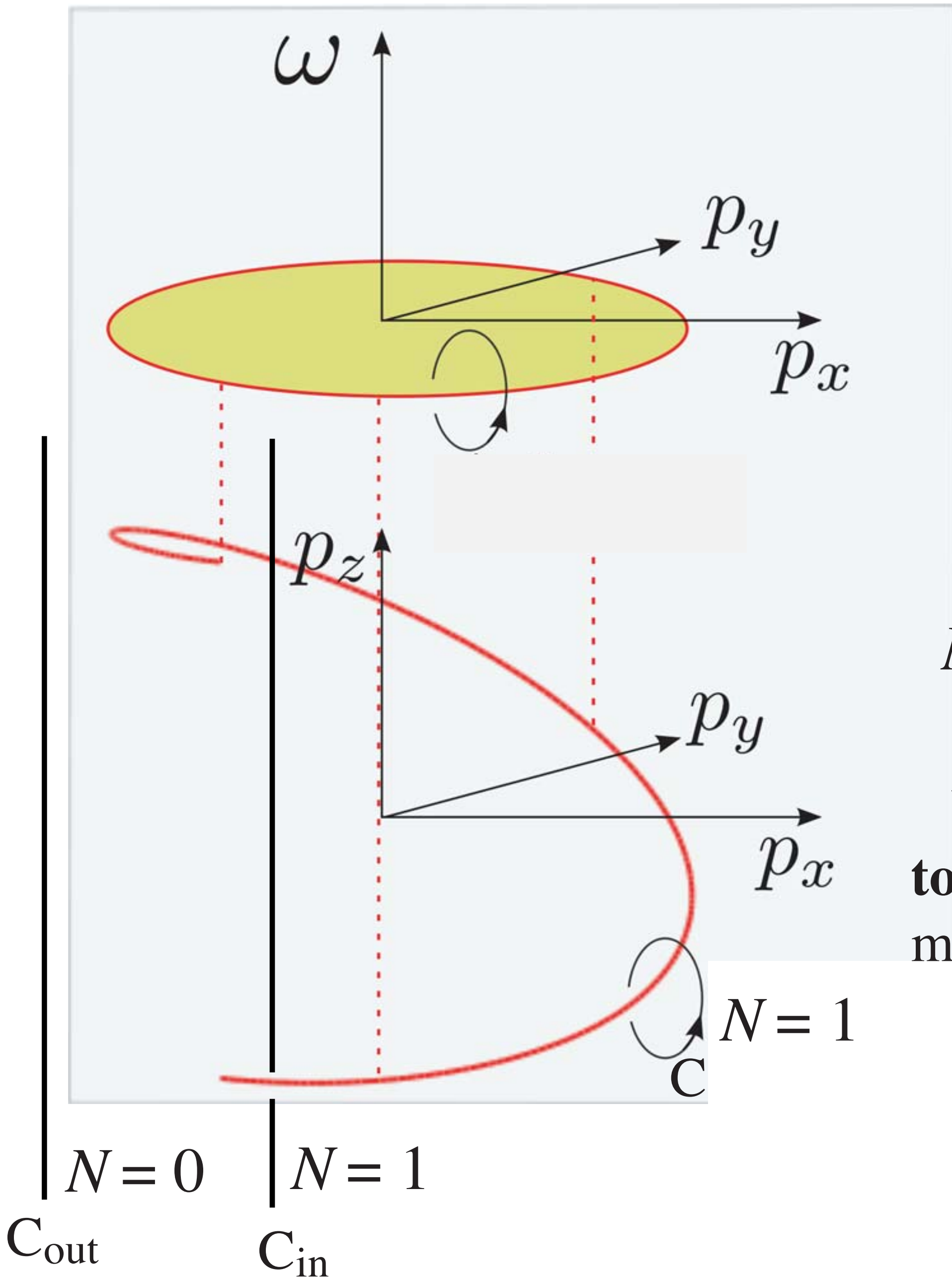

$$N = \frac{1}{4\pi i} \, \mathbf{tr} \left[\mathbf{K} \oint_C dl \, \mathbf{H}^{-1} \nabla_l \, \mathbf{H} \right]$$

at each (p_x,p_y) except the boundary of circle one has 1D fully gapped state (insulator)

$N_{out}(p_x,p_y) = 0$ trivial 1D insulator

$N_{in}(p_x,p_y) = 1$ topological 1D insulator

topological insulator has 1D gapless **edge state**
manifold (p_x,p_y) of edge states forms **flat band**

Nodal spiral generates flat band on the surface

projection of nodal spiral on the surface determines boundary of flat band

lowest energy states:
surface states form the flat band

energy spectrum in bulk
(projection to p_x , p_y plane)

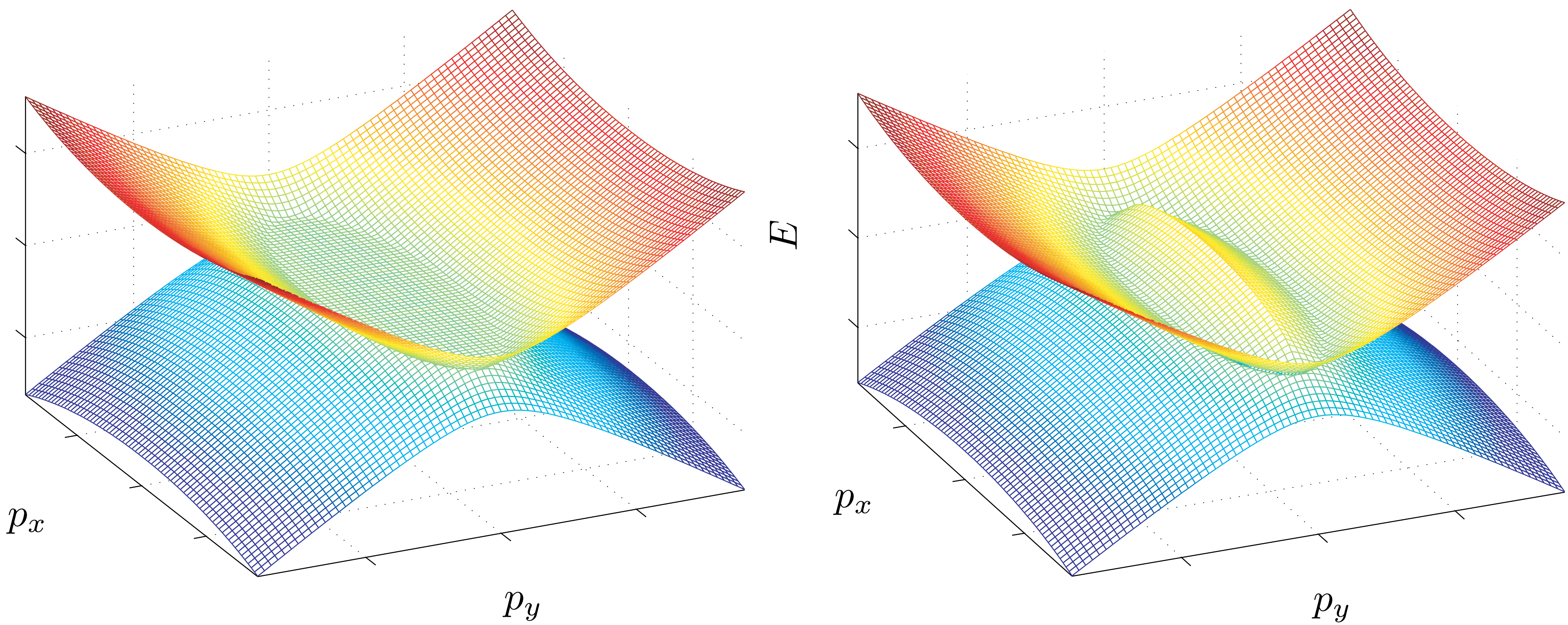

Modified nodal spiral in rhombohedral graphite: spiral of Fermi surfaces (McClure 1969)

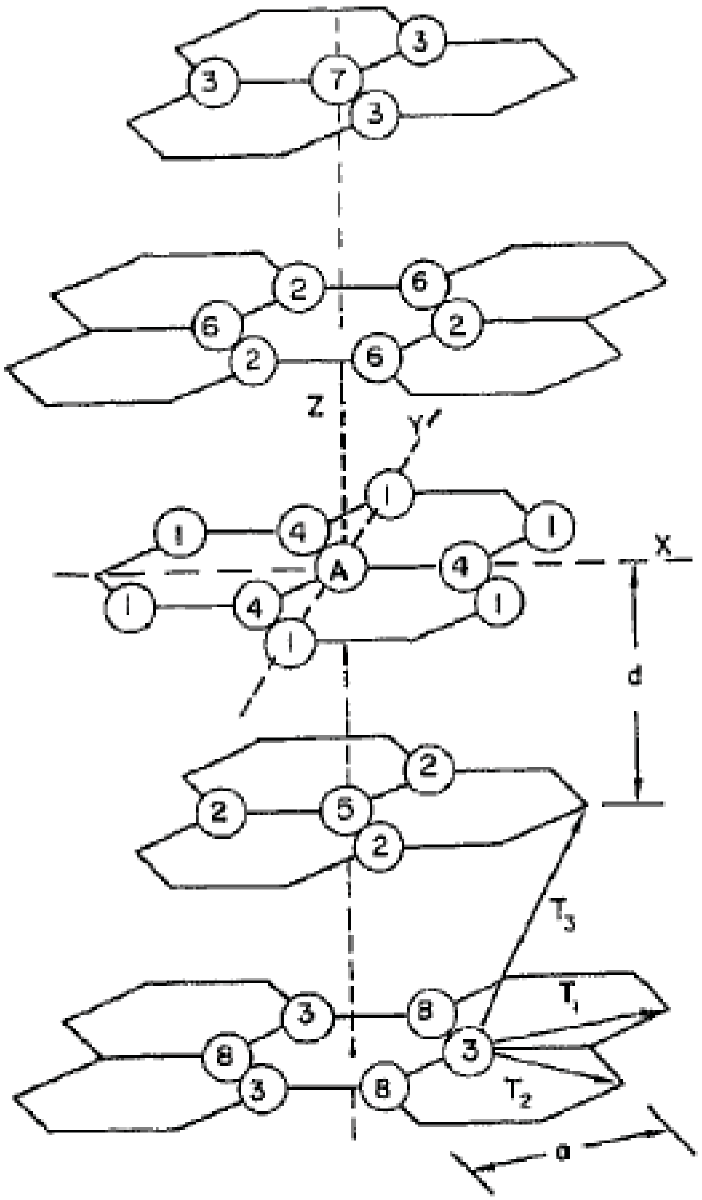

Fig. 1. The crystal lattice of rhombohedral graphite. The numbering of the groups of neighbors of the central A atom is explained in the text.

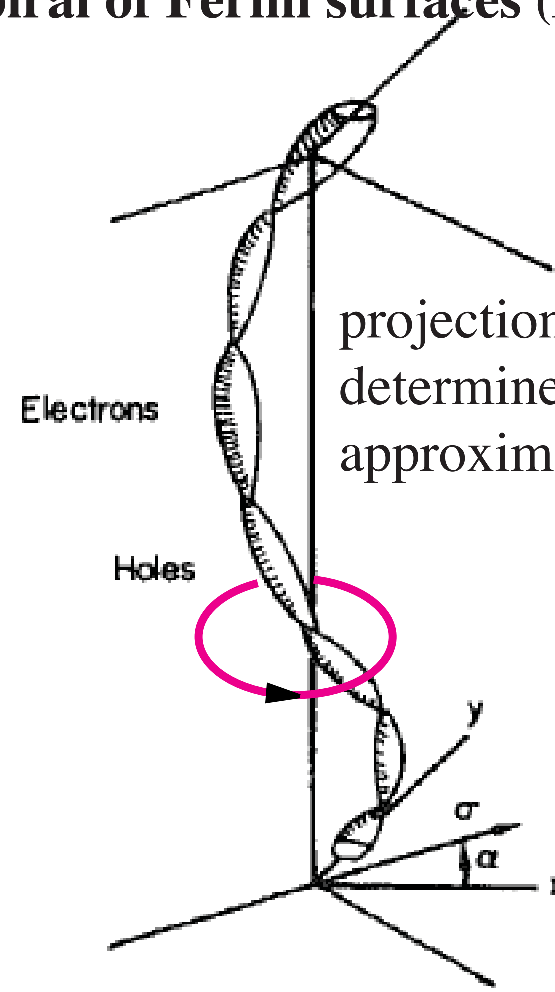

projections on surfaces determine approximate flat band

Fig. 2. The Fermi surface of rhombohedral graphite. The surface is centered on one of the six vertical zone edges. The widths of the surfaces have been magnified by more than an order of magnitude.

for conventional graphite: approximate flat band on the lateral surface

Flat band on the graphene edge

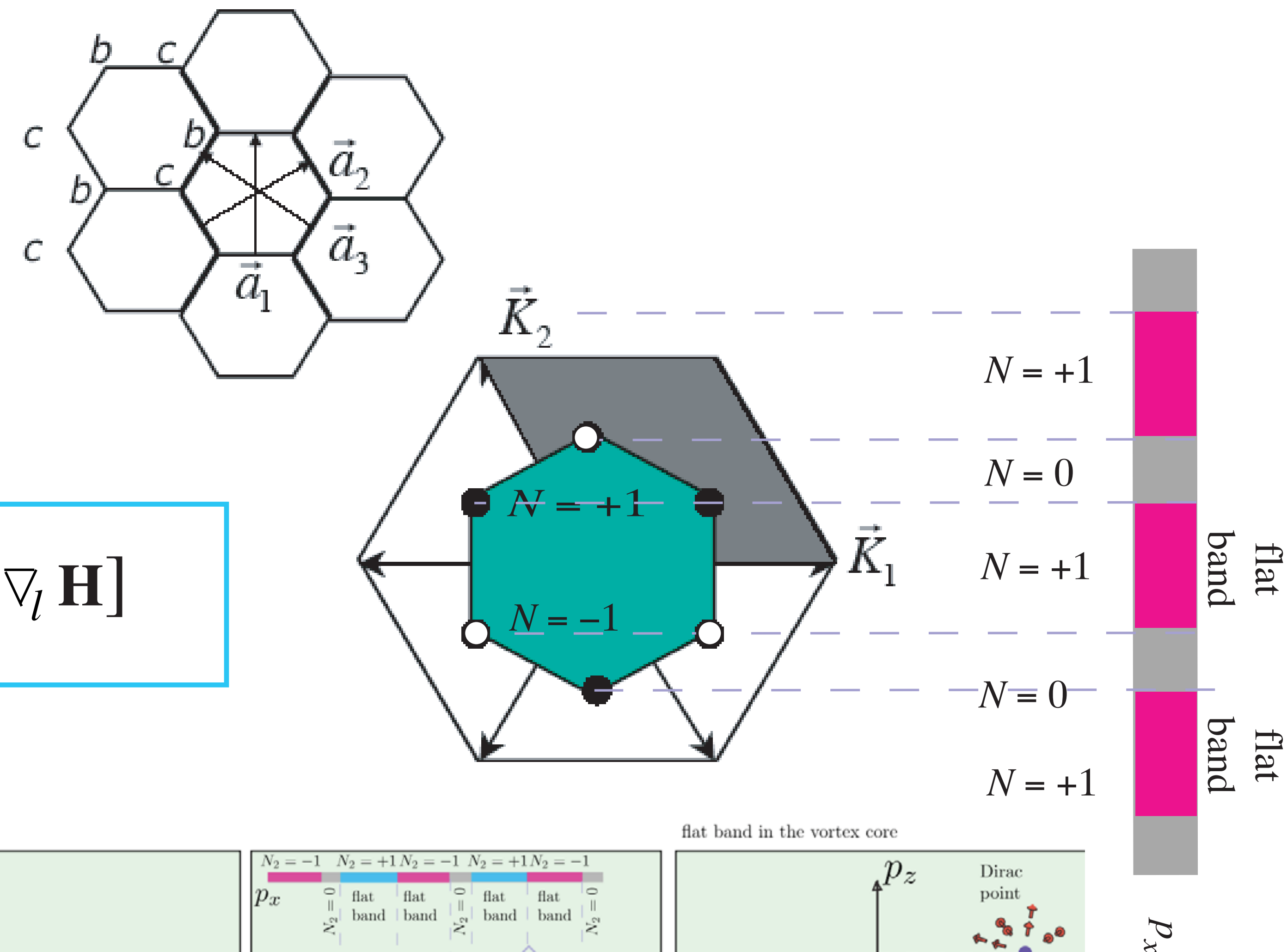

$$N = \frac{1}{4\pi i}\, \mathbf{tr}\, [\mathbf{K} \oint dl\, \mathbf{H}^{-1} \nabla_l\, \mathbf{H}]$$

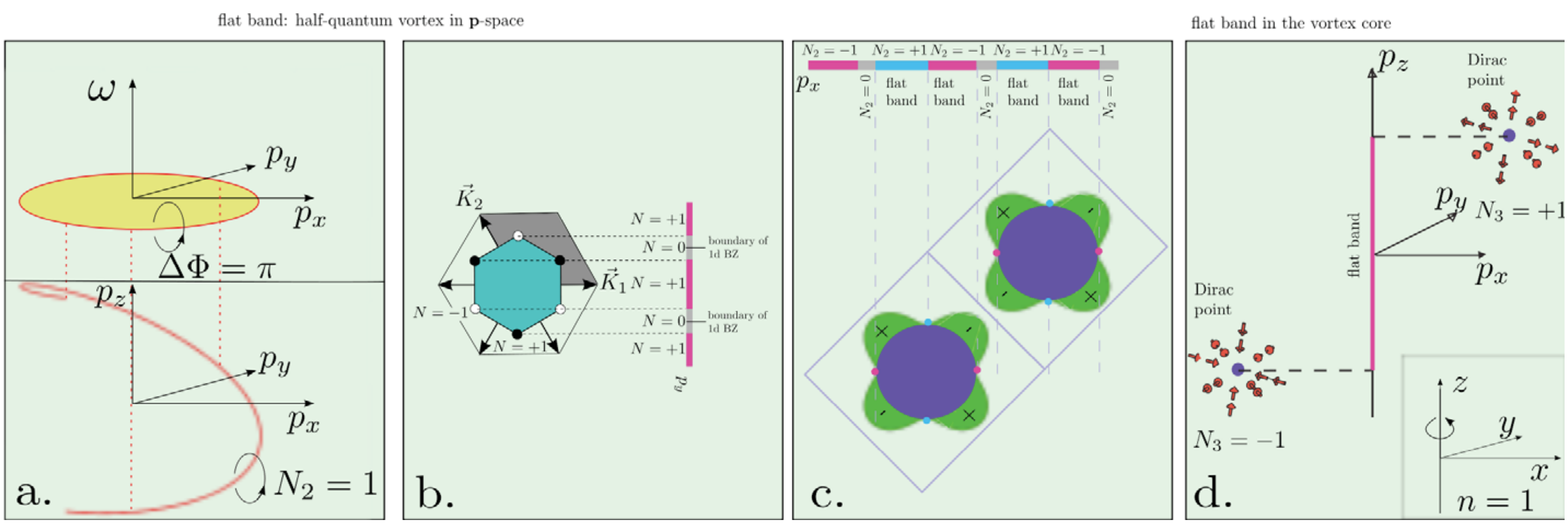

Surface superconductivity in topological semimetals: route to room temperature superconductivity

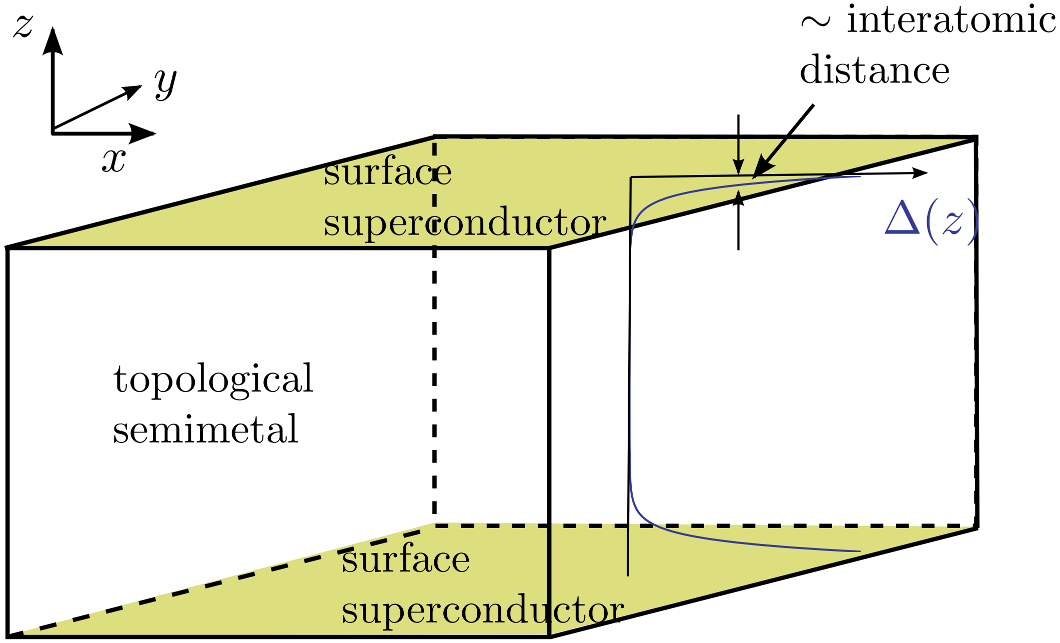

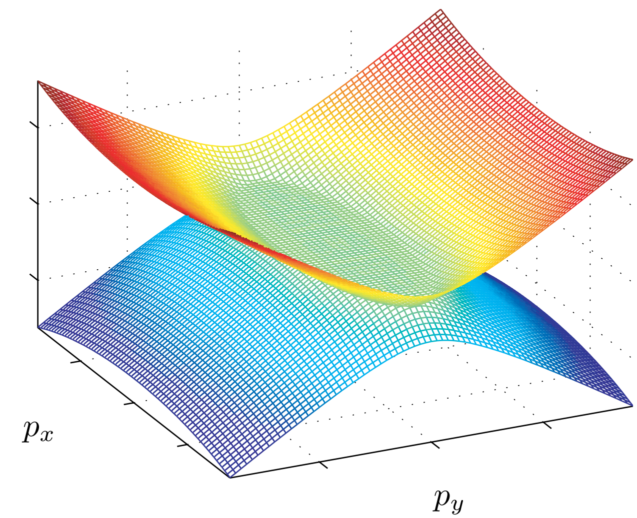

Extremely high DoS of flat band gives high transition temperature:

$$1 = g \int \frac{d^2p}{2h^2} \frac{1}{E(p)}$$

normal superconductors:
exponentially suppressed
transition temperature

$$T_c = T_F \exp\left(-1/g\nu\right)$$

interaction ***DOS***

$$\mathrm{DoS} = \nu(\varepsilon) \sim \varepsilon^{2/N-1}$$

N is number of layers

flat band superconductivity:
linear dependence
of T_c on coupling g

$$T_c \sim g S_{\mathrm{FB}}$$

coupling ***flat band area***

$N = 4$: $\nu(\varepsilon) \sim \varepsilon^{-1/2}$ Kopaev (1970); Kopaev-Rusinov (1987)

T.T. Heikkila, N.B. Kopnin & GV
Flat bands in topological media
Pis'ma ZhETF **94**, 252 (2011)

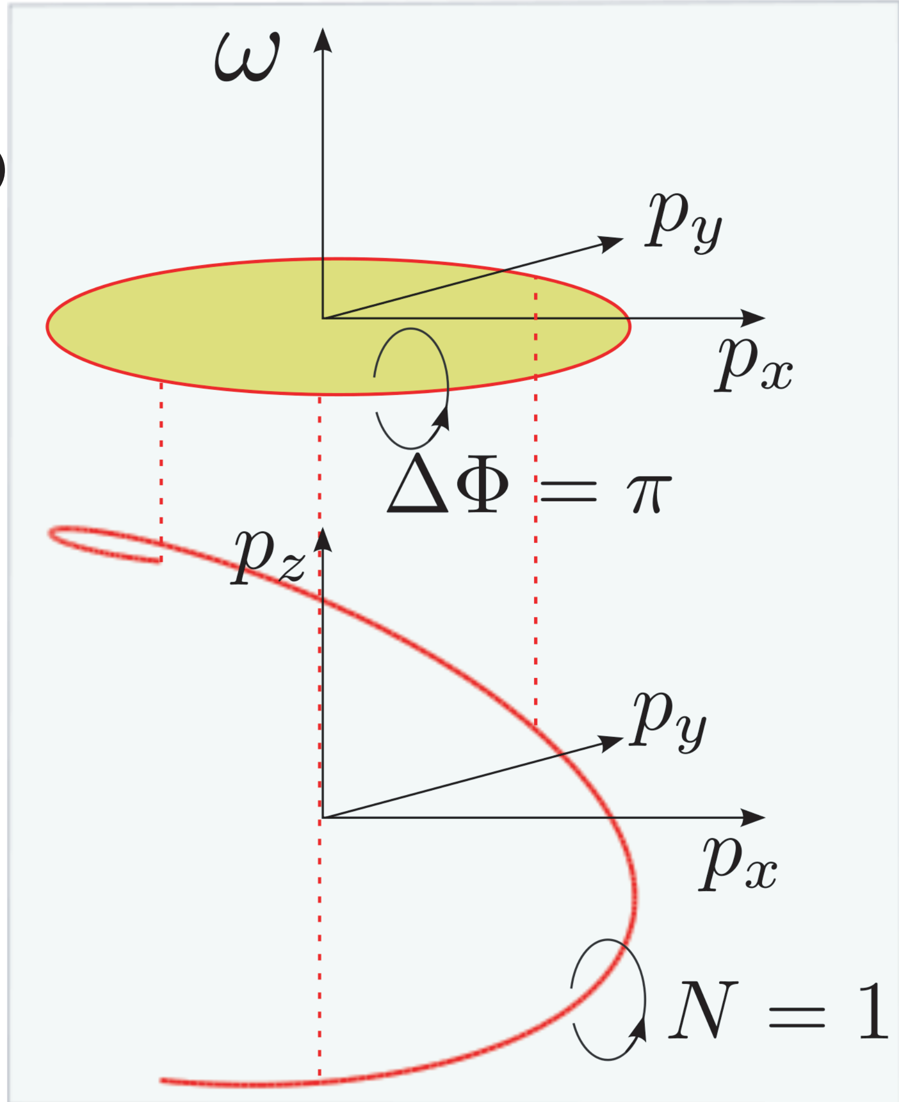

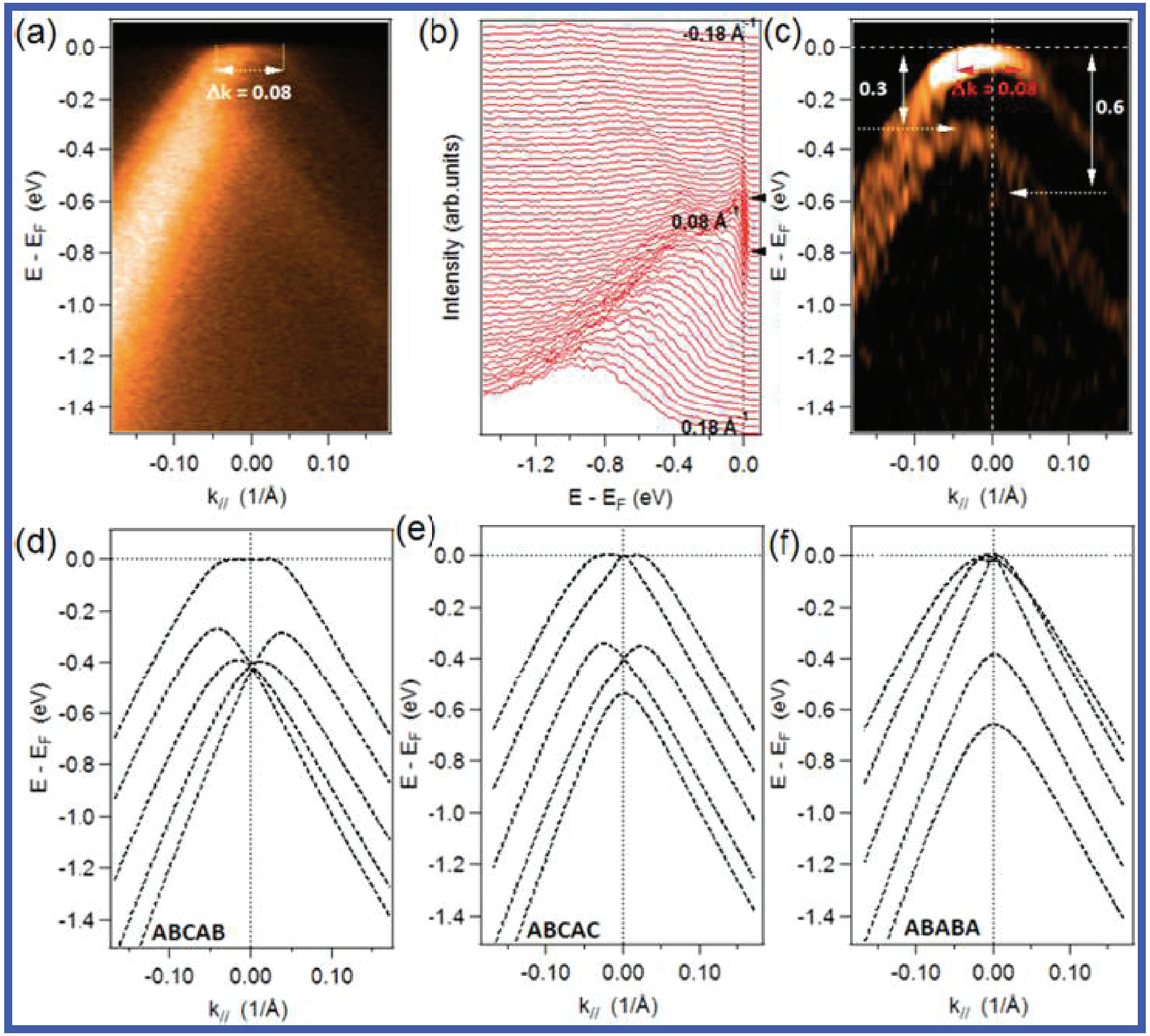

Figure 4. Electronic structure of multilayer graphene. (a) Dispersion of the π bands measured by ARPES. The spectra are measured with a photon energy of 60 eV and with scans oriented along the ΓK direction of the graphene Brillouin zone. (b) EDC of (a), showing the presence of a flat band. (c) Second derivative of the intensity ARPES data along the ΓK direction of the multilayer graphene. (d–f) Theoretical calculation of five layers with pure rhombohedral ABCAB, mixed rhombohedral–Bernal ABCAC, and pure Bernal ABABA sequence.

Evidence for Flat Bands near the Fermi Level in Epitaxial Rhombohedral Multilayer Graphene

Debora Pierucci,[†] Haikel Sediri,[†] Mahdi Hajlaoui,[†,‡] Jean-Christophe Girard,[†] Thomas Brumme,[§]

Published online
10.1021/acsnano.5b01239

interface superconductivity

nature materials

LETTERS

PUBLISHED ONLINE: 24 NOVEMBER 2014 | DOI: 10.1038/NMAT4153

Superconductivity above 100 K in single-layer FeSe films on doped $SrTiO_3$

Jian-Feng Ge[1], Zhi-Long Liu[1], Canhua Liu[1,2*], Chun-Lei Gao[1,2], Dong Qian[1,2], Qi-Kun Xue[3*], Ying Liu[1,2,4] and Jin-Feng Jia[1,2*]

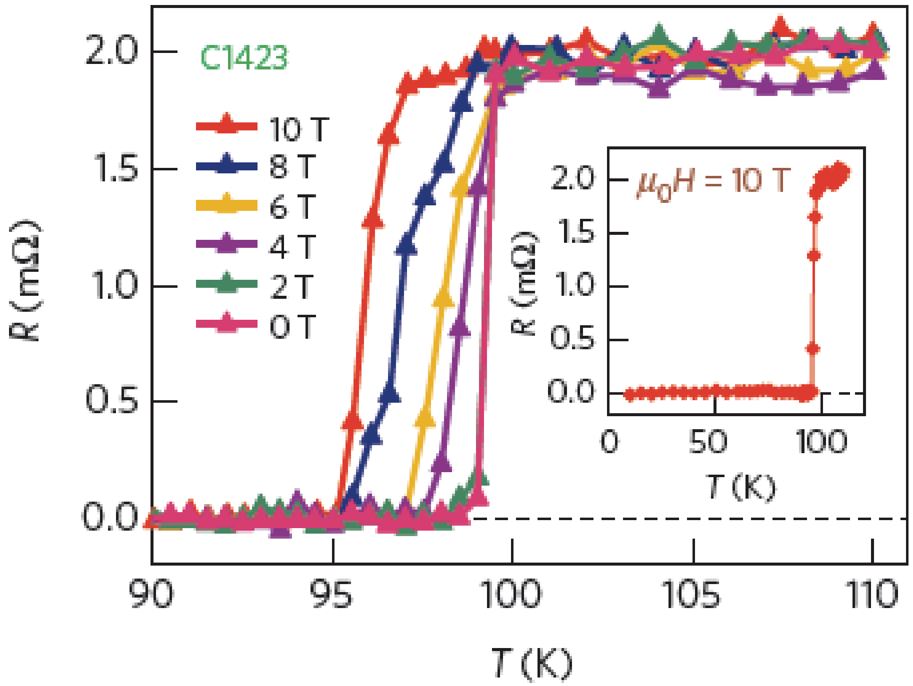

Ballestar et al.,
NJP 15,
023024
(2013)

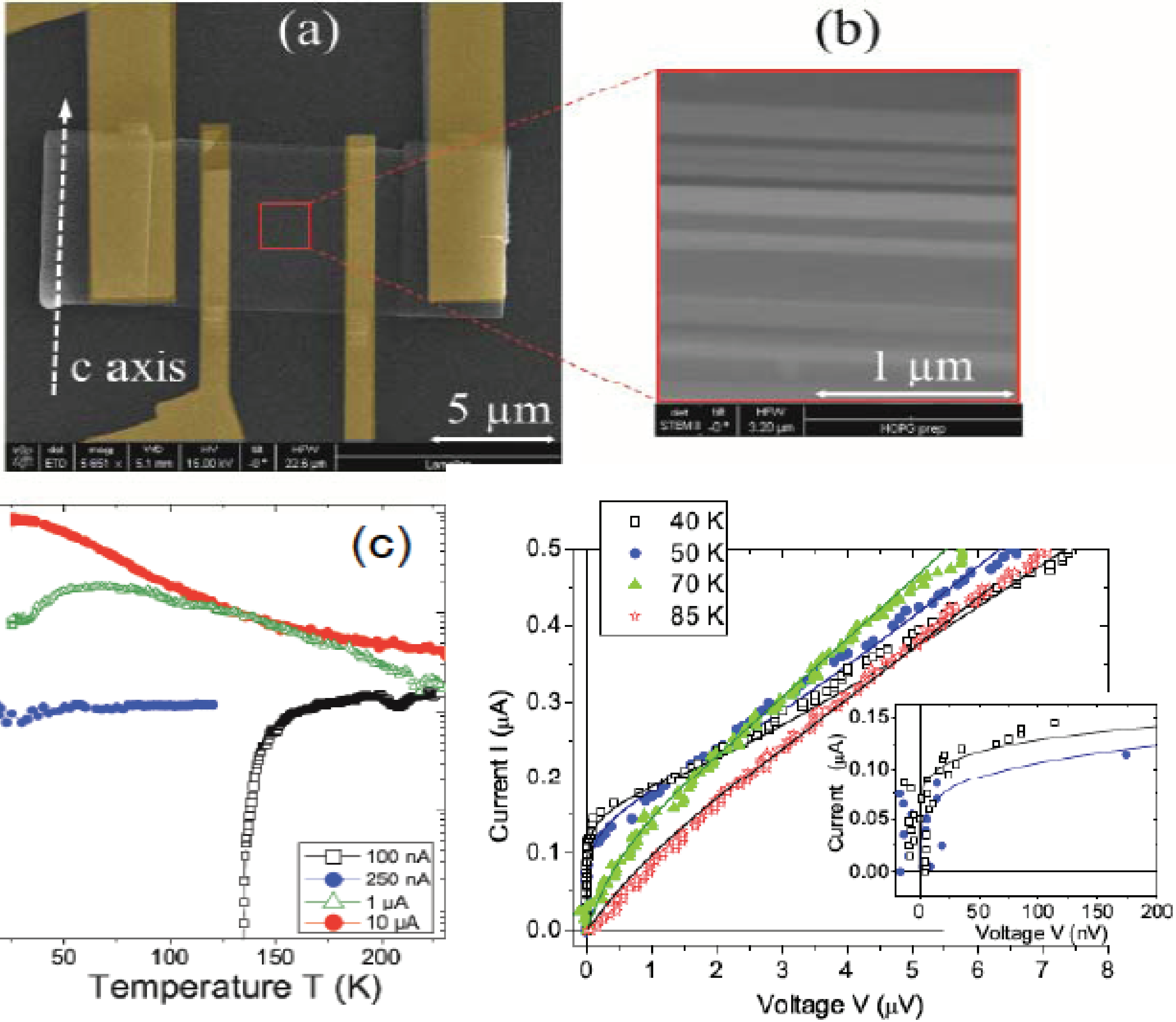

Flat band on graphene edge & on edge dislocation in graphite

1D flat band on graphene edge (Ryu-Hatsugai)

projections of Dirac points to the edge determine boundaries of the flat band

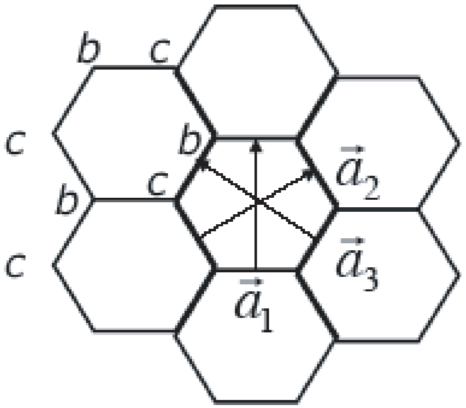

$$N = \frac{1}{4\pi i}\,\mathbf{tr}\left[\mathbf{K}\oint dl\; \mathbf{H}^{-1}\nabla_l\, \mathbf{H}\right]$$

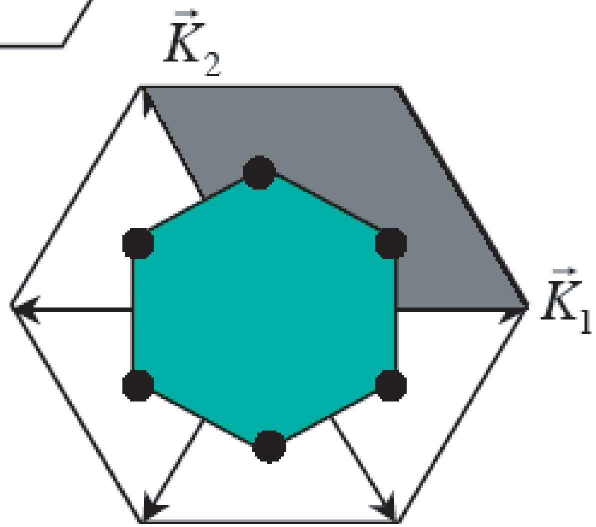

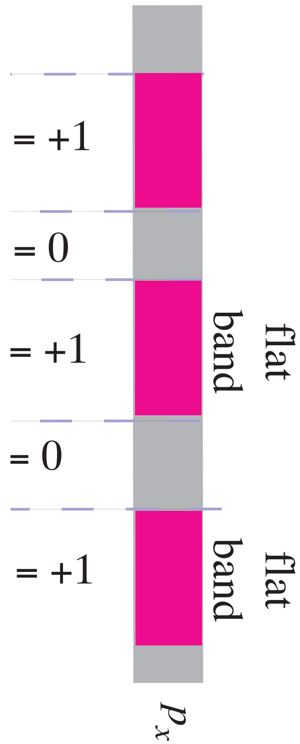

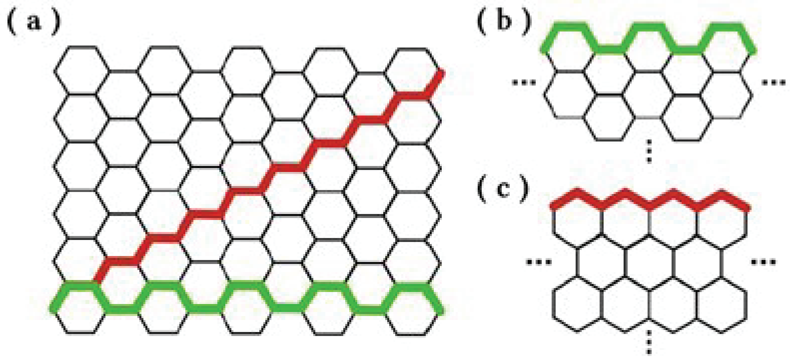

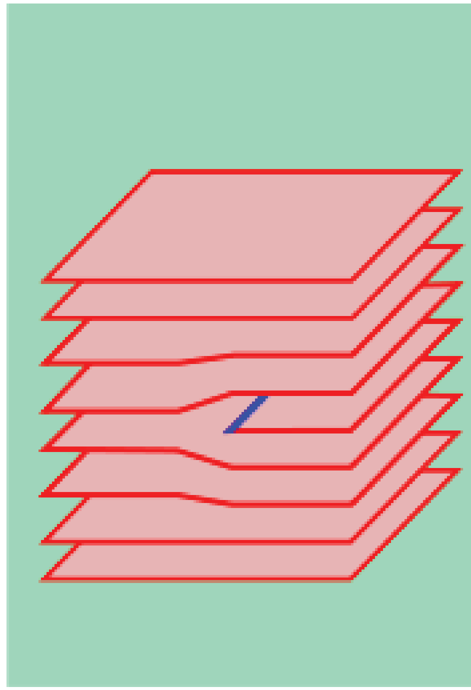

edge dislocation in graphite is the edge of graphene sheet dislocation contains 1D flat band

Twist interfaces in graphite

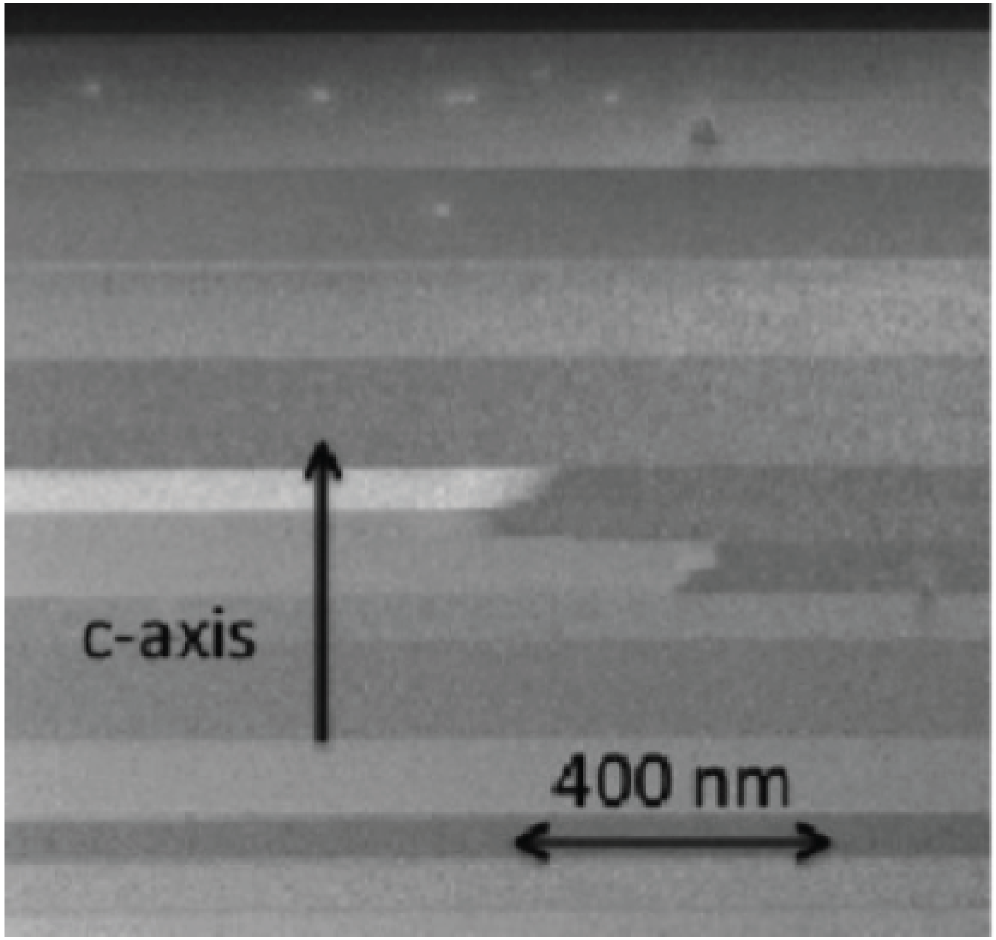

Esquinazi, et al

misfit dislocations network at interface

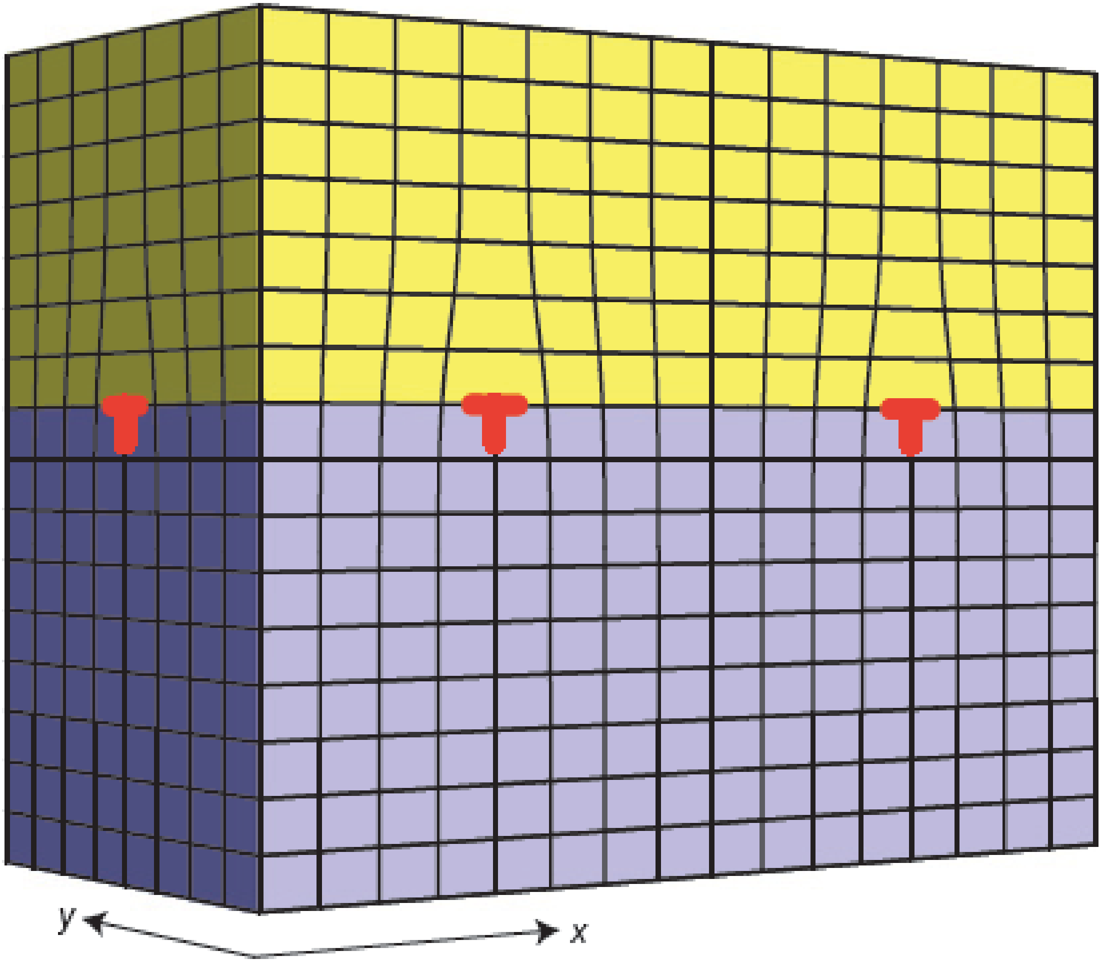

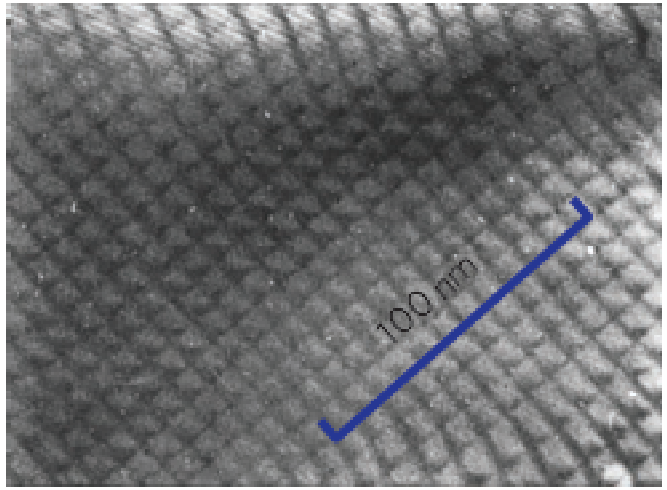

POLAR PHASE OF SUPERFLUID 3He in NAFEN

Engineering new topological superfluids by nanostructural confinement.

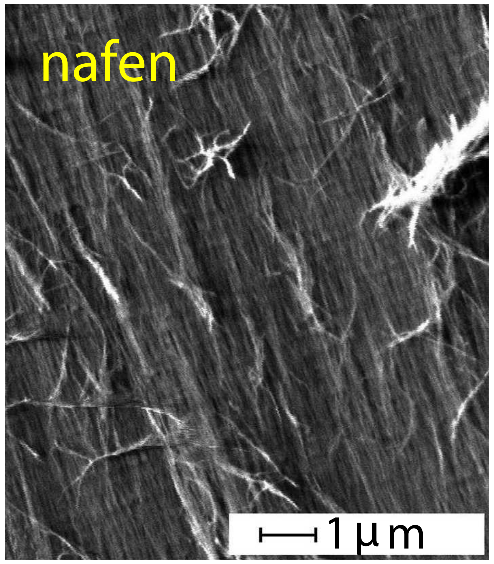

$$A_{\mu j} = \Delta\, d_\mu\, m_j\, e^{i\phi}$$

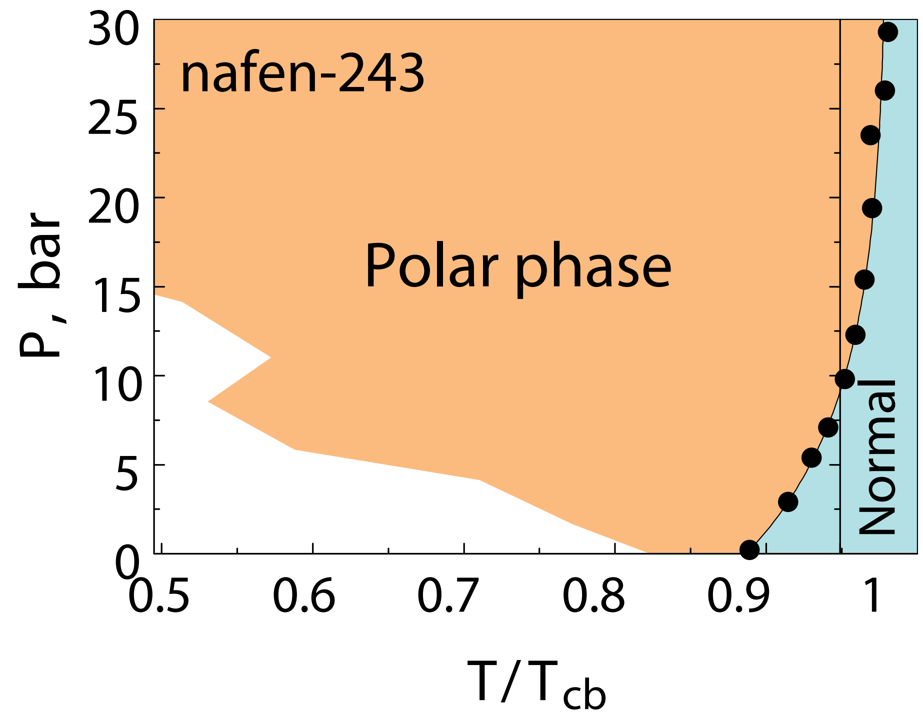

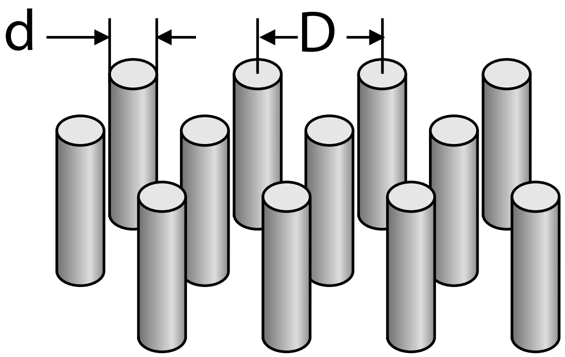

	open	d, nm	D , nm
nafen-90	98%	8	47
nafen-243	94%	9	32

$$H = \left(\frac{p^2}{2m} - \mu\right)\tau_3 - c\tau_1\sigma_z p_z$$

Dmitriev et al, PRL (2015) [arXiv:1507.04275]

Dirac nodal line & surface flat band in polar phase of 3He in NAFEN

$$A_{\mu j} = \Delta\, d_\mu\, m_j\, e^{i\phi}$$

$$H = \left(\frac{p^2}{2m} - \mu\right)\tau_3 - c\tau_1\sigma_z p_z$$

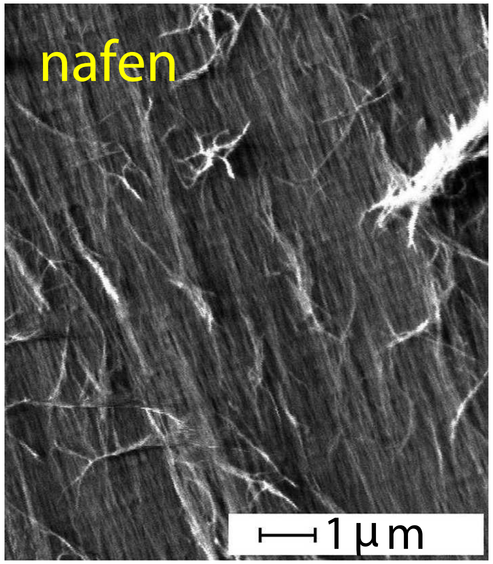

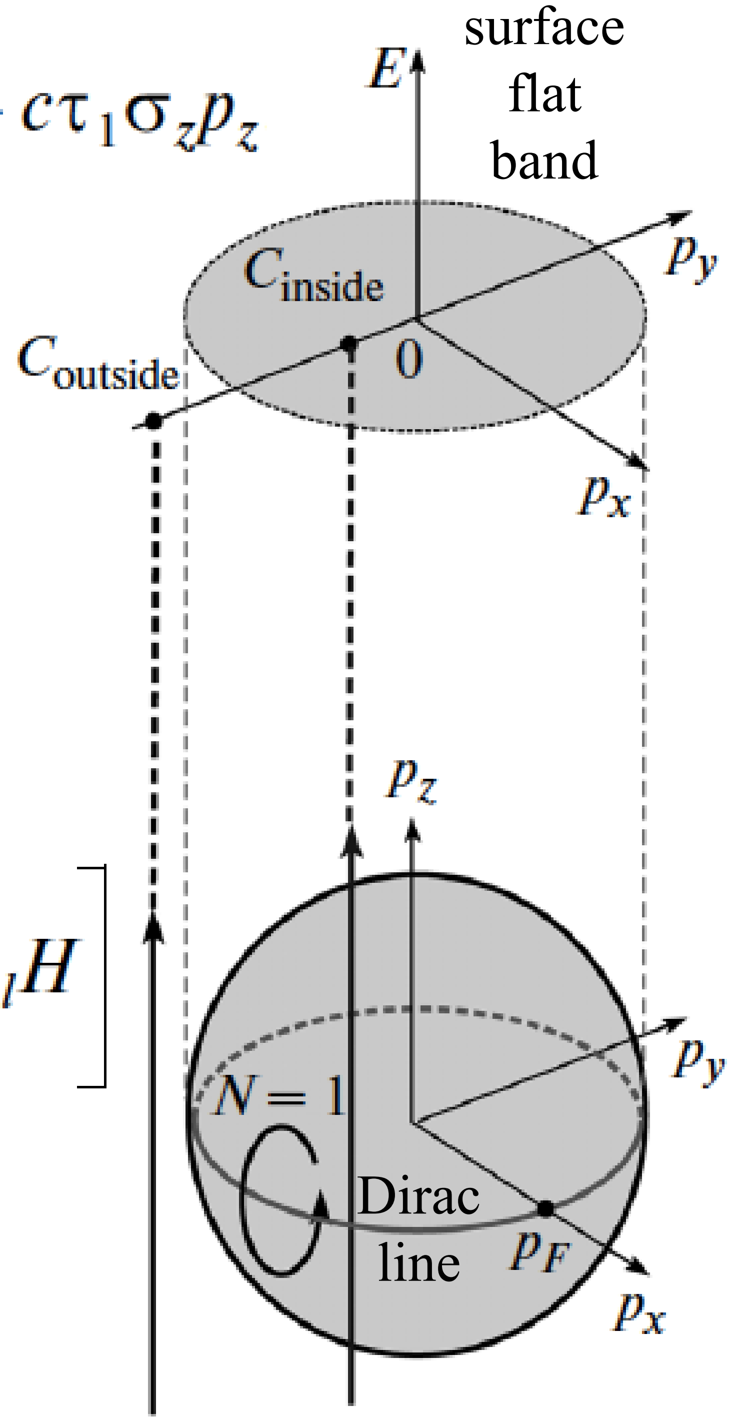

topological invariant
for line node

$$N_K = \frac{1}{4\pi i}\mathrm{Tr}\left[K\oint_C dl\, H^{-1}\nabla_l H\right]$$

nexus - combined topology in graphite

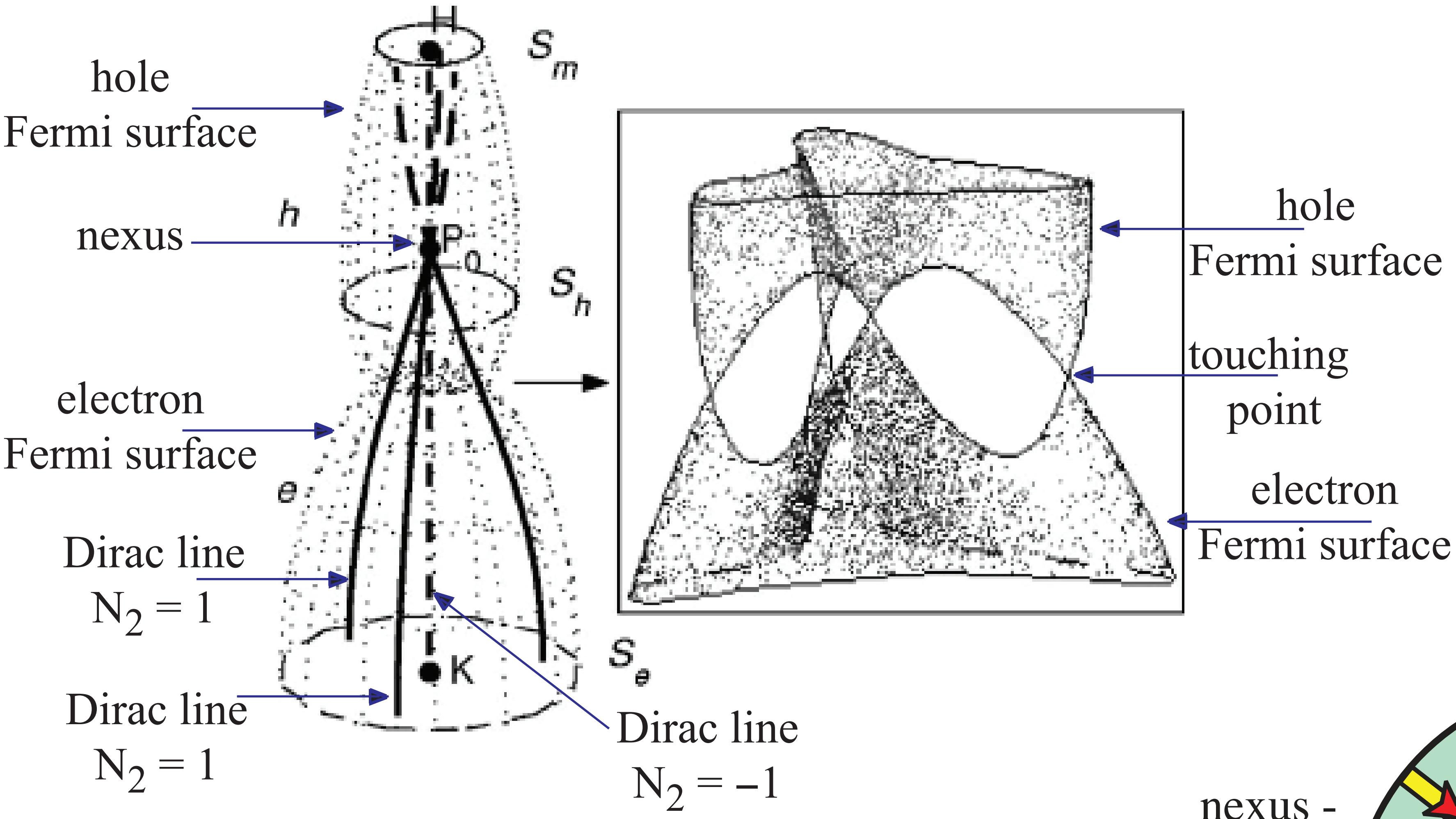

PHYSICAL REVIEW B 73, 235112 (2006)

Band-contact lines in the electron energy spectrum of graphite

G. P. Mikitik and Yu. V. Sharlai

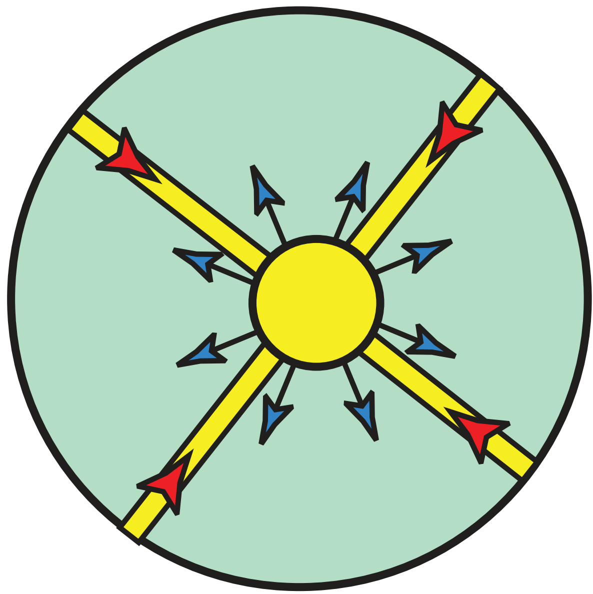

5. Fully gapped topological matter

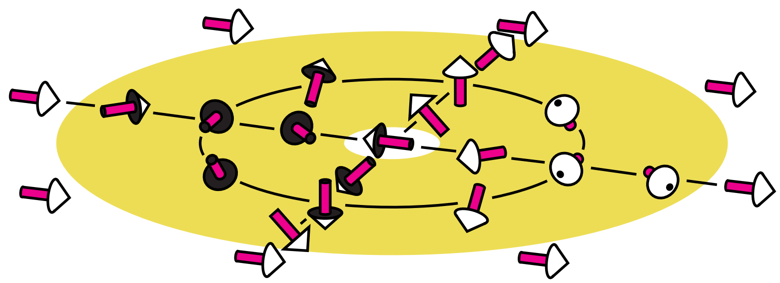

skyrmions in p-space

emergent relativistic fermions as edge states

$$N_3 = \frac{1}{8\pi} e_{ijk} \int dS^k \; \hat{\mathbf{g}} \cdot (\nabla_{p_i} \hat{\mathbf{g}} \times \nabla_{p_j} \hat{\mathbf{g}})$$

around Fermi point

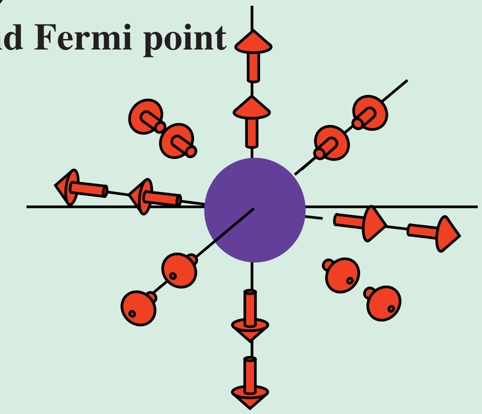

3+1vacuum with massless fermions

dimensional reduction

Fully gapped 2+1 vacuum

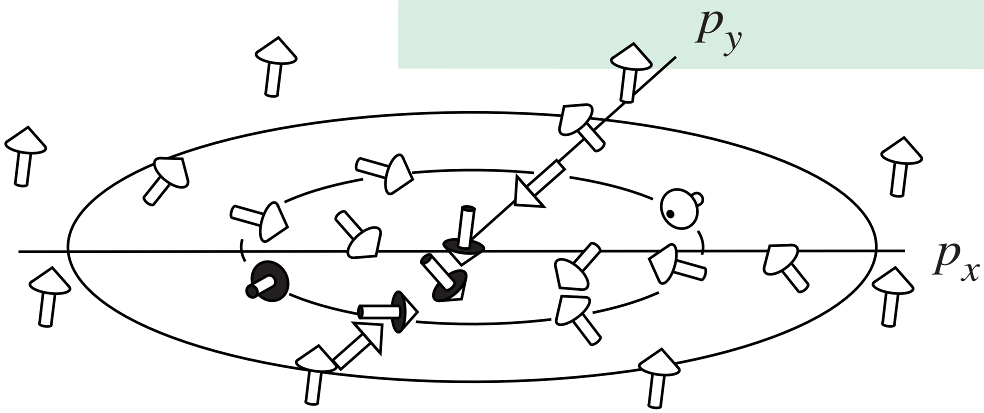

dimensional reduction

$$\tilde{N}_3 = \frac{1}{8\pi} e_{ijk} \int dp_x dp_y \; \hat{\mathbf{g}} \cdot (\nabla_{p_x} \hat{\mathbf{g}} \times \nabla_{p_y} \hat{\mathbf{g}})$$

over the whole 2D momentum space
or over 2D Brillouin zone

gapless 1+1 edge states

Fully gapped 4+1 vacuum gives 3+1 relativistic fermions (Kaplan, arXiv:1112.0302)

topological insulators & gapped superconductors in 2+1

topological insulator =
bulk insulator
with topologically protected
gapless states on the boundary

topological gapped superconductor =
superconductor with gap in bulk
but with topologically protected
gapless states on the boundary

p-wave 2D superconductor (Sr_2RuO_4 ?), ^{3}He-A thin film,
CdTe/HgTe/Cd insulator quantum well, planar phase film

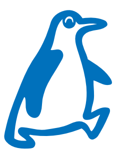

who protects gapless states?

generic example:

$$H = \begin{pmatrix} \dfrac{p^2}{2m} - \mu & c(p_x + ip_y) \\ c(p_x - ip_y) & -\dfrac{p^2}{2m} + \mu \end{pmatrix} \qquad p^2 = p_x^{\,2} + p_y^{\,2}$$

How to extract useful information on energy states from this Hamiltonian
without solving equation

$$H\psi = E\psi$$

Topological invariant in momentum space

$$\mathrm{H} = \begin{pmatrix} \frac{p^2}{2m} - \mu & c(p_x + ip_y) \\ c(p_x - ip_y) & -\frac{p^2}{2m} + \mu \end{pmatrix}$$

$$\mathrm{H} = \begin{pmatrix} g_3(\mathbf{p}) & g_1(\mathbf{p}) + i\, g_2(\mathbf{p}) \\ g_1(\mathbf{p}) - i\, g_2(\mathbf{p}) & -g_3(\mathbf{p}) \end{pmatrix} = \boldsymbol{\tau} \cdot \mathbf{g}(\mathbf{p})$$

$$p^2 = p_x^{\ 2} + p_y^{\ 2}$$

fully gapped 2D state at $\mu \neq 0$

$$\boxed{\tilde{N}_3 = \frac{1}{8\pi}\, e_{ijk} \int dp_x dp_y \;\; \hat{\mathbf{g}} \cdot (\nabla_{p_x} \hat{\mathbf{g}} \times \nabla_{p_y} \hat{\mathbf{g}})}$$

GV, JETP **67**, 1804 (1988)

Skyrmion (coreless vortex) in momentum space at $\mu > 0$

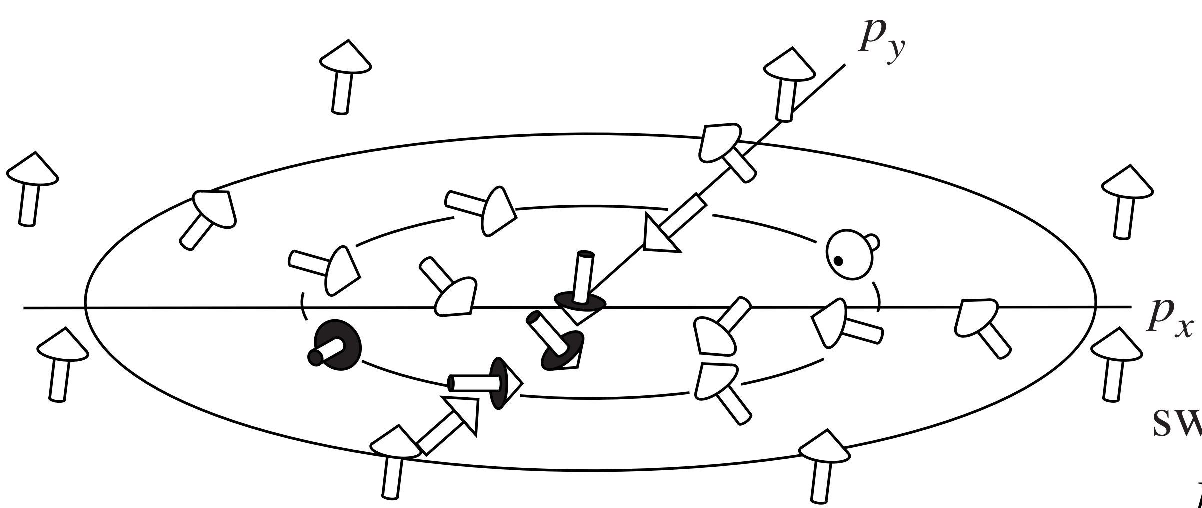

unit vector

$\hat{\mathbf{g}}(p_x, p_y)$

sweeps unit sphere

$\tilde{N}_3\ (\mu > 0) = 1$

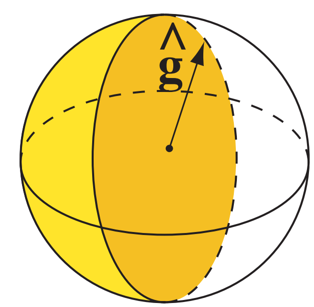

quantum phase transition:
from topological to non-topologicval insulator/superconductor

$$H = \begin{pmatrix} \frac{p^2}{2m} - \mu & c(p_x + ip_y) \\ c(p_x - ip_y) & -\frac{p^2}{2m} + \mu \end{pmatrix} = \begin{pmatrix} g_3(\mathbf{p}) & g_1(\mathbf{p}) + i\, g_2(\mathbf{p}) \\ g_1(\mathbf{p}) - i\, g_2(\mathbf{p}) & -g_3(\mathbf{p}) \end{pmatrix} = \boldsymbol{\tau} \cdot \mathbf{g}(\mathbf{p})$$

Topological invariant in momentum space

$$\boxed{N_3 = \frac{1}{8\pi}\, e_{ijk} \int dp_x dp_y \;\; \hat{\mathbf{g}} \cdot (\nabla_{px} \hat{\mathbf{g}} \times \nabla_{py} \hat{\mathbf{g}})}$$

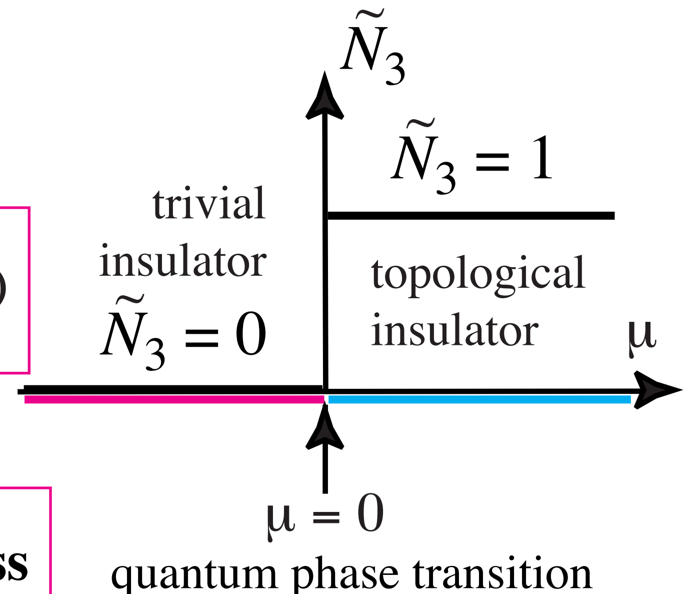

intermediate state at $\mu = 0$ must be gapless

$\Delta\widetilde{N}_3 \neq 0$ is origin of fermion zero modes at the interface between states with different $\widetilde{N}_3$

p-space invariant in terms of Green's function & topological QPT

$$\boxed{\tilde{N}_3 = \frac{1}{24\pi^2} e_{\mu\nu\lambda}\, \mathbf{tr} \int d^2p\, d\omega\, \mathbf{G}\nabla^{\mu}\mathbf{G}^{-1}\,\mathbf{G}\nabla^{\nu}\mathbf{G}^{-1}\mathbf{G}\nabla^{\lambda}\mathbf{G}^{-1}}$$

GV & Yakovenko
J. Phys. CM **1**, 5263 (1989)

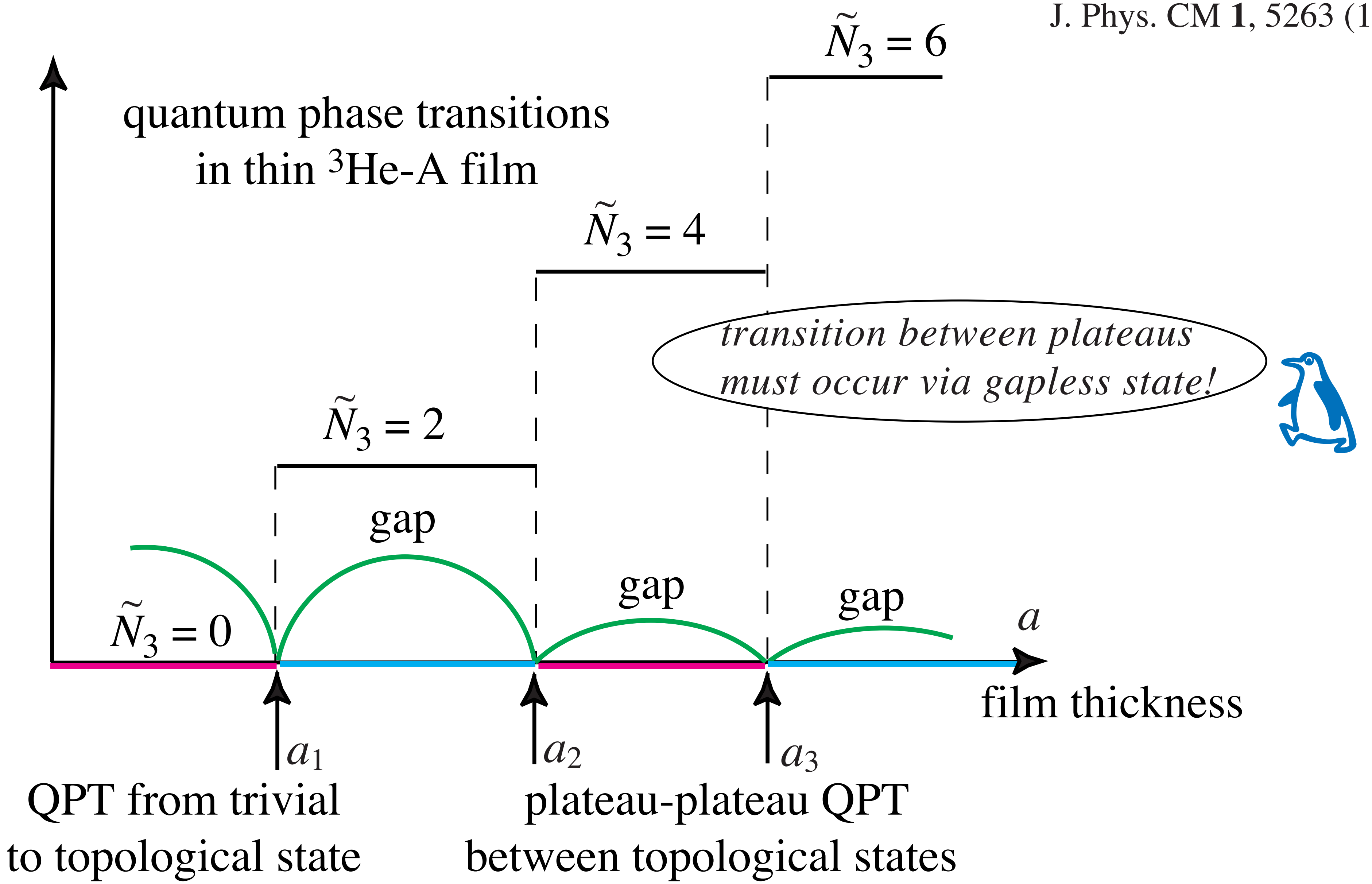

topological quantum phase transitions

transitions between **ground states (vacua)** of the **same symmetry**,
but **different topology** in **momentum space**

example: QPT between gapless & gapped matter

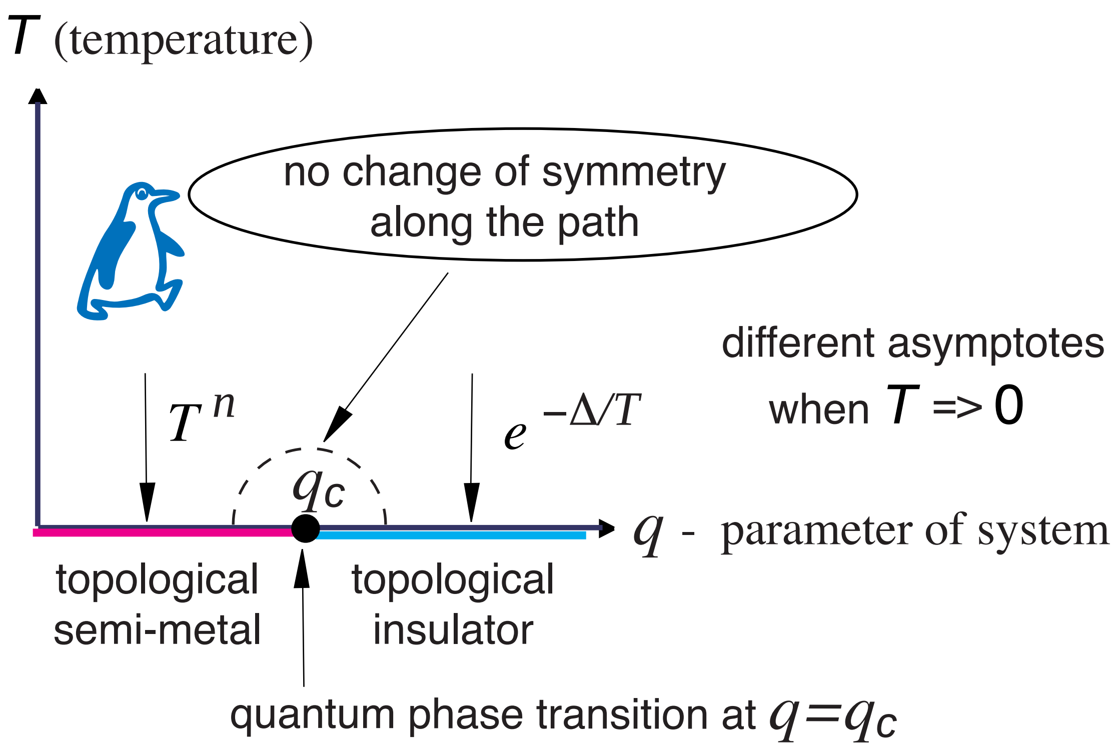

other topological QPT:
Lifshitz transition,
transtion between topological and nontopological superfluids,
plateau transitions,
confinement-deconfinement transition, ...

QPT interrupted
by thermodynamic transitions

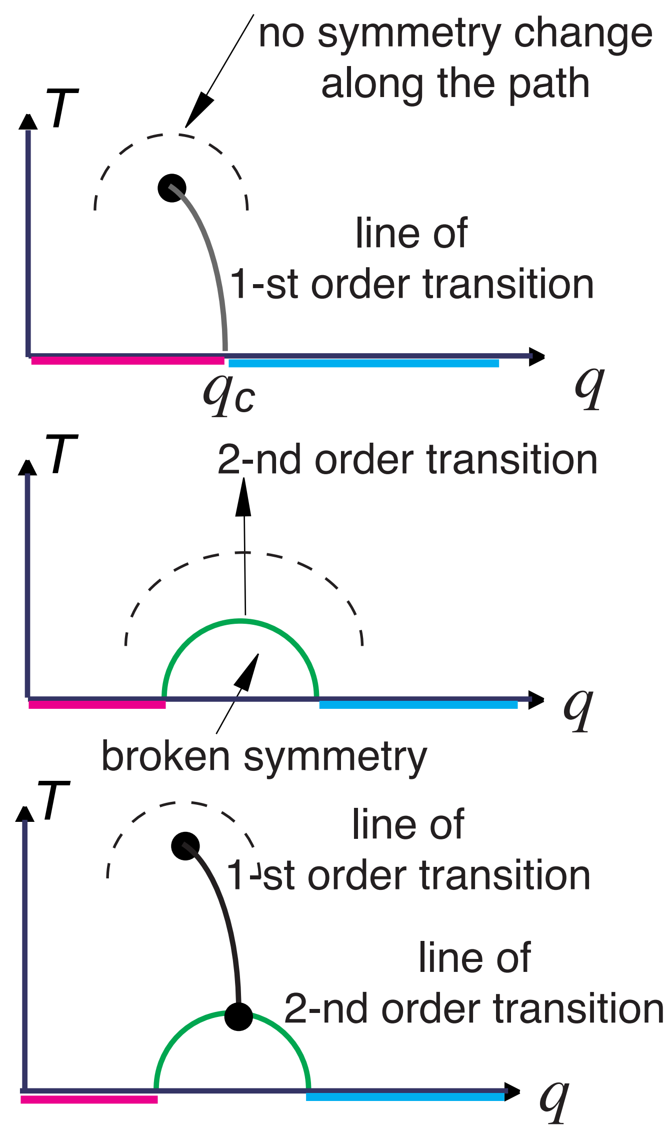

interface between two 2+1 topological insulators or gapped superfluids

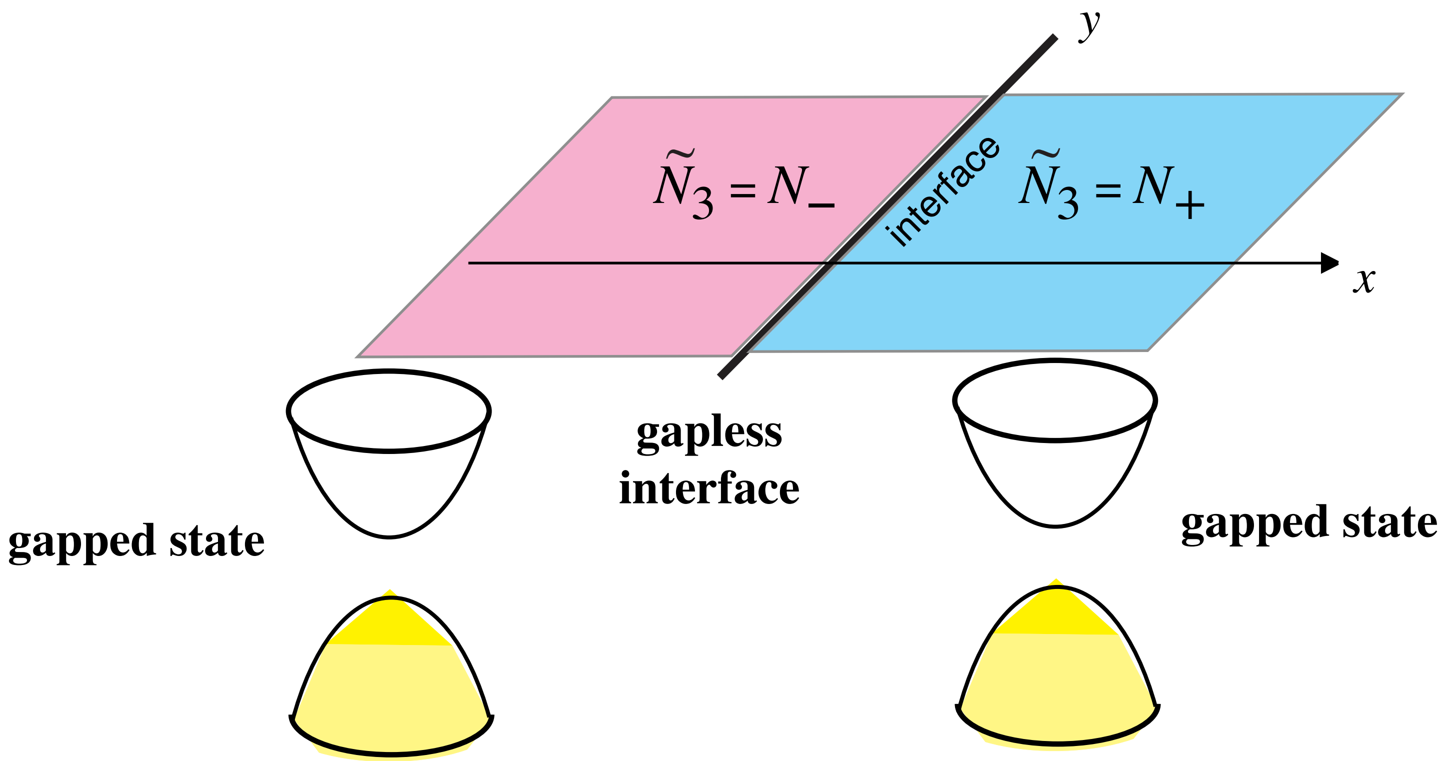

* domain wall in 2D chiral superconductors:

$$H = \begin{pmatrix} \frac{p^2}{2m} - \mu & c(p_x + i\, p_y \tanh x) \\ c(p_x - i\, p_y \tanh x) & -\frac{p^2}{2m} + \mu \end{pmatrix}$$

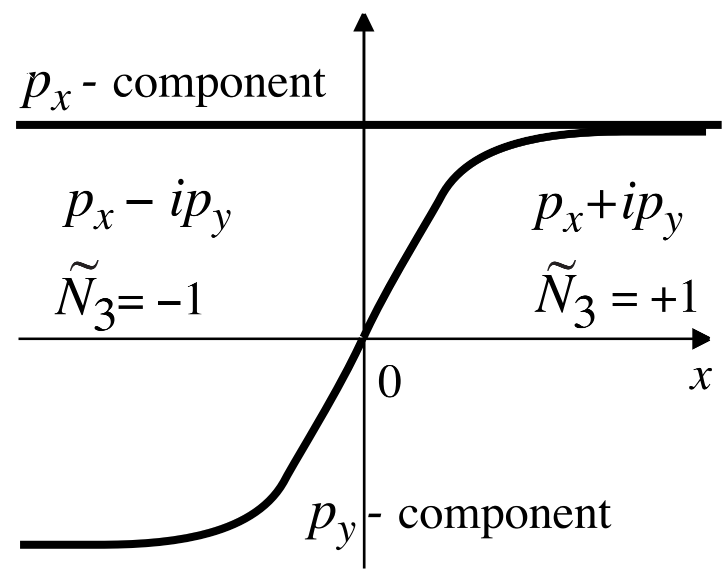

Edge states at interface between two 2+1 topological insulators or gapped superfluids

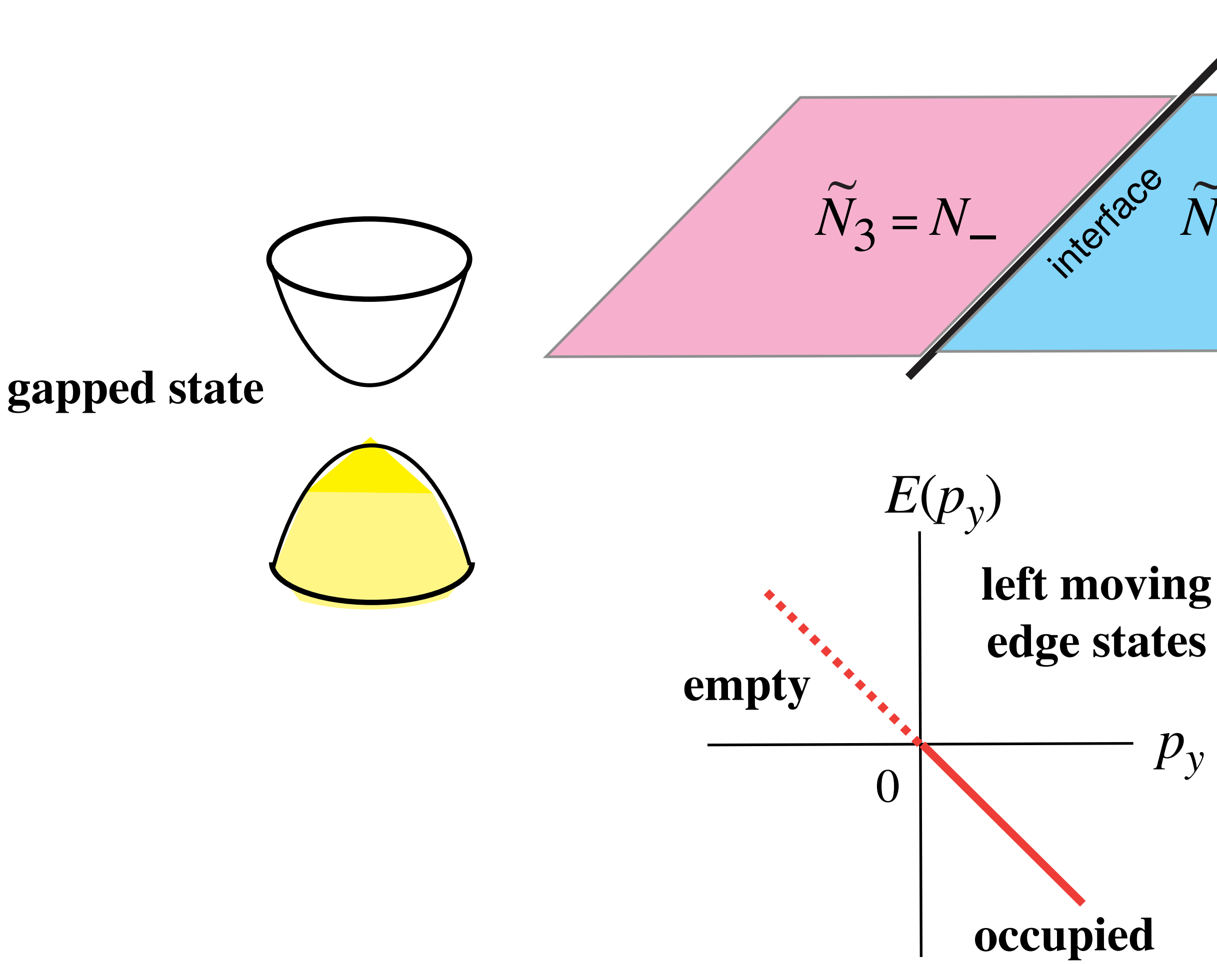

GV JETP Lett. **55**, 368 (1992)

Index theorem:
number of fermion zero modes
at interface:

$$\nu = N_+ - N_-$$

Edge states and currents

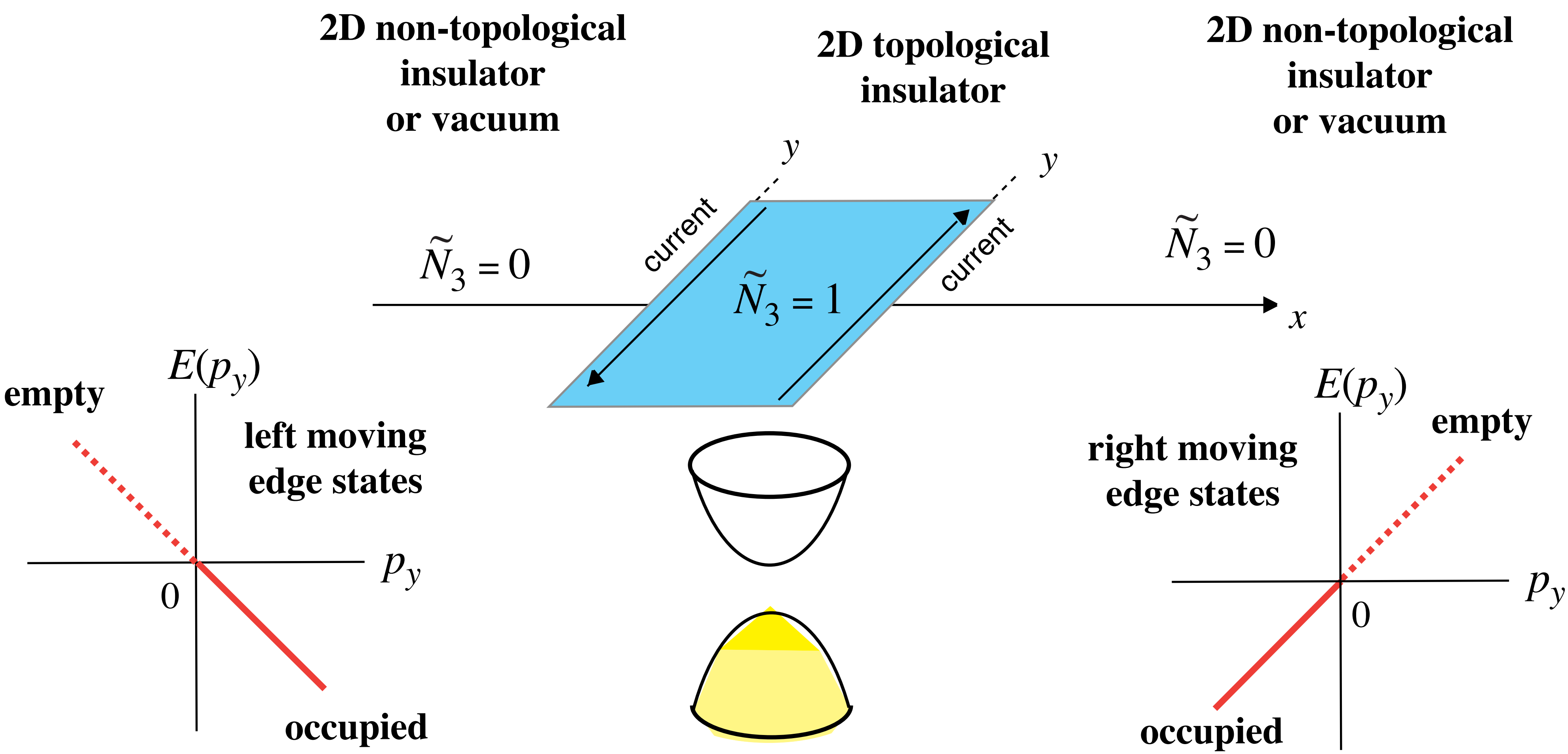

current $J_y = J_{\mathrm{left}} + J_{\mathrm{right}} = 0$

Edge states & intrinsic QHE: topological invariant determines Hall quantization

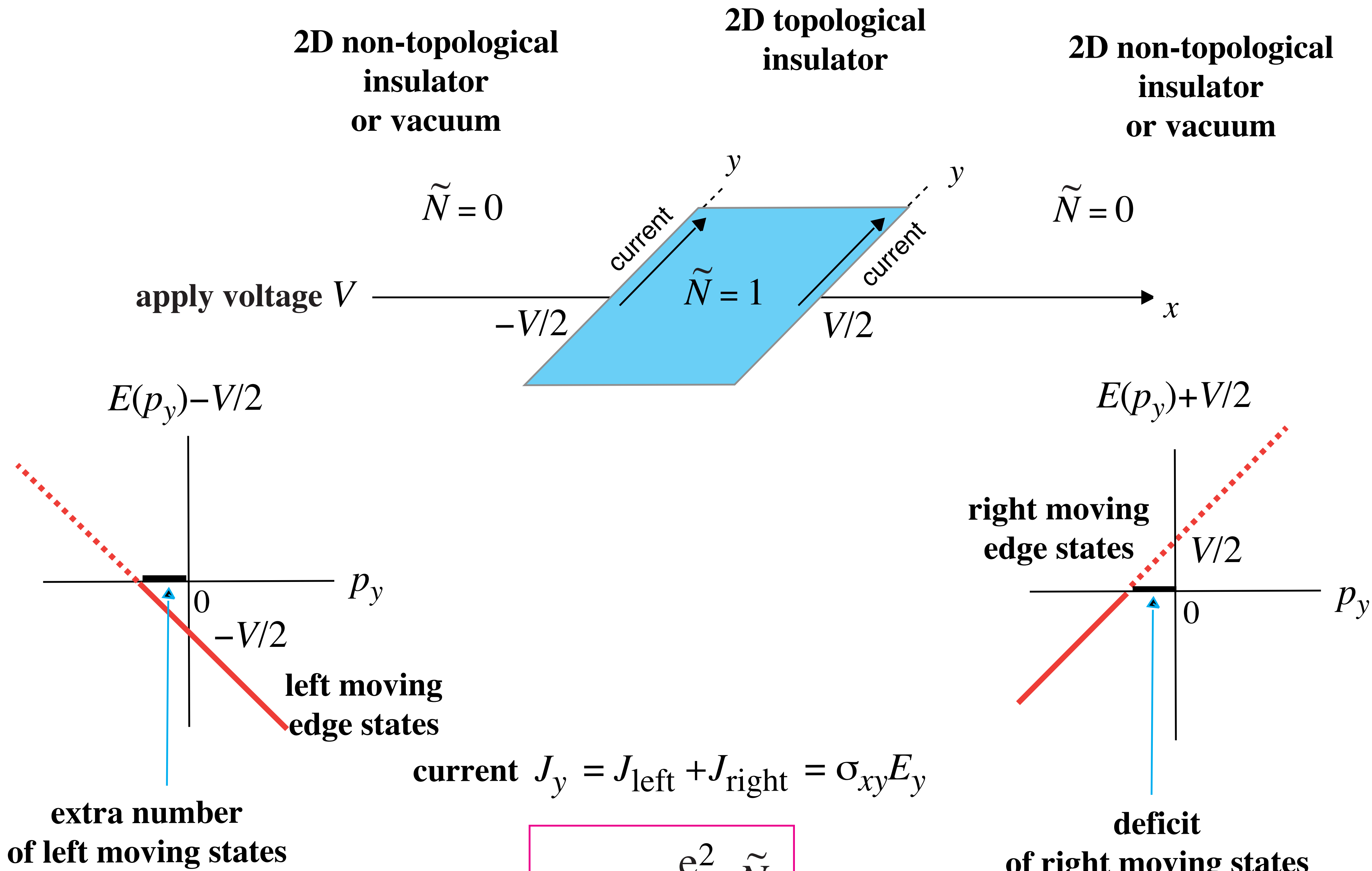

current $J_y = J_{\mathrm{left}} + J_{\mathrm{right}} = \sigma_{xy} E_y$

$$\boxed{\sigma_{xy} = \frac{e^2}{4\pi} \tilde{N}}$$

Intrinsic quantum Hall effect & momentum-space invariant

$$S_{CS} = \frac{e^2}{16\pi}\,\tilde{N}_3\, e^{\mu\nu\lambda} \int d^2x\, dt\, A_\mu\, F_{\nu\lambda}$$

p-space invariant — **r**-space invariant

A_μ - electromagnetic field

electric current $J_x = \delta S_{CS} / \delta A_x = \frac{e^2}{4\pi} \tilde{N}_3\, E_y$

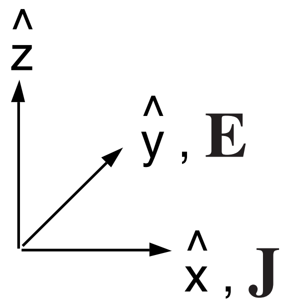

quantized intrinsic Hall conductivity
(without external magnetic field)

$$\boxed{\sigma_{xy} = \frac{e^2}{4\pi} \tilde{N}_3}$$

GV & Yakovenko
J. Phys. CM **1**, 5263 (1989)

film of topological quantum liquid

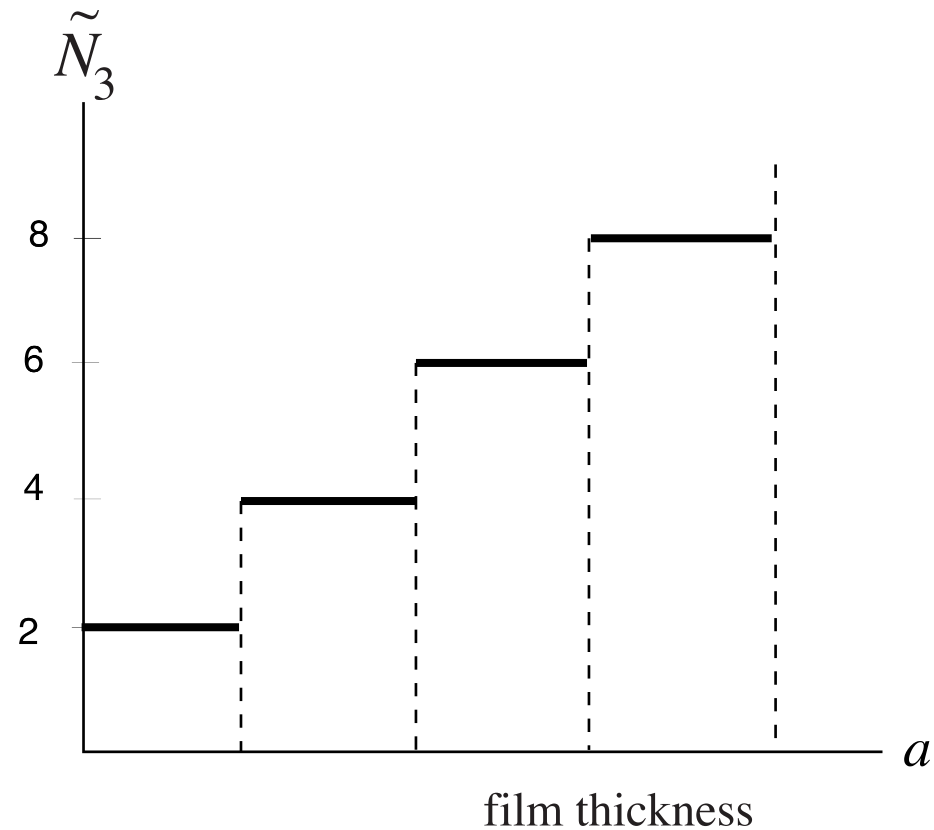

general Chern-Simons terms & momentum-space invariant

(interplay of ***r***-space and ***p***-space topologies)

$$\boxed{S_{CS} = \frac{1}{16\pi}\,\tilde{N}_{3IJ}\, e^{\mu\nu\lambda}\int d^2x\, dt\, A_\mu^{\ I} F_{\nu\lambda}^{\ J}}$$

***r*-space invariant**

***p*-space invariant protected by symmetry**

dimensional reduction
of chiral anomaly in 3+1

$$\boxed{\tilde{N}_{3IJ} = \frac{1}{24\pi^2} e_{\mu\nu\lambda} \mathbf{tr}\left[\int d^2p\, d\omega\, K_I K_J\, \mathbf{G}\nabla^\mu \mathbf{G}^{-1}\, \mathbf{G}\nabla^\nu \mathbf{G}^{-1} \mathbf{G}\nabla^\lambda \mathbf{G}^{-1}\right]}$$

K_I - charge interacting with gauge field $A_\mu^{\ I}$

gauge fields can be
real, artificial or auxiliary

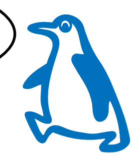

$K=e$ for electromagnetic field A_μ

$K=\hat{\sigma}_z$ for effective spin-rotation field $A_\mu^{\ z}$ $\left(A_0^{\ z} = \gamma H^{\ z}\right)$

$$id/dt - \gamma\hat{\sigma}\cdot\mathbf{H} = id/dt - \hat{\sigma}\cdot\mathbf{A}_0$$

applied Pauli magnetic field plays the role of components of effective SU(2) gauge field $A_\mu^{\ i}$

Intrinsic spin-current quantum Hall effect & momentum-space invariant

spin current $J_x^{z} = \dfrac{1}{4\pi}\left(\gamma N_{ss}\, dH^{z}/dy + N_{se}\, E_y\right)$

spin-spin QHE

spin-charge QHE

2D singlet superconductor:

$$\boxed{\sigma_{xy}^{\mathrm{spin/spin}} = \frac{N_{ss}}{4\pi}}$$

s-wave: $N_{ss} = 0$

$p_x + ip_y$: $N_{ss} = 2$

$d_{xx\text{-}yy} + id_{xy}$: $N_{ss} = 4$

film of planar phase of superfluid ^{3}He

$$\boxed{\sigma_{xy}^{\mathrm{spin/charge}} = \frac{N_{se}}{4\pi}}$$

GV & Yakovenko
J. Phys. CM **1**, 5263 (1989)

spin quantum Hall effect: planar phase film of 3He & 2D topological insulator

$$\mathrm{H} = \begin{pmatrix} \frac{p^2}{2m} - \mu & c(p_x + i\, p_y \sigma_z) \\ c(p_x - i\, p_y \sigma_z) & -\frac{p^2}{2m} + \mu \end{pmatrix}$$

$$\boxed{\tilde{N}_3 = \frac{1}{24\pi^2} e_{\mu\nu\lambda} \mathbf{tr} \left[\int d^2p\, d\omega\, \mathbf{G} \nabla^{\mu} \mathbf{G}^{-1} \mathbf{G} \nabla^{\nu} \mathbf{G}^{-1} \mathbf{G} \nabla^{\lambda} \mathbf{G}^{-1} \right] = 0}$$

$$\boxed{\tilde{N}_{se} = \frac{1}{24\pi^2} e_{\mu\nu\lambda} \mathbf{tr} \left[\int d^2p\, d\omega\, \sigma_z \mathbf{G} \nabla^{\mu} \mathbf{G}^{-1} \mathbf{G} \nabla^{\nu} \mathbf{G}^{-1} \mathbf{G} \nabla^{\lambda} \mathbf{G}^{-1} \right]}$$

$$\tilde{N}_3^{+} = +1 \qquad \tilde{N}_3^{-} = -1$$

$$\tilde{N}_3 = \tilde{N}_3^{+} + \tilde{N}_3^{-} = 0 \qquad \tilde{N}_{se} = \tilde{N}_3^{+} - \tilde{N}_3^{-} = 2$$

spin quantum Hall effect

spin current $J_x^{z} = \frac{1}{4\pi} N_{se} E_y$ $\boxed{\text{spin-charge QHE}}$

$$\boxed{\sigma_{xy}^{\text{spin/charge}} = \frac{N_{se}}{4\pi}} \qquad N_{se} = 2$$

GV & Yakovenko
J. Phys. CM **1**, 5263 (1989)

Intrinsic spin-current quantum Hall effect & edge state

spin current $J_x^{\,z} = \dfrac{1}{4\pi}\left(\gamma N_{ss}\, dH^z/dy + \underbrace{N_{se}}_{\text{spin-charge QHE}} E_y\right)$

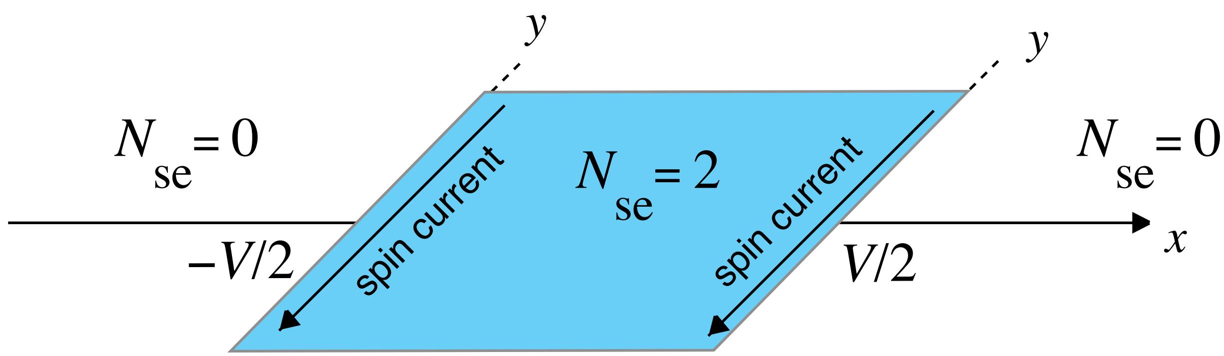

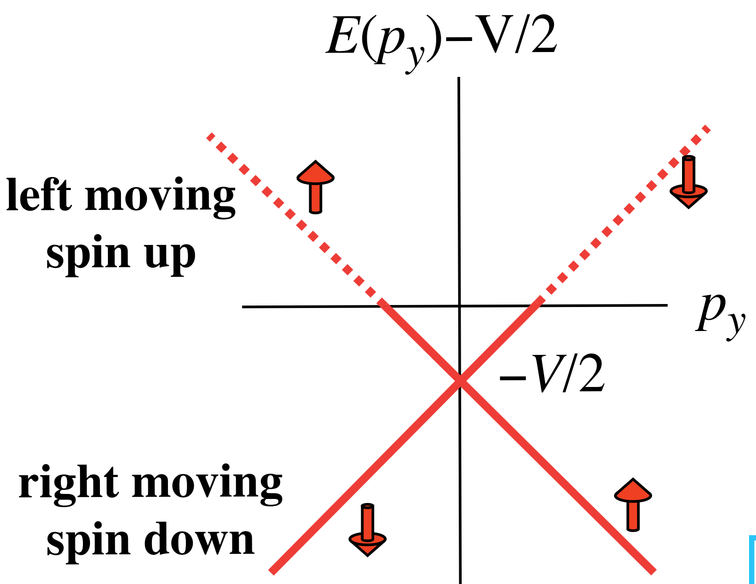

$$\sigma_{xy}^{\text{spin/charge}} = \frac{N_{se}}{4\pi}$$

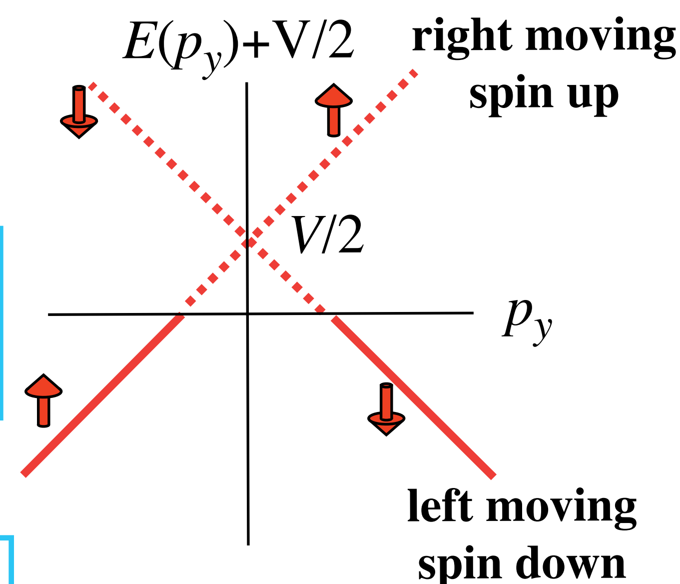

electric current is zero
spin current is nonzero

3D topological superfluids / insulators / semiconductors / vacua

gapless topologically
nontrivial vacua

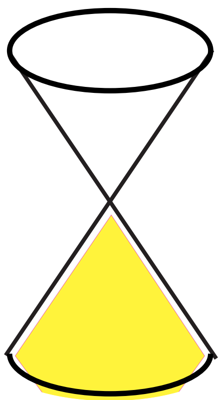

3He-A,
Standard Model
above electroweak transition,
semimetals,
4D graphene
(cryocrystalline vacuum)

fully gapped topologically
nontrivial vacua

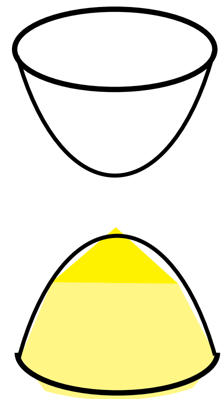

3He-B,
Standard Model
below electroweak transition,
topological insulators,
triplet & singlet
chiral superconductor, ...

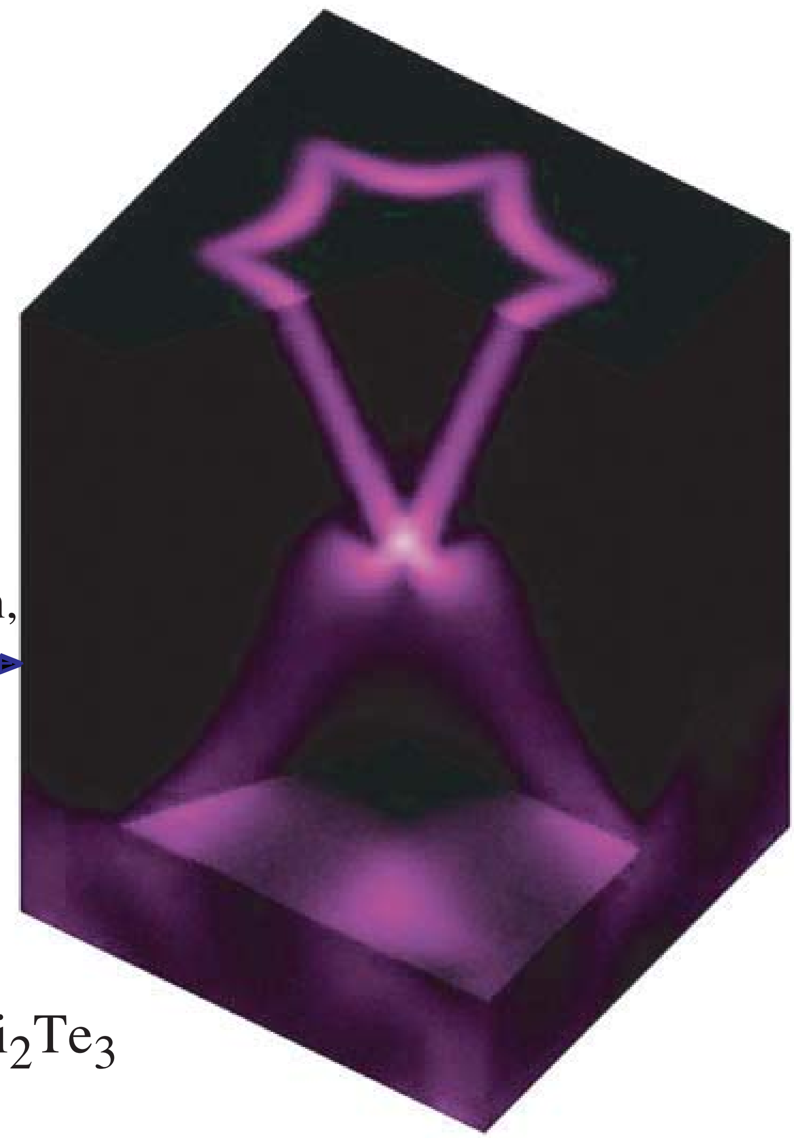

Bi_2Te_3

Present vacuum as semiconductor or insulator

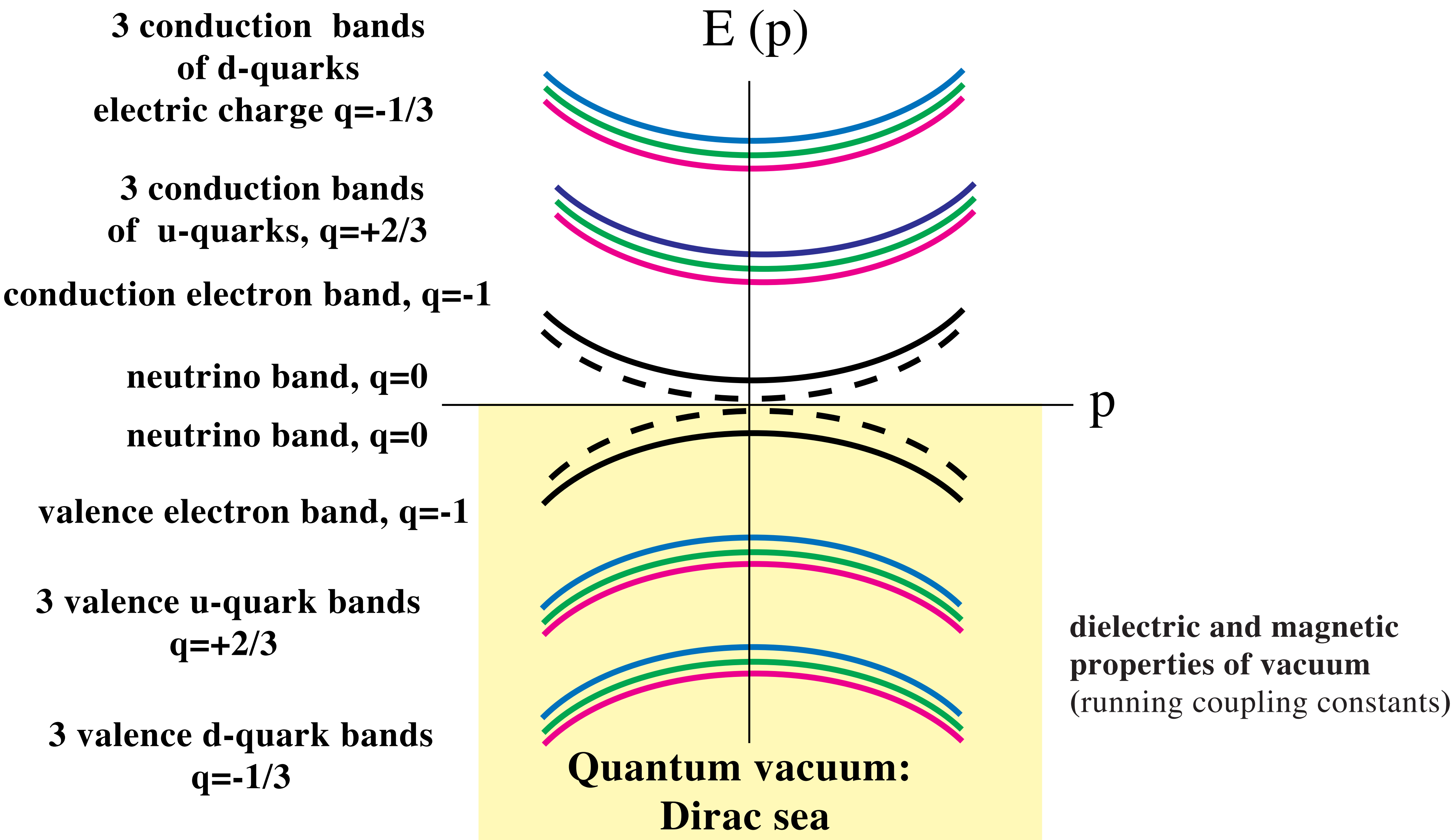

electric charge of quantum vacuum

$$Q = \sum_a q_a = N\,[-1 + 3\times(-1/3) + 3\times(+2/3)\,] = 0$$

fully gapped 3+1 topological matter

superfluid ^{3}He-B, topological insulator Bi_2Te_3 , present vacuum of Standard Model

* Standard Model vacuum as topological insulator

Topological invariant protected by symmetry

$$N_K = \frac{1}{24\pi^2}\, e_{\mu\nu\lambda}\, \mathbf{tr} \int dV\, K\, \mathbf{G}\, \nabla^\mu\, \mathbf{G}^{-1}\, \mathbf{G}\, \nabla^\nu\, \mathbf{G}^{-1} \mathbf{G}\, \nabla^\lambda\, \mathbf{G}^{-1}$$

over 3D momentum space

G is Green's function at $\omega=0$, K is symmetry operator **GK** =+/− **KG**

Standard Model vacuum: $K=\gamma_5$ $\mathbf{G}\gamma_5 = -\gamma_5\mathbf{G}$

$$N_K = 8n_g$$

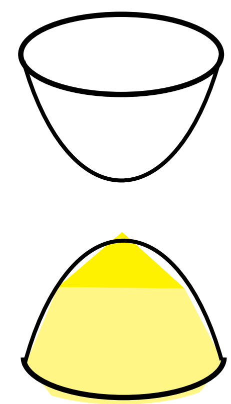

8 massive Dirac particles in one generation

topological superfluid ^{3}He-B

$$H\tau_2 = -\tau_2 H$$

$$K = \tau_2$$

$$H = \begin{pmatrix} \dfrac{p^2}{2m^*} - \mu & c_B \sigma\cdot\mathbf{p} \\ c_B \sigma\cdot\mathbf{p} & -\dfrac{p^2}{2m^*} + \mu \end{pmatrix} = \left(\frac{p^2}{2m^*} - \mu\right)\tau_3 + c_B \sigma\cdot\mathbf{p}\,\tau_1$$

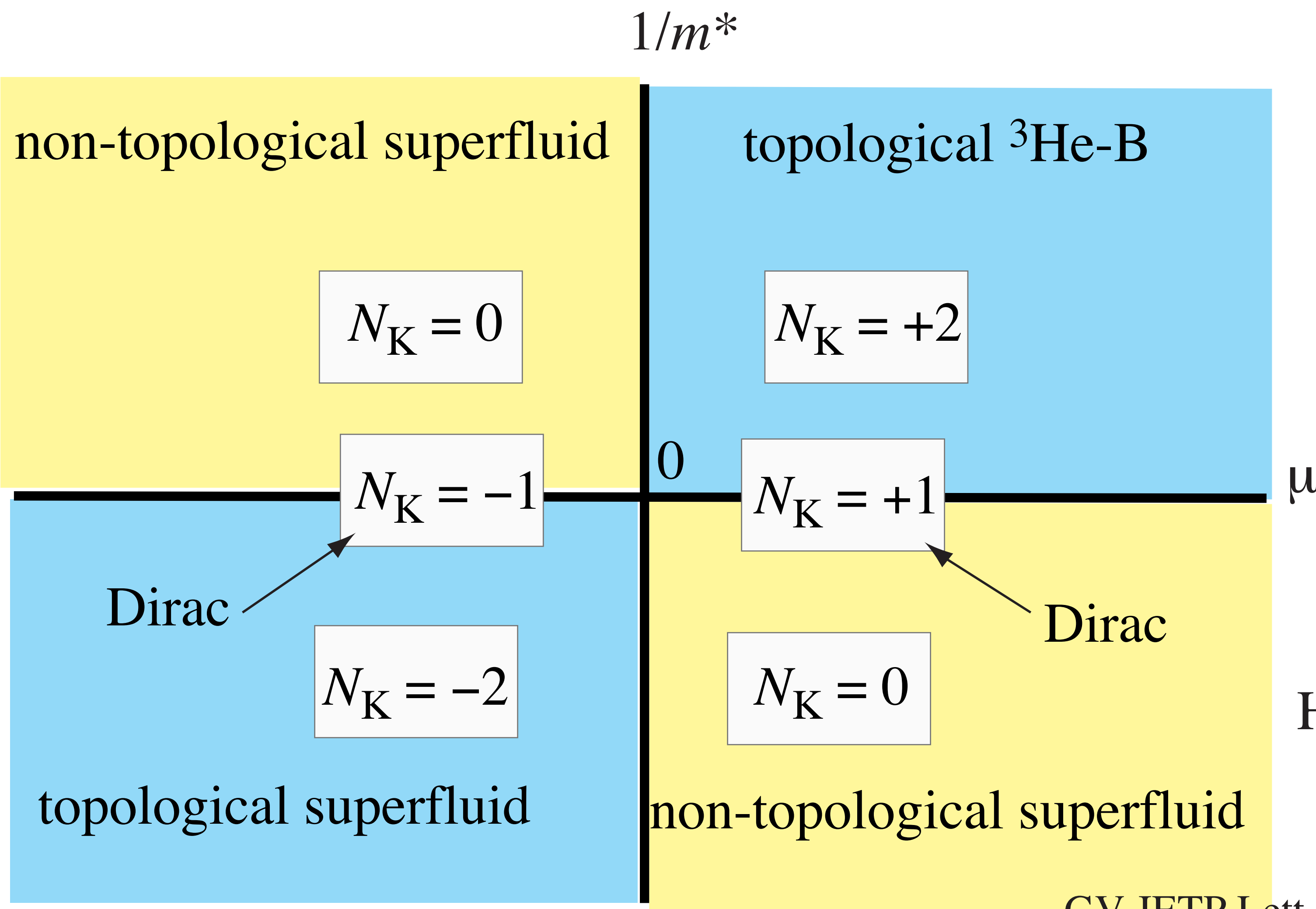

Dirac vacuum

$$1/m^* = 0$$

$$H = \begin{pmatrix} -M & c_B \sigma\cdot\mathbf{p} \\ c_B \sigma\cdot\mathbf{p} & +M \end{pmatrix}$$

GV JETP Lett. **90**, 587 (2009)

Boundary of 3D gapped topological superfluid

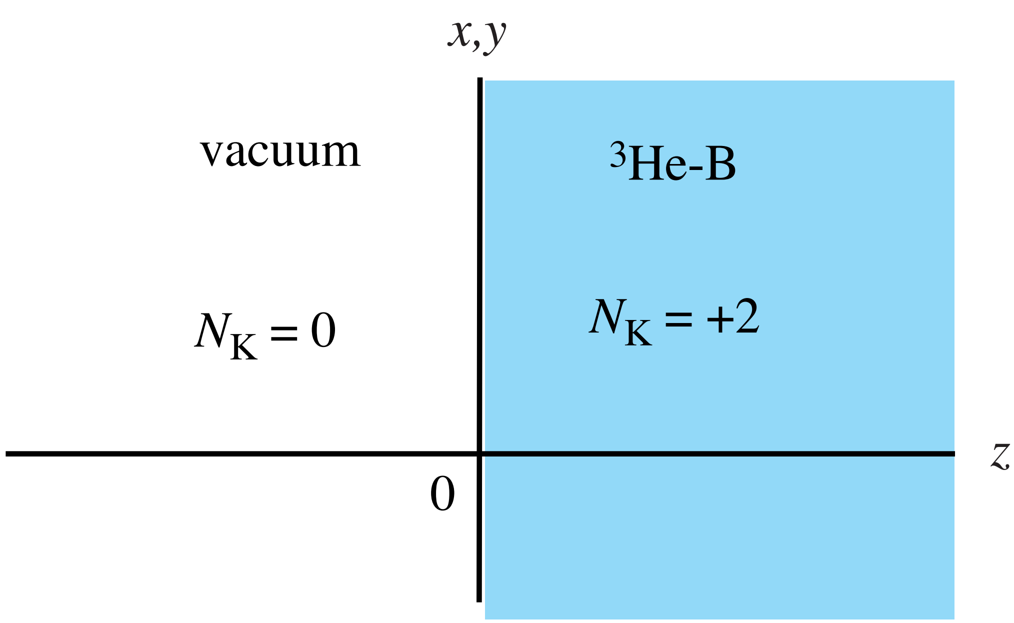

$$H = \begin{pmatrix} \frac{p^2}{2m^*} - \mu + U(z) & c_B \sigma\cdot\mathbf{p} \\ c_B \sigma\cdot\mathbf{p} & -\frac{p^2}{2m^*} + \mu - U(z) \end{pmatrix}$$

spectrum of Majorana fermion zero modes

$$H_{zm} = c_B\, \hat{\mathbf{z}} \cdot \sigma \times \mathbf{p} = c_B\, (\sigma_x p_y - \sigma_y p_x)$$

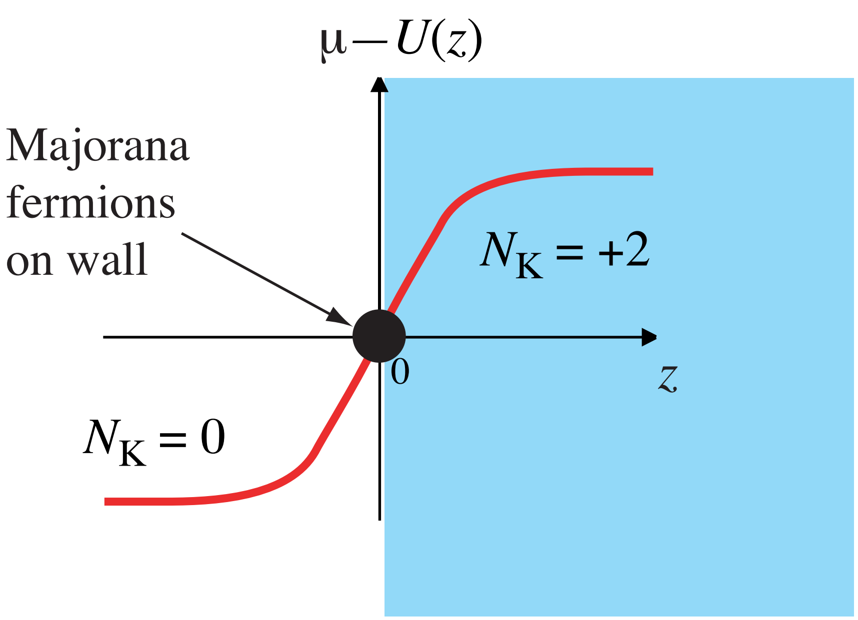

helical fermions

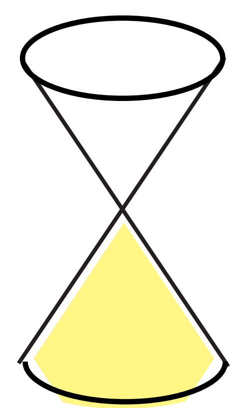

fermion zero modes on Dirac wall

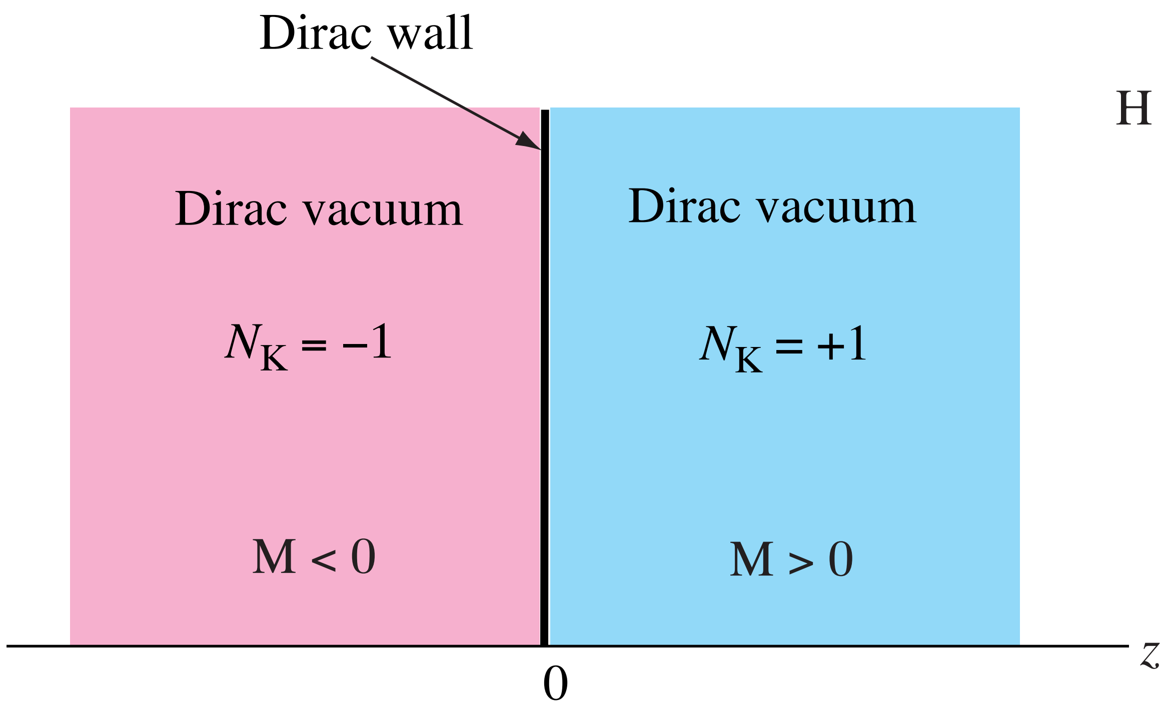

$$H = \begin{pmatrix} -M(z) & c\sigma\cdot\mathbf{p} \\ c\sigma\cdot\mathbf{p} & +M(z) \end{pmatrix}$$

Volkov-Pankratov,
2D massless fermions
in inverted contacts
JETP Lett. **42**, 178 (1985)

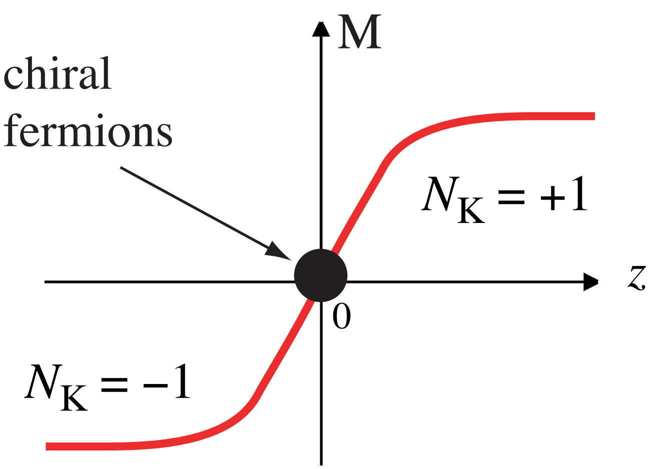

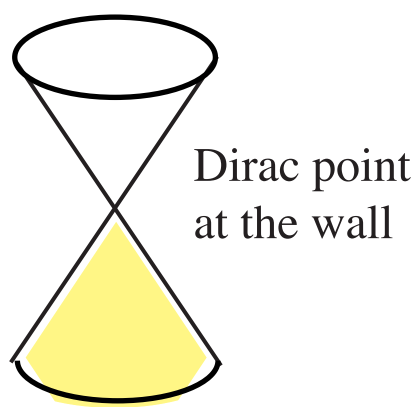

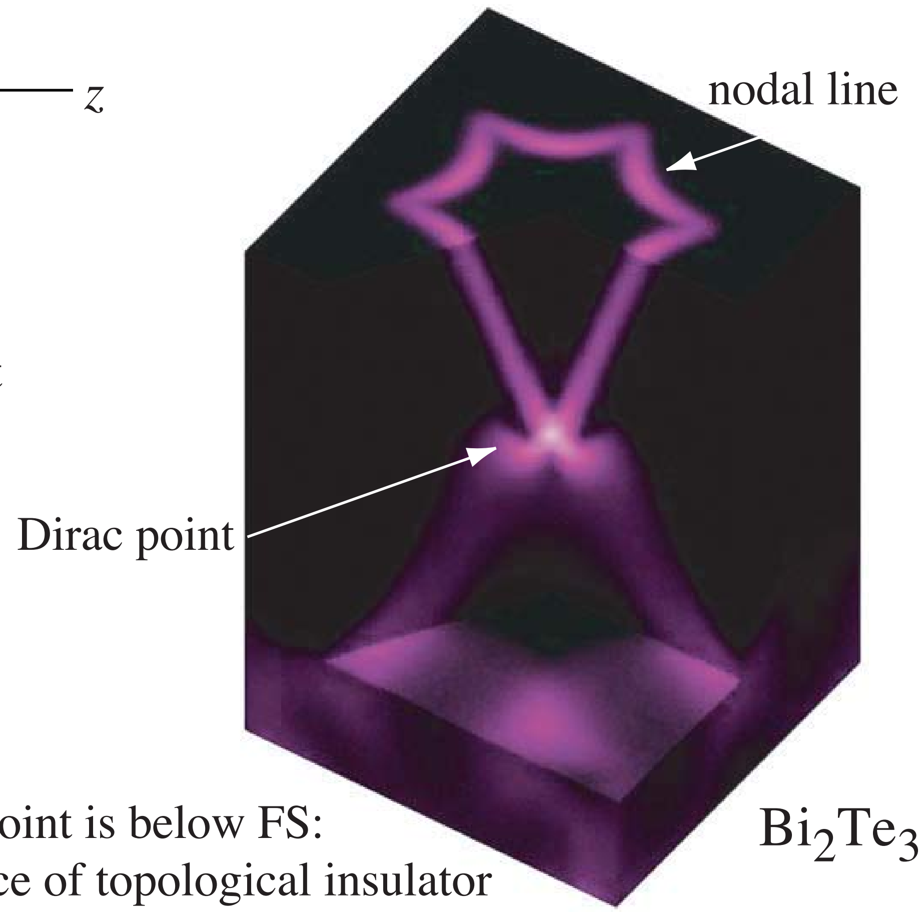

in Bi_2Te_3 Dirac point is below FS:
nodal line on surface of topological insulator

Majorana fermions: edge states
on the boundary of 3D gapped topological matter

$$H = \begin{pmatrix} \frac{p^2}{2m^*} - \mu + U(z) & c\sigma\cdot\mathbf{p} \\ c\sigma\cdot\mathbf{p} & -\frac{p^2}{2m^*} + \mu - U(z) \end{pmatrix}$$

* boundary of topological superfluid ^{3}He-B

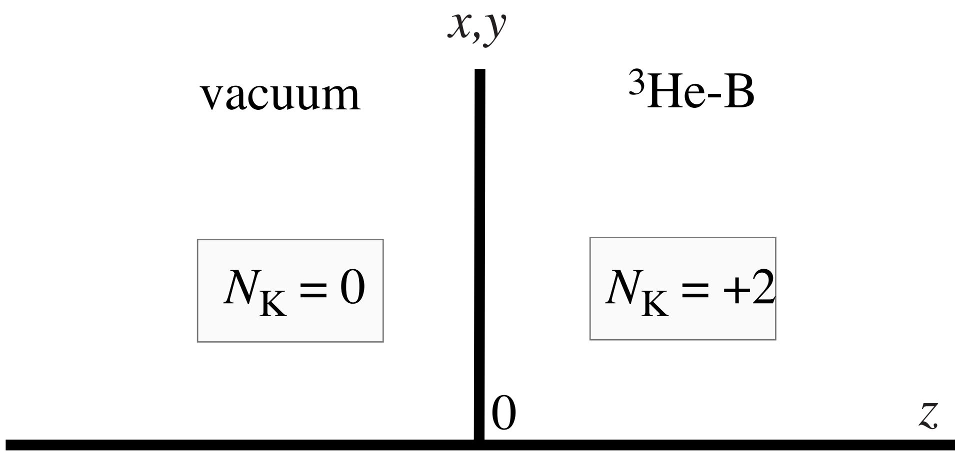

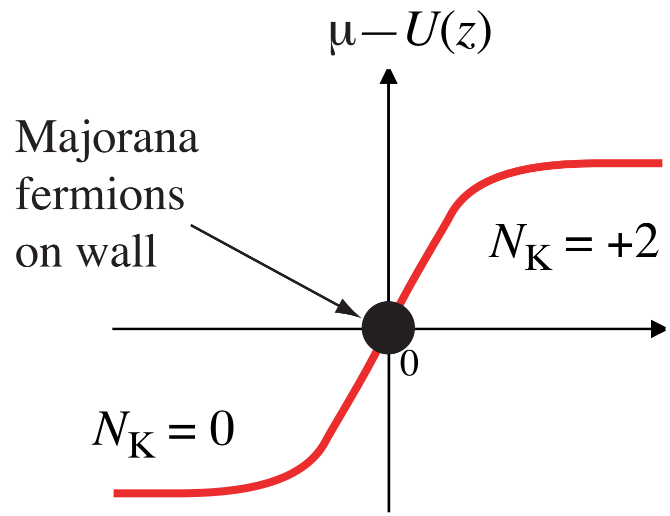

spectrum of fermion zero modes

$$H_{zm} = c\,(\sigma_x p_y - \sigma_y p_x)$$

helical fermions

* Dirac domain wall

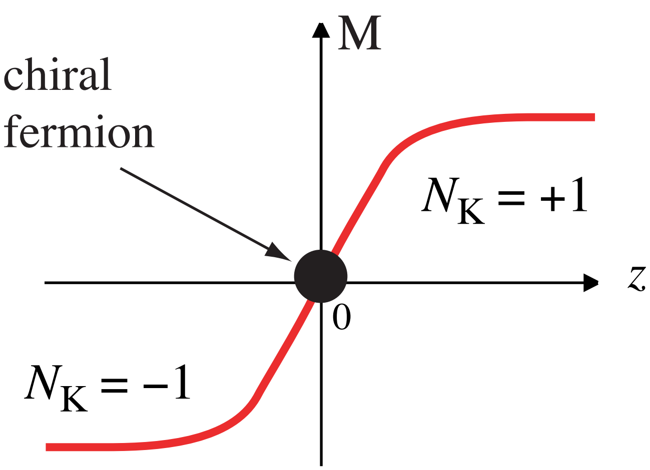

$$H = \begin{pmatrix} -M(z) & c\sigma\cdot\mathbf{p} \\ c\sigma\cdot\mathbf{p} & +M(z) \end{pmatrix}$$

Volkov-Pankratov,
2D massless fermions
in inverted contacts
JETP Lett. **42**, 178 (1985)

Majorana fermions on interface in topological superfluid ^{3}He-B

$$H = \begin{pmatrix} \frac{p^2}{2m^*} - \mu & \sigma_x c_x p_x + \sigma_y c_y p_y + \sigma_z c_z p_z \\ \sigma_x c_x p_x + \sigma_y c_y p_y + \sigma_z c_z p_z & -\frac{p^2}{2m^*} + \mu \end{pmatrix}$$

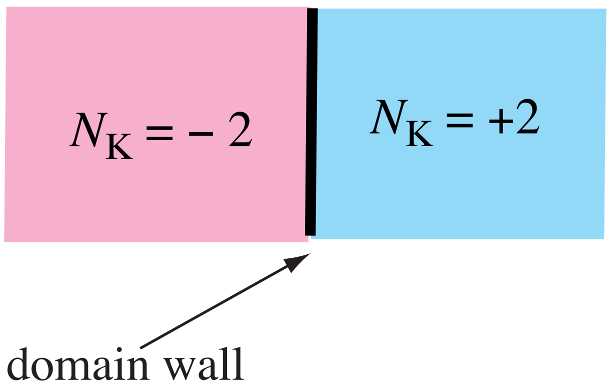

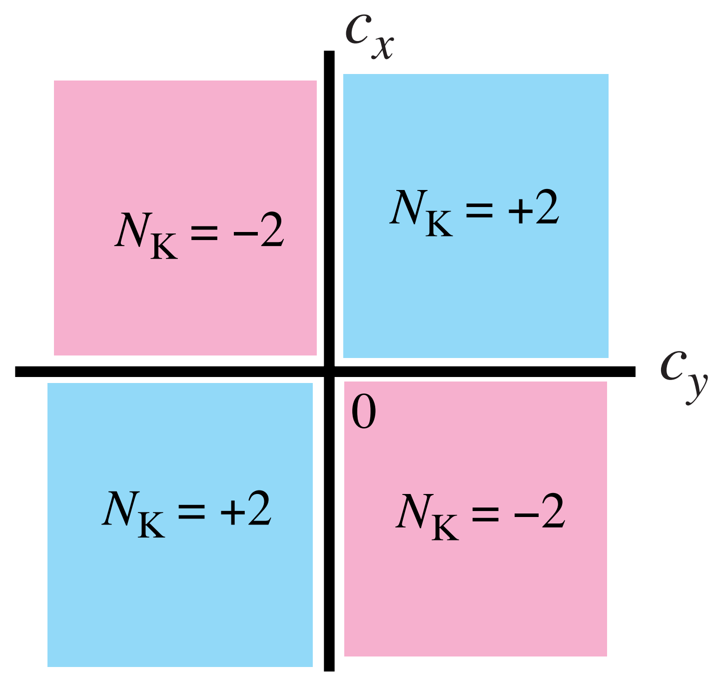

phase diagram

one of 3 "speeds of light" changes sign across wall

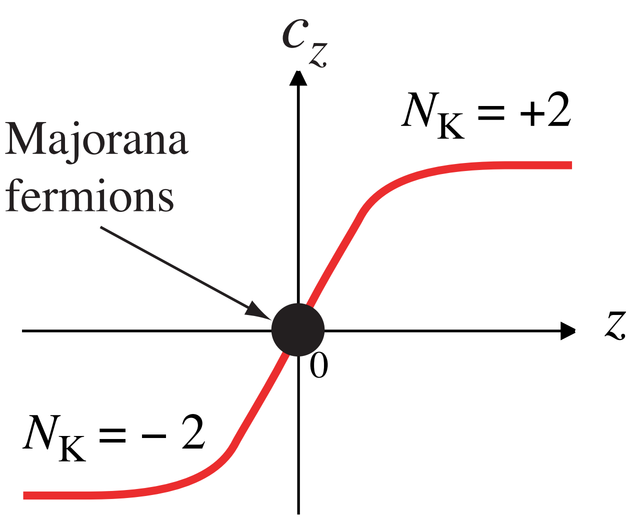

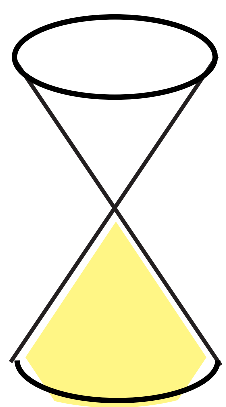

spectrum of fermion zero modes

$$H_{zm} = c\,(\sigma_x p_y - \sigma_y p_x)$$

Zero energy states in the core of vortices in topological superfluids

vortices in fully gapped 3+1 system

fermion zero modes in vortex core

Bound states of fermions on cosmic strings and vortices

Spectrum of quarks in core of electroweak cosmic string

quantum numbers: Q - angular momentum & p_z - linear momentum

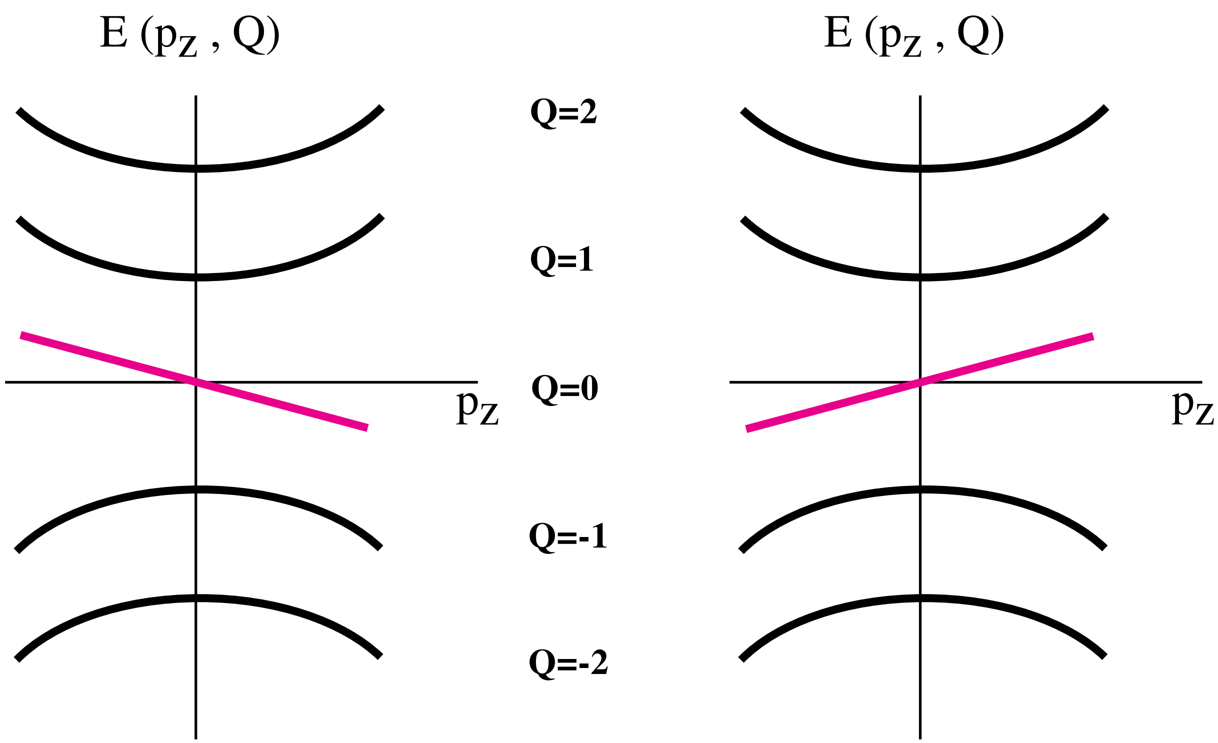

$E(p_z) = - cp_z$ for d quarks $\quad$ $E(p_z) = cp_z$ for u quark

asymmetric branches cross zero energy

Index theorem:

Number of asymmetric branches = N
N is vortex winding number

Jackiw & Rossi
Nucl. Phys. B**190**, 681 (1981)

Bound states of fermions on vortex in s-wave superconductor

$N_K = 0$

Caroli, de Gennes & J. Matricon, Phys. Lett. **9** (1964) 307

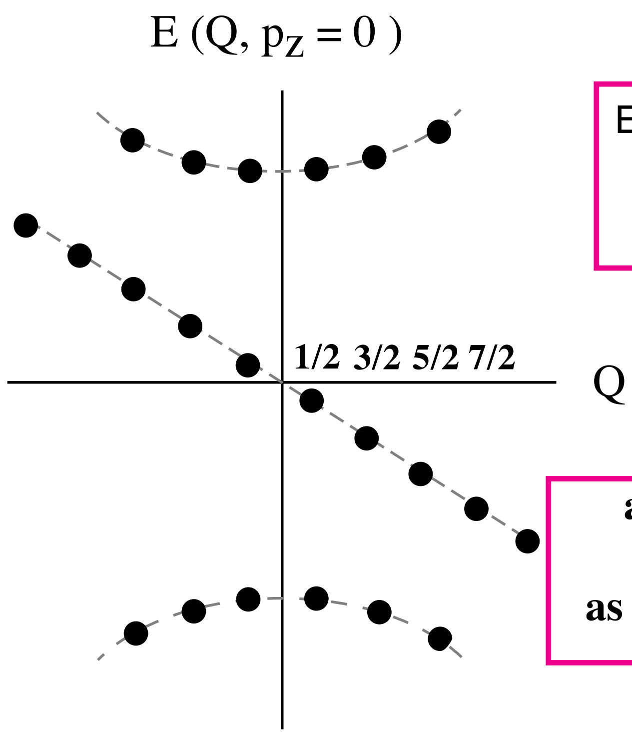

$E(Q,p_z) = - Q\, \omega_0\, (p_z)$

$\omega_0 = \Delta^2 / E_F << \Delta$

asymmetric branch as function of Q

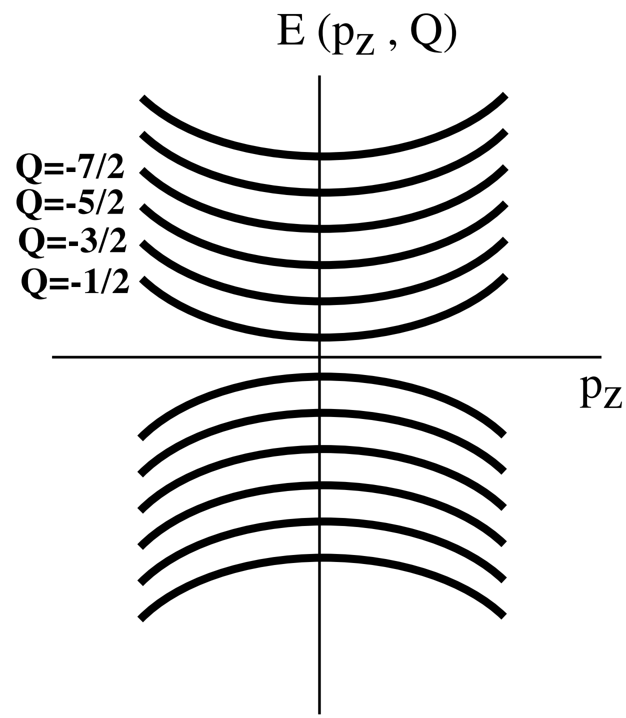

Angular momentum Q is half-odd integer in s-wave superconductor

no true fermion zero modes: no asymmetric branch as function of p_Z

Index theorem for approximate fermion zero modes:

Number of asymmetric Q-branches = 2N
N is vortex winding number

GV JETP Lett. **57**, 244 (1993)

Index theorem for true fermion zero modes?

is the existence of fermion zero modes related to topology in bulk?

fermions zero modes on symmetric vortex in 3He-B

topological ^{3}He-B at $\mu > 0$: $N_K = 2$

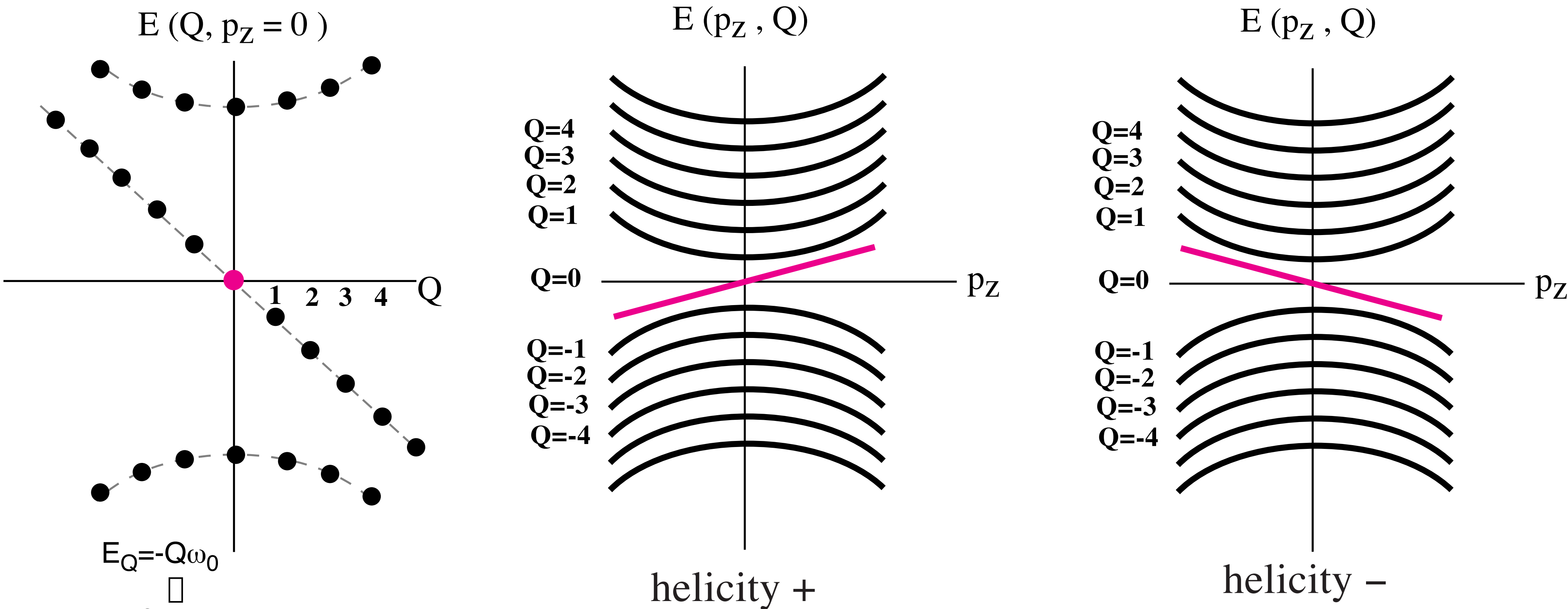

$E_Q = -Q\omega_0$

$\omega_0 = \Delta^2/E_F << \Delta$

Q is integer
for p-wave superfluid ^{3}He-B

gapless fermions on Q=0 branch form

1D Fermi-liquid

Misirpashaev & GV
Fermion zero modes in symmetric vortices in superfluid 3He,
Physica B **210**, 338 (1995)

fermions zero modes on symmetric vortex in 3He-B

topological ^{3}He-B at $\mu > 0$: $\boxed{N_K = 2}$

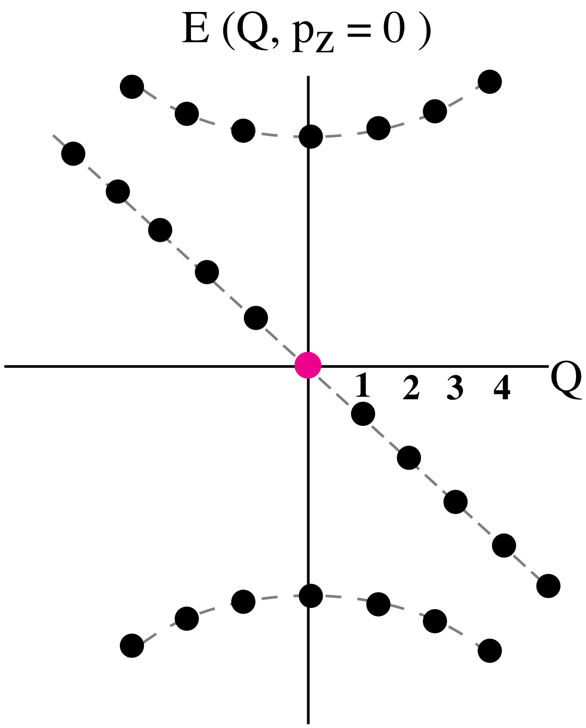

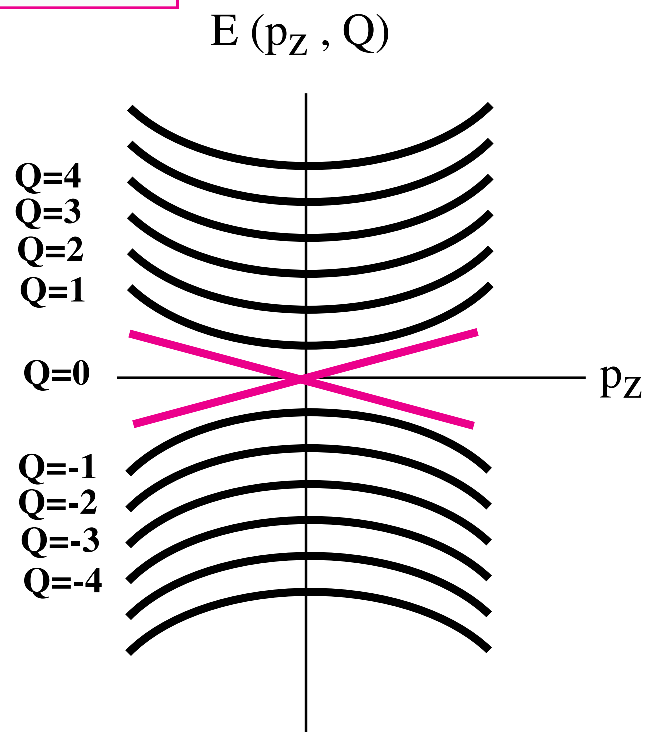

$E_Q = -Q\omega_0$

$\omega_0 = \Delta^2/E_F << \Delta$

Q is integer
for p-wave superfluid ^{3}He-B

gapless fermions on Q=0 branch form

$\boxed{\text{1D Fermi-liquid}}$

Misirpashaev & GV
Fermion zero modes in symmetric vortices in superfluid 3He,
Physica B **210**, 338 (1995)

topological quantum phase transition in bulk & in vortex core